1-1-2004

Target selection for antisense oligonucleotide induced exon skipping in the dystrophin gene

Stephen J. Errington
Edith Cowan University

Edith Cowan University

Copyright Warning

USE OF THESIS

The Use of Thesis statement is not included in this version of the thesis.

TARGET SELECTION FOR ANTISENSE OLIGONUCLEOTIDE INDUCED EXON SKIPPING IN THE DYSTROPHIN GENE

By

Stephen John Errington

Bachelor of Science (Human Biology)

A Thesis Submitted in Partial Fulfilment of the Requirements for the award of Master of Science (Human Biology)

Faculty of Communications, Health and Science

School of Biomedical and Sports Science

Edith Cowan University

Western Australia

Abstract

Duchenne Muscular Dystrophy (DMD), and the milder allelic Becker muscular dystrophy (BMD), are X-linked recessive muscle wasting disorders characterised by mutations in the dystrophin gene. DMD occurs at a frequency of approximately 1 in 3500 male newborns and life expectancy is typically less than 30 years. Due to progressive muscle wasting, affected boys are restricted to a wheelchair by the age of 12 years. The most common cause of death is pneumonia, compounded by cardiac involvement.

Mutations that disrupt the dystrophin reading frame, or prevent the synthesis of either terminus, preclude the synthesis of a fully functional dystrophin. The subsequent loss of membrane integrity results in a severe DMD phenotype, as these weakened but still functional muscle fibres are subject to continuous cycles of damage and regeneration. Conversely, BMD mutations are generally found to be in-frame deletions where a shorter but semi-functional protein with intact amino and carboxyl termini has been synthesised. BMD has an incidence almost ten times less than DMD. While the distribution of myopathy parallels DMD, the onset and progression of BMD is variable and generally less severe and some affected individuals are virtually asymptomatic.

From clinical studies on many patients with BMD, there is no doubt that some dystrophin, even if of reduced quantity and/or quality, can be of significant biological and functional advantage. Rare, naturally occurring dystrophin-positive, 'revertant' fibres have been found in over 50% of DMD patients. These revertant fibres are thought to result from the production of alternatively spliced dystrophin transcripts that bypass particular exons in the defective mRNA transcript to maintain the reading frame and produce a shorter, semi-functional protein. The presence of these fibres has led to the possibility of a new genetic therapy for DMD utilising small single-stranded fragments of nucleic acid called antisense oligonucleotides (2'OMeAOs). These 2'OMeAOs can be applied to the dystrophin gene to either restore the reading frame in the case of frame-shifting deletions, by skipping one or more flanking exons, or to target the disease-causing exons for removal from the final message. In this manner, the induced transcript could be translated into a shorter, but presumably semi-functional, dystrophin. Thus, the DMD phenotype would be potentially converted to a milder BMD-like phenotype.

At the commencement of this project, previous studies had targeted 2'OMeAOs to either of the consensus acceptor or donor splice sites or to a less well defined exon splicing enhancer sequence (ESE). However, none had compared these regions within the same exon or across species. The principal aim of this study, therefore, was to identify the target(s) within the dystrophin pre-mRNA most amenable to specific and efficient 2'OMeAO-induced exon skipping. An additional aim was to then apply the knowledge gained to mimic a naturally occurring revertant transcript, by inducing the removal of multiple exons.

Motifs involved in pre-mRNA splicing of mouse or human dystrophin exons 19 to 25 and 46 were targeted by 2'OMeAOs complexed with one of several transfection reagents. Cultured *H-2K* normal and *mdx* mouse, and normal and dystrophic human myotubes were transfected with 2'OMeAOs, either individually or in combinations. RT-PCR studies were undertaken to ascertain the extent of the 2'OMeAO-induced exon skipping and to determine if there might be a preferred motif at which to direct future 2'OMeAOs. We report varying efficiency of 2'OMeAO-induced removal of each exon of the dystrophin gene assessed by targeting a variety of splicing motifs. Furthermore, no alterations in other regions of the final dystrophin transcript were detected as a consequence of these 2'OMeAO treatments.

The results presented in this thesis suggest that the sensitivity of acceptor, donor or ESE splicing motifs to modulation by 2'OMeAOs is unique to the exon selected for removal and less dependent on the targeted sites. Therefore, there does not appear to be one specific splicing motif that can be universally targeted. Each mutation may have to be treated individually, assessing the best motifs on an exon to exon basis.

Declaration

I certify that this thesis does not, to the best of my knowledge and belief:

(i) incorporate without acknowledgment any material previously submitted for a degree or diploma in any institution of higher education;

(ii) contain any material published or written by another person except where due reference is made in the text; or

(iii) contain any defamatory material.

I also grant permission for the Library at Edith Cowan University to make duplicate copies of my thesis as required

Signature: _____

Date: 21/10/2004

Acknowledgements

Many thanks to my supervisors, Associate Professor Steve Wilton and Dr Sue Fletcher. It has been a privilege to learn from you both. Your guidance and support as well as your motivation and commitment to scientific endeavour during the course of this project was greatly appreciated. Additionally, your tireless efforts on behalf of the boys and their families are inspirational and I feel fortunate to have been able to contribute to this vital research. Lastly, thank you for the opportunities to attend the conferences in Pittsburgh, Vancouver and Brisbane.

To my principal supervisor at Edith Cowan University, Professor Alan Bittles, I also express my sincere thanks for your support and level-headed advice throughout the course of this degree.

Christo Mann, you taught me almost all the protocols used in this study and much much more. Your patient and generous nature was a wonderful example. Thankyou for your crazy humour and continual support and friendship.

To the rest of the Gene Therapy group, Kaite Honeyman, David Martino, Graham McClorey, Bijanka Gebski and Meina Lee, I wish to express my gratitude for the help and friendship you have shown me over the last few years. You have each played important roles as colleagues and friends during this time and I am very grateful to have shared this time with you.

To the girls downstairs, Rachael, Tina and Kate, as well as the "gang of four" Mark, Penny, Marissa and Claire, many thanks for the friendship and assistance you have provided during the course of my research.

I have left until last my family and friends, without whom this thesis would not have been possible. Thankyou mostly to my wonderful wife Hannah for your tireless support and encouragement throughout the course of this project.

List of Figures

List of Tables

Abbreviations

2'OMeAO	2'-O-methyl (chemical modification to antisense oligonucleotides).
A	Adenosine
AAV	Adeno-associated virus
AO	Antisense oligonucleotide
AV	Adenovirus
BFGF	Bovine fetal growth factor
BMD	Becker muscular dystrophy
bp	Base pairs
C	Cytosine
CEE	Chick embryo extract
CFTR	Cystic fibrosis transmembrane conductance regulator
CM	Minimum effective concentration
C50	Concentration of 50nM
CO	Chimeric oligonucleotides
DMD	Duchenne muscular dystrophy
DMEM	Dulbecco's modification of Eagle's medium
DMSO	Dimethyl sulphoxide
DNA	Deoxyribonucleic acid
dNTP	Deoxynucleotide triphosphate
DOTAP	N-[1-(2,3-dioleoyloxy]-N, N, N-trimethylammonium propane methylsulphate
DOPE	dioleoyl phosphatidylethanolamine
dpi	dots per inch
DTT	Dithiothreitol
EDTA	Ethylenediamine tetra acetic acid
ERS	Exon recognition sequence
ESE	Exonic splicing enhancer
FCS	Fetal calf serum
FITC	Fluorescein isothiocyanate
G	Guanosine
g	Gram

GRMD	Golden retriever muscular dystrophy
H-2K	*H-2K*^{b}-tsA58 (either normal, *mdx*, or both cell types as indicated)
HDMD	Human Duchenne muscular dystrophy
HIV-1	Human immunodeficiency virus
HS	Horse serum
HSV	Herpes simplex virus
hTERT	Human telomerase reverse transcription
IFN-γ	Interferon gamma
IGF-1	Insulin-like growth factor 1
IV	Intravenous
kb	Kilobases
kDa	Kilodaltons
L	Litre
M	Molar
m	Milli
mRNA	Messenger ribonucleic acid
n	Nano
nNOS	Neuronal nitric oxide synthase
NO	Nitric oxide
ODN	Oligodeoxynucleotide
PBS	Phosphate buffered saline
PCR	Polymerase chain reaction
PEI	Polyethyleneimine
PNA	Peptide nucleic acids
PO	Phosphodiester
PS	Phosphorothioate
Pu	Purine
Py	Pyrimidine
RBA	RNA binding assay
RESCUE-ESE	Relative enhancer and silencer classification by unanimous enrichment
RNA	Ribonucleic acid
RNaseH	Ribonuclease H enzyme

RT	Reverse transcription
snRNP	Small nuclear ribonucleoprotein particles
SR	Serine/arginine rich
SV40	Simian virus 40
T	Thymine
Tag	T antigen (of SV40)
T_m	Annealing temperature
U	Uracil
UV	Ultraviolet
µ	Micro
°C	Degrees Celsius

Table of Contents

Chapter 1 - Introduction

1.1 Duchenne and Becker muscular dystrophy

Duchenne muscular dystrophy (DMD), and the milder allelic Becker muscular dystrophy (BMD), are X-linked recessive muscle wasting disorders caused by mutations in the dystrophin gene (Hoffman, Brown & Kunkel, 1987; Koenig et al., 1989). DMD occurs at a frequency of approximately 1 in 3500 male newborns (Koenig et al., 1987) and life expectancy is typically less than 30 years (Emery, 2002).

The main clinical feature of DMD, muscle weakness, becomes evident early in childhood. Initially, affected boys have difficulty running and climbing stairs, and most require a wheelchair by the age of 12 years. Mental impairment is also a common clinical feature, with approximately 20% of affected boys having IQs under 70 (Emery, 2002). The most common cause of death is pneumonia, compounded by cardiac involvement. Without assisted ventilation, few of those affected live beyond their third decade (Emery, 2002).

BMD has an incidence almost ten times less than DMD (Heald, Anderson, Bushby & Shaw, 1994), with a broad spectrum of phenotypes. Although the distribution of myopathy parallels DMD, the onset and progression of BMD is variable and generally less severe (Emery, 2002), and some affected individuals are virtually asymptomatic (England et al., 1990).

Genomic deletions in the human dystrophin gene account for approximately 60% of the DMD mutations (Koenig et al., 1989), while the remaining cases arise from genomic duplications and nonsense, splicing and missense mutations. Although genetic counselling can reduce the incidence of DMD, an estimated one third of all reported cases arise from *de novo* mutations in the dystrophin gene (Worton, 1992), emphasising the urgent need for an effective treatment for this disorder.

1.2 The dystrophin gene and protein

The dystrophin gene, currently the largest known human gene, consists of 79 exons spanning approximately 2.4 megabases (Hoffman et al., 1987; Roberts, Bobrow & Bentley, 1992b) and undergoes extensive pre-mRNA processing to produce a number

of isoforms (Feener, Koenig & Kunkel, 1989; Sadoulet-Puccio & Kunkel, 1996). The major muscle specific transcript of 14kb (Anderson & Kunkel, 1992) represents only 0.02 to 0.12% of the mRNA in either human or mouse cardiac or skeletal muscle (Chelly, Kaplan, Maire, Gautron & Kahn, 1988). It has been estimated that this transcript requires approximately 16 hours for complete synthesis and is co-transcriptionally spliced, with the 5' end of the transcript spliced before transcription of the 3' end is complete (Tennyson, Klamut & Worton, 1995). Tennyson et al. (1995) suggested that this mechanism may have developed in response to the need to restrict the number of splice sites available by the end of transcription, as a means to maintain splicing fidelity. This is of particular significance considering that the length of the introns, accounting for 99.4% of the sequence in total (Ahn & Kunkel, 1993), requires the precise and orderly splicing of the 79 exons to take place across large physical distances (Tennyson et al., 1995).

The tissue-specific expression of dystrophin isoforms is based on transcriptional control by seven to eight different promoters (Sadoulet-Puccio & Kunkel, 1996; Culligan, Mackey, Finn, Maguire & Ohlendieck, 1998). Three full-length (427kDa) dystrophin isoforms have been confirmed, each controlled by a tissue-specific promoter. The brain dystrophin isoform has been localised in neurons of the cerebral and cerebellar cortices, while the Purkinje-cell isoform is the predominate type found in the cerebellum (Ahn & Kunkel, 1993; Gorecki et al., 1992). The muscle isoform, expressed in skeletal, smooth and cardiac muscle (Bies et al., 1992), has been found to be localised to the muscle plasma membrane and t-tubules, tightly bound to the glycoprotein complex (Hoffman et al., 1987; Zubrzycka-Gaarn et al., 1988). This protein consists of four distinct structural domains - the N-terminal (actin-binding) domain, which connects dystrophin to the subsarcolemmal cytoskeleton, the central rod, which gives the protein elasticity, the cysteine-rich domain, which anchors dystrophin to the extracellular matrix, and the C-terminal domain, which binds to dystrophin-associated proteins (Hoffman et al., 1987; Koenig, Monaco & Kunkel, 1988).

It is thought that one of the primary roles of this isoform is in contributing to muscle fibre stability through mechanical reinforcement and protection of the sarcolemma from membrane stresses during muscle contraction (Petrof, Shrager, Stedman, Kelly & Sweeney, 1993; Vilquin et al., 1998; Zubrzycka-Gaarn, Hutter, Karpati, Klamut & Bulman, 1991). Supporting this hypothesis is the fact that muscles

lacking dystrophin are susceptible to mechanical injury and undergo repeated cycles of necrosis and regeneration, leading to a gradual replacement of muscle by fatty fibrous tissue (Anderson & Kunkel, 1992; Harper et al., 2002). Dystrophin performs this critical role despite amounting to only 0.002% of total muscle protein (Radojevic, Lin & Burgunder, 2000). The localisation of dystrophin to neural and vascular tissues also suggests that there may be vasculogenic or neurogenic components involved in the progressive skeletal muscle pathology observed in DMD (Hoffman et al., 1988).

1.3 Dystrophin mutations and disease severity

The reading frame hypothesis proposed by Monaco, Bertelson, Liechti-Gallati, Moser and Kunkel (1988) suggested that the different phenotypes expressed in DMD and BMD depended on the break-point of the mutation and its effect on the translation of downstream codons. For example, if the sum of the nucleotides within an deleted region was not a multiple of three, the reading frame would not be maintained and the resulting frame-shift would lead to the generation of a premature stop codon. These frameshift mutations (typically resulting in DMD) lead to the premature termination of protein synthesis during translation. Mutations which prevent the synthesis of the carboxyl terminal of dystrophin have been shown to result in a severe phenotype (Prior et al., 1993; Roberts, Coffey, Bobrow & Bentley, 1992a), as both the actin binding and carboxyl termini are required to form functional dystrophin (Buiman, Murphy, Zurzycka-Gaarn, Worton & Ray, 1991).

In contrast, BMD mutations are generally found to be in-frame deletions which maintain the reading frame and termini, resulting in the production of a shorter but semi-functional protein (Monaco et al., 1988; Koenig et al., 1989). It appears that deletions of large portions of the central rod region can be associated with mild BMD phenotypes (England et al., 1990), although there appears to be a threshold effect whereby central in-frame deletions of more than 36 exons result in DMD phenotypes (Fanin et al., 1996).

Depending upon the position and nature of the mutation, BMD patients typically have less severe symptoms with later onset and/or variable progression of muscle degradation (Emery, 2002). From clinical studies on many patients with BMD, there is no doubt that some dystrophin, even if of reduced quantity and quality, can be of significant biological and functional advantage (Anderson & Kunkel, 1992). Examples

include a patient with a deletion of exons 3 to 9 who played competitive badminton and went undiagnosed until his mid 60s (Heald et al., 1994). Another patient had 46% of the dystrophin coding sequence missing and still remained ambulant until 61 years of age (England et al., 1990).

A study by Koenig et al. (1989) reported that the reading frame hypothesis predicted the correct clinical phenotype in approximately 92% of cases. Alternative splicing events which would overcome the effect of the original mutation by restoring the reading frame (Chelly et al., 1988), and very rare missense mutations where crucial binding domains have been corrupted (Prior et al., 1993), could account for the remaining 8% of patients not characterised by Monaco's hypothesis.

1.4 Revertant fibres

The discovery of rare, naturally-occurring dystrophin-positive fibers in DMD patients has led to the possibility of a new genetic therapy for DMD. These revertant fibres occur singly or in clusters and may represent up to 10% of the total muscle fibre population (Sherratt, Vulliamy, Dubowitz, Sewry & Strong, 1993; Uchino et al., 1995). Immunohistochemical staining has identified revertant fibres in the skeletal muscle of up to 50% of DMD patients (Klein et al., 1992; Uchino et al., 1995), as well as the dog (GRMD) and mouse (*mdx*) models of DMD (Hoffman, Morgan, Watkins & Partridge, 1990; Schatzberg et al., 1998; Sherratt et al., 1993). The frequency of revertant fibres has been shown to increase with age and X-irradiation treatment in *mdx* mice (Hoffman et al., 1990).

The natural mechanism by which the original mutation is overcome, resulting in restoration of the reading-frame, remains unclear. Mechanisms proposed to account for the presence of dystrophin in these revertant fibres include secondary somatic genomic mutations and alternative mRNA splicing (Hoffman et al., 1990; Klein et al., 1992; Lu et al., 2000; Wilton, Dye, Blechynden & Laing, 1997). The low frequency and apparent clonal development of revertant fibres seem to support secondary somatic genetic events rather than alternative splicing (Hoffman et al., 1990). It has been reported that such an event, either by deletion or through a mutation affecting a splice site, can remove exons from the dystrophin gene such that the reading frame is restored (Klein et al., 1992; Thanh, Man, Helliwell & Morris, 1995; Winnard, Mendell, Prior, Florence & Burghes, 1995). However, *in situ* hybridisation studies in *mdx* mice using a genomic

probe spanning exon 23 demonstrated that the majority of revertant fibres had not undergone any gross genomic deletions to remove exon 23, supporting some alternative mRNA splicing mechanism (Lu et al., 2000). As there is evidence for both, it is possible that these two main theories explaining the presence of revertant fibres are not mutually exclusive (Dickson, Hill & Graham, 2002; Wilton, Dye & Laing, 1997).

Research using exon-specific antibodies has suggested that revertant fibres skip multiple exons, up to 30 at one time, in order to restore the reading frame (Lu et al., 2000). Although revertant transcripts appear to be translated into at least partially functional 'Becker-like' dystrophin proteins (Lu et al., 2000), there have been conflicting reports as to whether there is a relationship between the presence of revertant fibres and the severity of the DMD phenotype. A study by Nicholson (1993) reported a relationship between the abundance of dystrophin-positive fibres and the age at which independent ambulation was no longer possible. However, a later study failed to find a correlation between the presence of revertant fibres and the clinical course of the disease, citing inter- and intra-individual variability as the probable cause of this discrepancy (Fanin et al., 1995). The authors suggested that the low levels of fibres produced would be likely to limit their functional significance. Nevertheless, the very existence of these fibres represents a rationale for a possible therapeutic approach to reduce the clinical severity of DMD, provided that the frequency of revertants could be raised to biologically significant levels (Sherratt et al., 1993; Wilton, Dye, Blechynden & Laing, 1997).

In addition, the natural occurrence of revertant fibres suggests that an approach which increases the frequency of these fibres may avoid the possibility of triggering an immune response, such as that reported to occur following the introduction of full length dystrophin by gene transfer into dystrophic muscles (Ohtsuka, Udaka, Yamashiro, Yagita & Okumura, 1998). Many of these individuals will not have been exposed to dystrophin previously, except in the form of revertant fibres, and may perceive the introduced protein as a neoantigen (Ferrer, Wells & Wells, 2000). However, targeted exon skipping based on the exons commonly removed in revertant fibre transcripts may result in a less immunogenic product (Lu et al., 2000).

1.5 Pre-mRNA splicing

Pre-mRNA splicing involves the precise excision of introns from the primary gene transcript and the joining of exons to form the mature RNA. This intricate process is catalysed within the spliceosome, a large ribonucleoprotein complex consisting of five small nuclear ribonucleoprotein particles (snRNP), U1, U2, U4, U5 and U6, as well as approximately 80 - 100 non-snRNP proteins (Adams, Rudner & Rio, 1996; Kole & Sazani, 2001).

To ensure that intron cleavage and exon ligation is exact, the consensus splice sites are distinguished by the almost invariant dinucleotides GU at the 5' acceptor site and AG at the 3' donor site of the intron (Shapiro & Senapathy, 1987). In addition, the 3' splice site is associated with an upstream polypyrimidine tract and degenerate branch point motif (Tanaka, Watakabe & Shimura, 1994). The components that initially recognise the splice sites are the U1snRNP, which pairs with the 5' splice site, and the protein factor U2AF, which binds to the polypyrimidine tract within the 3' splice site sequence (Black, 1995). These factors trigger the formation of the spliceosome. Cleavage at the 5' splice site, with ligation of the intron 5' end to an adenosine residue at the branch point, is followed by cleavage at the 3' splice site and ligation of the two exons (Black, 1995). It is thought that the splicing of pre-mRNA transcripts generally occurs in a 5' to 3' direction, although there is evidence to suggest that the splicing of introns may also occur in a non-linear progression (Kessler, Jiang & Chasin, 1993).

Large genes, such as the dystrophin gene contain a high number of exons and very long introns, which presents a challenge to efficient and precise transcription and splicing processes. In some regions, the 5' and 3' splice sites must be correctly paired across large physical distances (200kb or more) while avoiding the inappropriate exclusion of exons (Berget, 1995; Black, 1995; Horowitz & Krainer, 1994).

Positive elements for pre-mRNA splicing include the strength of the 5' and 3' splice sites (determined by how well they conform to the consensus sequences) and the branch point sequence (Chabot, 1996; Dominski & Kole, 1994). However, mRNA contains many "cryptic" sequences which closely resemble the splice site consensus sequences of true splice sites (Black, 1995). Thus, individual splice site strength alone may not be sufficient to account for the high specificity observed in splice site selection, indicating the presence of additional elements involved in exon recognition (Reed, 1996; Watakabe, Tanaka & Shimura, 1993).

Several factors have been suggested to affect the selection of splice sites and subsequent spliceosome assembly, including the spacing of each splicing element (Berget, 1995; Reed, 1996), the length of the exon (Dominski & Kole, 1994) and the order of intron removal, through a change in secondary structure or approximation of protein binding sites (Kessler et al., 1993). These factors may help to explain why cryptic splice sites are not well recognised.

In addition, there is growing evidence that internal exon sequences can efficiently stimulate inclusion of an exon, presumably through recognition by the splicing machinery. These exon splicing enhancers (ESEs) may act by co-operating with, or compensating for, functionally weak splice sites, allowing more efficient recognition of the target exon (Dominski & Kole, 1996; Lam & Hertel, 2002). The terms ERS and ESE have been used interchangeably in the literature, but ESE is now considered a general term for any sequence that promotes exon inclusion during splicing (Xu, Teng & Cooper, 1993), whereas an ERS is defined as a purine-rich ESE (Tanaka et al., 1994). It is important to note, however, that not every purine-rich exon sequence functions as an ERS. For example, it has been reported that purine-rich sequences from three exons of the dystrophin gene (exons 43, 46 and 53) showed varying degrees of splicing enhancer activity ranging from very little (exon 46) to powerful (exon 43), suggesting that each exon in the dystrophin transcript may be subject to the influence of different splicing elements (Ito, Takeshima, Sakamoto, Nakamura & Matsuo, 2001).

The mechanisms by which ESEs enhance exon inclusion remain unclear (Ito et al., 2001). It has been suggested that ESEs form an RNA secondary structure which either directly influences exon selection or improves the accessibility of splicing factors to the binding sites (Watakabe et al., 1993; van Deutekom & van Ommen, 2003). In addition, exonic splicing enhancers serve as binding sites for serine/arginine rich (SR) proteins (Lam & Hertel, 2002; Liu, Zhang & Krainer, 1998), which are thought to interact with the 5' splice site, the U1 snRNP, and the U2AF protein, providing a bridge between the splice sites during splicing (Black, 1995). It is thought that the activity of these bound SR proteins, sequence context and the distance between the ESE and the intron, determines the strength of an ESE (Graveley, Hertel & Maniatis, 1998), although the optimal distance may be protein specific and thus variable between exons (Liu, Chew, Cartegni, Zhang & Krainer, 2000).

In addition to sequences which enhance the inclusion of exons, less well characterised sequences which inhibit splicing, known as exonic or intronic splicing silencers, also exist (Blencowe, 2000; Fairbrother & Chasin, 2000). It is thought that these sequences, which can be either purine or pyrimidine rich, bind a diverse array of proteins and may have a role in suppressing the use of cryptic splice sites, thereby favouring the selection of true splice sites (Fairbrother & Chasin, 2000).

1.6 Animal models of DMD

Animal models, including dystrophin-deficient dogs, mice and cats, play an important role in DMD research by providing genetic and/or biochemical homologues of their human counterparts (Cooper, 1993). Golden Retriever dogs with muscular dystrophy (GRMD) exhibit a similar but more severe phenotype to that seen in DMD (Howell et al., 1998; Valentine et al., 1992). This disorder arises from a point mutation in the acceptor splice site of intron 6 of the GRMD dystrophin gene, resulting in the exclusion of exon 7 from the mRNA (Sharp et al., 1992). Affected dogs have raised serum creatine kinase levels, display progressive muscle atrophy with fatty infiltration (although to a lesser degree than observed in DMD), develop cardiomyopathy, and have a shortened life span, secondary to cardiac and respiratory failure (Nonaka, 1998; Valentine et al., 1992).

The *mdx* mouse commonly serves as an animal model for DMD as it also exhibits an absence of dystrophin in its muscle tissue (Sicinski et al., 1989). The skeletal muscle of *mdx* mice demonstrates dystrophic changes such as muscle fibre necrosis and regeneration, with the diaphragm most severely affected (Nonaka, 1998). In the *mdx* mouse the absence of dystrophin is caused by a nonsense mutation at position 3185 in exon 23 of the dystrophin gene, leading to premature termination of dystrophin synthesis (Sicinski et al., 1989). As a model for DMD, the *mdx* mouse is convenient and economical, but it is limited in its clinical similarity to the human disease. By comparison, the GRMD dog more accurately reflects the human DMD phenotype, but is more difficult and expensive to maintain as a colony (Cooper, 1989). In consideration of these different models, the *mdx* mouse appears most appropriate for DMD laboratory experiments, whereas the GRMD dog may be an essential model for preclinical studies before human trials.

1.7 Therapies for DMD

The objective of most therapeutic approaches to the treatment of DMD is to raise the quantity of functional dystrophin in all dystrophic tissues to clinically significant levels.

Many gene replacement or modification strategies are being tested; however there are numerous technical problems that must be overcome before any of these therapies can be used safely and effectively, as briefly considered below.

1.7.1 Cell-mediated treatment

One approach to the treatment of genetic disorders involving muscle is myoblast transplantation, where mononucleated precursor cells isolated from normal donor tissues are propagated in cell culture before injection into diseased muscle (Coovert & Burghes, 1994; Smythe, Hodgetts & Grounds, 2000). However, transplanted myoblasts have a tendency to remain localised near the injection site, rather than migrating to distant damaged sites (Blau & Springer, 1995). Additionally, implanted myoblasts were shown to have poor survival rates, typically less than 1% (Mendell et al., 1995), with the majority of donor cells failing to survive for more than one hour after injection (Smythe et al., 2000). This poor survival is thought to be caused by immune rejection of the implanted myoblasts (Hodgetts, Spencer & Grounds, 2003).

In another cell-mediated approach, injection of genetically marked bone marrow into damaged muscles of immunodeficient mice revealed that the bone marrow cells are able to undergo myogenic differentiation and contribute to regeneration of the damaged muscle fibres (Ferrari et al., 1998). In another study, it was reported that intravenous injection of either haematopoetic stem cells or muscle-derived stem cells into irradiated *mdx* mice resulted in dystrophin expression in up to 10% of the muscle fibres within an individual mouse. Of the dystrophin-positive fibres, 10 - 30% contained donor nuclei (Gussoni et al., 1999). More recently, stem cells derived from blood vessels (mesoangioblasts) have been demonstrated to reconstitute dystrophin expression following intravenous injection in dystrophic mice (Sampaolesi et al., 2003). This approach may be a promising development in the treatment of DMD, particularly as systemic delivery appears possible, at least within the mouse.

1.7.2 Gene replacement

Gene replacement aims to introduce normal or semi-functional genes into cells which lack the product of that gene (Karpati & Acsadi, 1993). In treating DMD, the main aim has been to supply dystrophin minigenes, consisting of partial or full-length dystrophin cDNAs driven by a suitable promoter, to muscle cells (Acsadi et al., 1991; Ragot et al., 1993). Further development of novel plasmid and viral vectors has allowed greater delivery of cDNAs to skeletal myocytes (reviewed by Fletcher, Wilton & Howell, 2000; Marshall & Leiden, 1998).

Unfortunately, even if gene replacement therapies were developed successfully in skeletal muscle, the absence of the two other major full length dystrophin products found in the brain and heart would still remain a problem (Karpati & Acsadi, 1993). For this reason, and to avoid multiple injections into the muscle to achieve transgene delivery, a systemic delivery system would be advantageous (Hartigan-O'Connor & Chamberlain, 2000). Furthermore, it is possible that not all of the symptoms of DMD can be alleviated by replacement of only the full length dystrophin isoform (Culligan et al., 1998).

1.7.2.1 Non-viral vectors

Non-viral delivery systems, such as cationic liposomes, DNA protein complexes and direct injection of naked plasmid have the advantages of being non-infectious and potentially less immunotoxic when used *in vivo* (reviewed by Fletcher et al., 2000). By comparison with virus-based systems, non-viral vectors are easier to manufacture, allow the delivery of larger inserts and may be particularly suitable for the delivery of oligonucleotides to mammalian cells (reviewed by Romano, Michel, Pacilio & Giordano, 2000). Unfortunately, non-viral vectors have demonstrated low transfection efficiencies (Marshall & Leiden, 1998) and lack target specificity (Romano et al., 2000). Liposome-mediated delivery of plasmid DNA also increases host immune responses compared to naked plasmid DNA (Romano et al., 2000).

The use of plasmid RNA and DNA injected directly into mouse skeletal muscle to modify gene expression was first demonstrated by Wolff and colleagues (Wolff et al., 1990). Subsequent studies in dystrophic muscle used expression plasmids containing 12 kb human dystrophin cDNA or a 6.3 kb BMD-like cDNA. These were directly injected

into *mdx* muscle and gave rise to approximately 1% dystrophin-positive fibres (Acsadi et al., 1991). A similar trial in GRMD dogs yielded dystrophin expression of up to 2.5% of fibres in skeletal muscles injected with plasmid containing a full length dystrophin gene or a dystrophin minigene (Howell et al., 1998). The authors concluded that for gene therapy to be useful as a treatment for DMD, more efficient expression will need to be achieved.

More recent research has aimed to improve efficiency by using an Epstein-Barr virus based plasmid 'minichromosome' injected into *mdx* muscle tissue (Tsukamoto et al., 1999). Over a ten-week period, this resulted in a statistically significant increase in the number of muscle fibres expressing dystrophin, compared with a conventional vector. In addition, the effects of direct intra-muscular injection of a plasmid expressing full-length dystrophin have been assessed in DMD and BMD patients (Romero et al., 2002).

Besides the standard DNA delivery methods discussed, several other innovative 'physical' approaches to enhance gene transfer into muscle have been trialled with varied success. These include muscle electroporation which hyper-permeabilises the myocytes (Vilquin et al., 2001), hyperosmotic pressure (Duchler et al., 2001), high velocity tissue bombardment ('gene-gun') (Zelenin et al., 1997) and ultrasound-mediated microbubble destruction (Frenkel, Chen, Thai, Shohet & Grayburn, 2002). However, a less invasive method of delivery will need to be developed for routine clinical use of plasmid vectors (van Deutekom & van Ommen, 2003).

1.7.2.2 Viral vectors

Retroviral, lentiviral, adenoviral and adeno-associated viral vectors have been employed to increase the efficiency and delivery of DNA transfer, but have been hindered by immunotoxicity and other factors (reviewed by Coovert & Burghes, 1994; Fletcher et al., 2000; Morgan, 1994).

Retroviruses are single-stranded RNA viruses which can efficiently integrate into the host genome, carrying gene products such as the dystrophin minigene, and transduce the host cell by reverse-transcribing their viral RNA (with insert) into DNA (Morgan, 1994). However, as viral insertion is random, the cell genome may be

disrupted, possibly leading to the inactivation of tumour suppressor genes or even induction of the expression of cellular oncogenes (Romano et al., 2000).

Additional limitations include a relatively small payload, as only an insert of approximately 8 kb can be carried, and the fact that most retroviruses require the presence of mitotically active host cells for transfer of the viral load and therefore do not infect mature myofibrils (Coovert & Burghes, 1994; Morgan, 1994). Lentiviruses, while able to transfect both dividing and non-dividing cells, have the disadvantage of being HIV-1 based, and so carry the potential danger of serum conversion to HIV-1 in the patient (Romano et al., 2000).

Adenoviruses are double-stranded DNA viruses which can be rendered replication-defective (Ragot et al., 1993; Romano et al., 2000). These altered viral particles enter the target cell through endocytosis and reside as autonomously replicating episomal units in the nucleus, but are not integrated into the host genome (Coovert & Burghes, 1994). The advantages of adenoviruses are that they can infect non-dividing cells and be prepared in large quantities. Unfortunately, they also have an insert-size limit of approximately 8 kb and, as they do not integrate into the host genome, can only provide transient gene expression (Hauser, Amalfitano, Kumar-Singh, Hauschka & Chamberlain, 1997; Mountain, 2000). Furthermore, they may trigger potent immune and inflammatory responses (Mountain, 2000).

A further development in adenoviral vectors has sought to overcome these limitations by removing all viral coding sequences, producing 'gutless' adenoviruses. This manipulation allowed the accommodation of up to 30 kb of foreign DNA (Kochanek et al., 1996). In addition, the expression of viral proteins is eliminated as all protein coding sequences are removed. The authors proposed that this would reduce the cellular immune response and allow longer-term expression of the transferred gene. A more recent study has reported restoration of functional dystrophin production to *mdx* muscle following single injections of gutted adenoviral vectors carrying full-length dystrophin cassettes (DelloRusso et al., 2002). Only a slight immune response to the injected material was observed.

Adeno-associated viruses (AAV) are single-stranded DNA viruses which can stably integrate into host DNA. One limitation is that they can carry only a small gene load of approximately 4 kb (Romano et al., 2000). Injection of AAV carrying micro-dystrophin gene constructs into dystrophic muscles of *mdx* mice have been reported to reverse the histopathological features of this disease (Fabb, Wells, Serpente

& Dickson, 2002; Harper et al., 2002; Sakamoto et al., 2002). However, substantial immune responses to AAV-delivered transgene products have been observed in dystrophic mice, causing destruction of transduced myofibres (Yuasa et al., 2002). In addition, it has been suggested that despite its apparent ability to prevent ongoing muscle damage, this approach may not be able to fully restore muscle strength (Harper et al., 2002; van Deutekom & van Ommen, 2003).

Several approaches have been attempted in order to yield higher transduction efficiencies with viral vectors. A study by van Deutekom et al. (1998) demonstrated that the use of cardiotoxin to generate a specific myofibre degeneration resulted in markedly higher levels of retroviral, herpes simplex viral, and adenoviral transduction of mature muscle compared to non-regenerating muscle. In addition, streptokinase treatment of myofibres was shown to increase the permeability of the extracellular matrix, resulting in higher levels of herpes simplex viral transduction.

1.7.3 Utrophin upregulation

The utrophin gene, encoding 74 exons spanning over 1Mb of genomic DNA, is widely expressed in many fetal and adult tissues (Pearce et al., 1993) and may be a developmental precursor of dystrophin (Lin & Burgunder, 2000). Studies on utrophin upregulation have been based on the hypothesis that utrophin, a protein which shares over 80% homology with dystrophin (Love, Byth, Tinsley, Blake & Davies, 1993), may offer protection against damage and necrosis in dystrophic muscle (Wilson, Cooper, Dux, Dubowitz & Sewry, 1994). Utrophin is expressed at the membrane surface of immature myotubes and becomes restricted to the neuromuscular junction in mature muscle (Davies, 1997). Utrophin constitutes part of the complex of proteins and glycoproteins which link the basal lamina to the cytoskeleton, providing muscle fibre membrane stability (Radojevic et al., 2000). Utrophin has been detected as sarcolemma staining of muscle cells obtained from DMD patients and *mdx* mice (Davies, 1997), and appears to increase in response to muscle degeneration and regeneration, particularly in DMD muscle (Pearce et al., 1993).

A truncated utrophin transgene, driven by the human skeletal α-actin promoter, was used to generate high level utrophin expression in *mdx* skeletal muscle and diaphragm, preventing development of dystrophic pathology (Tinsley et al., 1996). In addition, adenoviral delivery of mini-utrophin has been demonstrated to restore the

dystrophin-glycoprotein complex and prevent the dystrophic phenotype in animal models of DMD (Cerletti et al., 2003; Wakefield et al., 2000). A higher level of function was achieved, as demonstrated by muscle strength, following the expression of full-length utrophin mRNA in *mdx* mice (Gillis, 2002). In a different approach, overexpression of utrophin in *mdx* diaphragm muscle was stimulated by treatment with nitric oxide donors (Chaubourt et al., 2002). Utrophin upregulation may avoid the potential immune response associated with the delivery of dystrophin to previously dystrophin-deficient tissues (Hartigan-O'Connor & Chamberlain, 2000; van Deutekom & van Ommen, 2003; Wakefield et al, 2000). In addition, no toxic effects were observed following non-specific overexpression of full-length utrophin in a broad range of tissues in the *mdx* mouse (Fisher et al., 2001). Thus this approach remains a promising potential therapy for DMD once suitable compounds to upregulate this gene can be identified.

1.7.4 Genetic therapies

1.7.4.1 Short fragment homologous recombination

The introduction of short fragments (400 - 800 bp) of wild type DNA to the nuclei of mutant cells is thought to result in homologous replacement of the endogenous allele with the wild type counterpart, through utilisation of recombination gene repair (Goncz et al., 2001). In a study by Kapsa et al. (2001) a 603 bp wild-type PCR product was applied to *mdx* muscle cells, with 15 - 20% exhibiting conversion of *mdx* to wild-type transcripts. Despite the high level of gene repair reported, none of the corrected cells were shown to express dystrophin. *In vivo*, only 0.0005% to 0.1% of treated muscle cells exhibited gene repair, again with no expression of dystrophin. The authors attributed the lack of dystrophin expression to the observed drop in cell numbers after transfection, possibly due in part to the transfection agents used (Kapsa et al., 2001). However, it now appears likely that the high levels of correction were an artefact of the assay used for correction (A. Saxena, unpublished observations).

1.7.4.2 Chimeric oligonucleotides

Chimeric oligonucleotides (COs), also known as chimeraplasts, consist of self-complementary DNA and RNA nucleotides arranged in a double-hairpin configuration (Gamper et al., 2000). It is thought that COs with the appropriate sequence can anneal to the target region containing a point mutation. The COs could then act as a template, exploiting the cell's own mismatch repair mechanism, and induce the correction of the mutation (Rando, Disatnik & Zhou, 2000). COs have been shown to correct substitution, deletion and insertion mutations in yeast cells (Liu, Rice & Kmiec, 2001). However, as COs correct only single base mismatches, this approach would not be suitable for the 60% of patients with DMD who have large deletions in the dystrophin gene (Rando et al., 2000).

In a study by Rando et al. (2000), single doses of chimeric RNA/DNA oligonucleotides targeting the point mutation in exon 23 were injected into muscles of *mdx* mice. CO-mediated repair was low, with only 1% - 2% of the muscle fibres in the total muscle staining positive for dystrophin. These fibres were located directly around the needle track and injection site but they represented 10% - 20% of fibres staining positive for CO uptake and subsequent gene correction. It has been suggested that the muscle fibre correction rate must exceed 10 - 20% before this method could become a potential treatment for DMD (Fletcher et al., 2000). Rando and colleagues (2000) suggested that the efficiency of the procedure could have been enhanced by performing multiple injections, increasing the concentration of CO, use of a delivery vector or possibly IV injection. In a later study, the same group demonstrated CO-mediated gene repair in *mdx* muscle precursor cells, indicating that improved persistence of CO-mediated effects may be possible (Bertoni & Rando, 2002). While this approach remains inefficient, the potential for cumulative, more permanent gene correction warrants further optimisation (van Deutekom & van Ommen, 2003).

1.7.4.3 Antisense oligonucleotides

Of the genetic therapies, antisense oligonucleotides (AOs) represent an attractive approach to the regulation of specific gene expression. AOs are single-stranded fragments of nucleic acid approximately 10 - 40 bases in length and are composed of nucleotide sequences complementary to the mRNA or pre-mRNA sense strand

(Lavrovsky, Chen & Roy, 1997). The mechanism by which AOs exert their effect is through Watson-Crick base-pair hybridisation to the target sequence (Agrawal, 1996).

AOs were originally used to inhibit the replication of the Rous sarcoma virus by causing targeted downregulation of the viral mRNA in cell culture (Stephenson & Zamecnik, 1978). Many subsequent studies have investigated AOs as agents for specific downregulation of gene expression in the treatment of viral infections, cancers and inflammatory disorders (Agrawal, 1999; Lebedeva & Stein, 2001; Mercatante, Bortner, Cidlowski & Kole, 2001). This has resulted in the commencement of clinical trials and the approval of the first oligonucleotide drug, Vitravene™, for the treatment of an acquired disease, cytomegalovirus retinitis (Orr, 2001).

The first antisense agents used were unmodified oligodeoxynucleotides (ODNs), which were hampered by rapid degradation in the cellular environment caused by nuclease-mediated hydralisation of the phosphodiester (PO) bond (Seeberger & Caruthers, 1998). Efforts to alleviate these effects by modifying the ODN backbone resulted in the production of the first generation oligonucleotides. Of these, the AOs studied most extensively are the phosphorothioates (PS), where one of the non-bridging oxygen atoms of the PO moiety has been replaced by sulphur (Dias & Stein, 2002; Seeberger & Caruthers, 1998). Compared to the natural PO backbone, this modified linkage greatly enhances resistance to nucleases (Altmann, Cuenoud & Von Matt, 1998; Dias & Stein, 2002), although binding affinity is reduced (Guga, Koziolkiewicz, Okriszek & Stek, 1998).

The mechanisms of action through which AOs modulate gene expression can be divided into two main categories: in the first, duplexes formed by a PS AO and its complementary RNA act as substrates for RNaseH, an ubiquitous enzyme that specifically cleaves the RNA strand of the duplex (Altmann et al., 1998). In the second category, the AO can sterically interfere with pre-mRNA splicing or the translation of protein (Dias & Stein, 2002). However, PS AOs have a disadvantage in biological systems, as they tend toward non-specific protein binding, which may result in significant non-antisense side effects (Altmann et al., 1998; Crooke & Bennett, 1996).

Further attempts to ameliorate these side effects and enhance both binding affinity and nuclease resistance led to the development of AOs with a wide variety of ribose modifications, one of which includes the addition of a methyl group at the 2'-O position (Seeberger & Caruthers, 1998). Modifications at this position of the sugar molecule produces an oligonucleotide that resembles RNA more than DNA. This

increases the stability of the AO and allows the 2'-O-methyl antisense oligonucleotide (2'OMeAO) to hybridise to its complementary RNA target sequence without inciting RNaseH degradation of the resulting duplex (Lavrovsky et al., 1997).

1.7.4.3.1 Antisense oligonucleotides as modulators of splicing

In addition to downregulating gene expression, 2'OMeAOs have been shown to have potential in restoring the expression of genes inactivated by aberrant splicing mutations (Dominski & Kole, 1993; Sierakowska, Sambade, Agrawal & Kole, 1996). The requirements of 2'OMeAOs for splicing modification differ from those which aim to downregulate gene expression, in that the activation of RNaseH should be avoided (Sazani & Kole, 2003). In addition, the AOs must be able to effectively displace the splicing factors required for the normal processing of the pre-mRNA within the cell nucleus (Sazani & Kole, 2003). Possible pre-mRNA targets for 2'OMeAO hybridisation include the consensus splice sites, branch point sequence and internal exon sequences (Dunckley, Manohoran, Villiet, Eperon & Dickson, 1998; Mann et al., 2001; van Deutekom & van Ommen, 2003).

Modification of pre-mRNA splicing by 2'OMeAOs was initially demonstrated by Kole and colleagues in the β-globin gene, mutations of which result in β-thalassemia (Dominski & Kole, 1993). 2'OMeAOs were targeted to cryptic splice sites activated by intronic mutations, forcing the utilisation of the correct splice sites and restoring β-globin expression. Several other targets, including the CFTR gene and the Tau gene (reviewed in Sazani & Kole, 2003) have been found to be amenable to 2'OMeAO-mediated modification. Additionally, 2'OMeAOs have been applied to dystrophic cell lines carrying frame-shifting mutations (Aartsma-Rus et al., 2003; Dunckley et al. 1998; Mann et al., 2001; Pramono et al. 1996; van Deutekom et al., 2001; Wilton et al. 1999).

1.7.4.3.2 Antisense oligonucleotides and DMD

In 1990, Matsuo and colleagues described a patient with an intra-exon deletion of 52bp in exon 19 of the dystrophin gene which resulted in an out-of-frame mutation with a subsequent DMD phenotype (Matsuo et al., 1990). This mutation, despite the retention of the consensus splice sites, prevented correct exon 19 definition so that the

entire exon was excluded during processing, leading these researchers to believe that the deleted sequence of exon 19 contained a cis-acting element (i.e. an ESE) essential for accurate splicing of the flanking introns (Matsuo et al., 1991). Subsequently, a 31-mer 2'OMeAO complementary to the 5' region of the deleted sequence in dystrophin Kobe exon 19 was demonstrated to inhibit pre-mRNA splicing in a mini-gene in a dose- and time-dependent manner. It was noted that splicing efficiency was proportional to the number of polypurine stretches in exon 19, supporting the notion that these stretches are important for exon recognition (Takeshima, Nishio, Sakamoto, Nakamura and Matsuo, 1995). Additional studies by the same group induced highly efficient and specific skipping of dystrophin Kobe exon 19 in normal human lymphoblastoid cells by directing a 31-mer antisense oligodeoxynucleotide to the ESE of exon 19 (Pramono et al., 1996).

It has been suggested that targeting the DMD gene transcript to remove an exon containing a disease-causing nonsense mutation, or removing one or more exons flanking a deletion to restore the reading frame, should minimise the consequences of the dystrophin mutation. In this manner, the DMD gene is processed to produce an in-frame BMD-like mRNA with subsequent reading frame restoration (Matsuo, 1996; Wilton et al., 1999). This principle was demonstrated in *mdx* mice, with consistent and efficient 2'OMeAO-induced skipping of exon 23 by targeting the 5' splice site of intron 23 (Wilton et al., 1999). This re-directed processing of the pre-mRNA, such that the nonsense mutation in exon 23 was removed. Skipping of exon 23 did not disrupt the reading frame and near full length dystrophin was detected in 2'OMeAO-treated *mdx* cells and muscle (Mann et al., 2001). However, it was observed that these 2'OMeAOs also induced the sporadic removal of an adjacent exon, suggesting a potential lack of specificity or that the splicing of exons 22 and 23 are intimately linked (Mann et al., 2001; Wilton et al., 1999). A more recent study by the same group reported improvements to the design of the 2'OMeAOs, resulting in increased efficiency of exon skipping. 2'OMeAOs targeted to the 5' splice site, extending further into intron 23, induced greater levels of protein synthesis than previously reported (Mann, Honeyman, McClorey, Fletcher & Wilton, 2002). It was demonstrated that refining the region targeted by 2'OMeAOs could lead to detection of 2'OMeAO-induced mRNA transcripts in cell culture at transfection doses as low as 5nM.

In 2001, van Deutekom and colleagues applied 2'OMeAOs to a polypurine-rich sequence in dystrophin exon 46 and induced the precise excision of that exon from

dystrophin pre-mRNA in normal human cells. These AOs were then successfully applied to myotubes derived from a DMD patient with an exon 45 deletion, to restore the reading frame in that particular defective dystrophin transcript. The authors proposed that the specific skipping of exon 46 after targeting the ESE indicated that these motifs may be more efficient targets than the splice sites for precise exon skipping (van Deutekom et al., 2001). Subsequent studies by this group demonstrated the broad therapeutic potential of 2'OMeAOs. The individual skipping of an additional 11 dystrophin exons were induced by 2'OMeAOs in cultured normal human muscle cells (Aartsma-Rus et al., 2002). The authors suggested that the targeted skipping of one particular exon could be applied to a series of different mutations in order to restore the reading frame. This approach was then demonstrated in cultured muscle cells from DMD patients exhibiting a variety of mutations (Aartsma-Rus et al., 2003). In each case, the skipping of the exon required to restore the reading frame was induced, restoring dystrophin synthesis in over 75% of cells.

A limitation in these studies was the transient nature of dystrophin expression, which would necessitate periodic administration of the 2'OMeAO. An alternative approach to 2'OMeAO delivery was to achieve a more permanent bypass of a mutation in the dystrophin gene (De Angelis et al., 2002). Antisense sequences, targeting both the 5' and 3' splice sites of exon 51, were cloned into small nuclear RNAs (snRNAs) and delivered into human muscle cells by a recombinant virus. It is thought that these snRNPs would stably and efficiently produce the antisense sequences, leading to a more permanent antisense effect and reducing the need for repeated delivery. As the human cells were from a patient with an exon 48 to 50 deletion, the reading frame was effectively restored, resulting in dystrophin synthesis as demonstrated by Western blotting (De Angelis et al., 2002).

Although considerable advances in this field have been made, several parameters, including choice of target sequence, antisense drug design and safe and efficient delivery require further optimisation, with the ultimate aim of restoring dystrophin synthesis to therapeutic levels in all affected tissues (van Deutekom & van Ommen, 2003).

Chapter 2 - Materials

2.1 Cell lines

2.1.1 Mouse cells

Two conditionally immortal mouse cell lines were used in this project, *H-2K* normal and *H-2K mdx*. Both cell lines were derived from *H-2K*^{b}-tsA58 transgenic mice carrying a thermolabile T antigen (Jat et al. 1991; Morgan et al., 1994). These mice harbour a temperature sensitive (tsA58) strain of the immortalising simian virus 40 (SV40) large tumour antigen (Tag) under the control of a mouse major histocompatability complex *H-2K*^{b} class I promoter. This promoter is active in a broad range of tissues and acts to control the expression of the transgene. *H-2K* cells remain in a proliferative phase while exposed to high serum concentrations and the cytokine interferon-gamma and incubation at a constant 33°C. Increasing the cell culture temperature to 37°C inactivates the tsA58 Tag gene product, thus removing its immortalising function. Furthermore, exposure to low serum media stimulates terminal cell differentiation (Jat et al. 1991; Morgan et al., 1994).

2.1.2 Human cells

2.1.2.1 Primary human cells

Quadriceps muscle biopsies were obtained after informed consent from patients undergoing screening for susceptibility to general anaesthesia-induced malignant hyperthermia. The procedure was performed at Royal Perth Hospital, Western Australia from where the biopsy remnants were transported in ice to the laboratory and immediately subjected to enzymatic disassociation. All initial culturing of the primary human myoblasts was performed by Dr Sue Fletcher (Experimental Molecular Medicine Group) according to the protocol of Rando and Blau (1994).

2.1.2.2 Immortalised HDMD cells

The immortalised human DMD (HDMD) cell line was generously provided by Professor Jacques Tremblay (Université Laval, Quebec, Canada). These cells were initially obtained from a DMD patient with a deletion of dystrophin exons 46 to 51 inclusive. Immortalisation of the HDMD cells required subsequent transfection with two retroviruses. To delay senescence in these cells, they were first transfected with a retrovirus containing the SV40 large T antigen (Tag). After approximately 25 doublings, DMD-Tag, a clone of the transformed cells, was then infected with the human telomerase reverse transcription (hTERT) subunit retrovirus to activate telomerase, allowing the DMD-Tag cells to escape crisis and form the DMD-Tag-hTERT cell line (Seigneurin-Venin, Bernard & Tremblay, 2000).

2.2 Reagents and Suppliers

Reagent	Supplier
2'-O- methylated antisense oligonucleotides	Geneworks and CNND
40% acrylamide/Bis solution 19:1 (2.6% C)	Bio-Rad Laboratories
40% acrylamide/Bis solution 37.5:1 (2.6% C)	Bio-Rad Laboratories
Acetic acid, glacial (CH_3COOH)	BDH Laboratory Supplies
Acrylamide/Bis solution (40%, 37.5:1)	BioRad
Agarose (molecular biology grade)	Scientifix
Agarose, low melting point (LMP)	Promega
Ammonium persulphate (APS)	Sigma
Amphotericin B	Sigma
Baxter sterile water	Baxter Healthcare
Big Dye Terminator Sequencing Mix (Version 3.1)	ABI
Bovine fetal growth factor (BFGF)	Roche
Bromophenol Blue/Xylene Cyanol dye solution	Sigma

Reagent	Supplier
C. therm. Polymerase One-step RT-PCR system	Roche
Calcium chloride	BDH
Chick embryo extract (CEE)	Invitrogen
Chloroform	Sigma
Collagenase (grade II)	Invitrogen
Dimethyl sulphoxide (DMSO)	Sigma
Di-potassium hydrogen phosphate	Sigma
Di-sodium hydrogen orthophosphate dihydrate	BDH
Di-sodium hydrogen phosphate	Sigma
dNTPs	Promega
DOTAP	Biontex
Dulbecco's modified Eagle's Medium (DMEM)	Invitrogen
Ethanol	Merck
Ethidium bromide	Sigma
Ethylenediamine tetra acetic acid (EDTA)	Sigma
ExGen 500 (PEI)	MBI Fermentas
Fetal Calf Serum (FCS), heat inactivated	Invitrogen
Formamide	Sigma
Fungizone	Sigma
Glycerol	Sigma
Glycine	Sigma
HAMS's F10	Invitrogen
Horse Serum (HS), heat inactivated	Invitrogen
Hydrochloric acid	BDH Laboratory Supplies
Interferon-gamma (IFN-γ)	Roche Molecular Biochemicals
Isopropanol	Sigma
Lipofectamine 2000	Invitrogen

Reagent	Supplier
Lipofectin	Invitrogen
Matrigel	Becton Dickinson
Methanol	Selby Scientific
Mineral oil	Sigma
Molecular weight marker (100bp ladder)	Geneworks
Opti-MEM (Reduced Serum Media)	Invitrogen
PCR primers (sequencing grade)	Geneworks
Penicillin / Streptavidin solution	Sigma
Poly-D-Lysine, hydrobromide	Sigma
Potassium chloride (KCl)	Sigma
Potassium dihydrogen phosphate (KH_2PO_4)	Ajax Chemicals
QIAquick PCR Purification Columns	Qiagen
RNA-Bee (RNazol B)	Tel-Test
rNTPs	Promega
Sodium acetate, anhydrous (CH_3COONa)	BDH
Sodium bicarbonate ($NaHCO_3$)	Sigma
Sodium chloride (NaCl)	Sigma
Sodium hydroxide (NaOH)	APS Finechemicals
Sodium phosphate (Na_2PO_4)	Sigma
Streptomycin	Sigma
SyBr Gold	BioScientific Pty Ltd.
TEMED (N,N,N',N'-tetramethylethylenediamine)	Sigma
Titan One Tube RT-PCR System	Roche Molecular Biochemicals
Trypan blue	Sigma
Trypsin (lyophilised)	Invitrogen
Trypsin-EDTA solution (0.5% trypsin, 5.3mM EDTA)	Invitrogen
Tth Plus DNA polymerase	Fisher Biotech

Reagent	Supplier
Urea (CH_4N_2O)	Eastman Kodak
Versene	Life Technologies
Xylene	Rowe Scientific

Chapter 3 - Methods

3.1 Cell culture

3.1.1 Resurrection of cells

Stocks of cells were stored frozen as 1mL aliquots in liquid nitrogen until required. Each stock vial contained ~5 x 10^4 cells. Resurrection of a vial of cells was performed as quickly as possible to limit the amount of time the cells are exposed to DMSO, the cryopreservation agent. When DMSO reaches temperatures above 0°C, it exerts a toxic effect on the cells. Under sterile conditions in a laminar flow biological cabinet, the vial of cells was rapidly thawed by the dropwise addition of pre-warmed 10% HS, DMEM or 10% HS HAM's F10 according to the cell type (Table 3.1). As the cells thawed they were removed from the vial and placed into 9mL of the warm medium and then pelleted by centrifugation at ~3 000 x g for 5 minutes in a MSE Minor centrifuge. The supernatant was then removed and discarded and the pellet resuspended in 10mL of the relevant proliferative medium (Table 3.1) containing antibacterial and fungicidal agents. The final cell suspension was then transferred into a 75cm^2 flask pre-coated with 100µg/mL Matrigel solution. Incubation conditions for proliferation were dependant on the particular cell type. Both the primary human and HDMD cell lines were proliferated at 37°C and 5% CO_2 / 95% air atmosphere in a Sanyo MCO 17A model incubator. Proliferation of the H2K cell lines required the addition of 20µL (20 units/mL) interferon gamma (IFNγ) to the 10mL cell suspension and then incubation at 33°C and 10% CO_2 air atmosphere in a Sanyo MCO 17A model incubator. All cultures were checked daily and the media changed every second day.

Table 3.1 Culture medium for mouse and human cells.

Cell type	Resurrection	Proliferation	Differentiation	Cryopreservation
H2K normal and *mdx* mouse	DMEM 10% HS p/s/f	DMEM 20% FCS 10% HS 0.5% CEE p/s/f IFN-γ	DMEM 5% HS p/s/f	DMEM 10% HS p/s/f
Primary and DMD human	HAM's F10 10% HS p/s/f	HAM's F10 20% FCS 10% HS 0.5% CEE p/s/f BFGF (HDMD cells only)	DMEM 5% HS p/s/f	HAM's F10 10% HS p/s/f

Key DMEM - Dulbecco's Modified Eagle's Medium (Invitrogen)
HAMs F10 - (Invitrogen)
FCS - Fetal Calf Serum (Invitrogen)
CEE - Chick Embryo Extract (Invitrogen)
HS - Horse Serum (Invitrogen)
IFN-γ - Interferon-gamma (Roche Molecular Biochemicals)
BFGF - Bovine fetal growth factor (Roche Molecular Biochemicals)
p/s/f - antibacterial agents Penicillin and Streptavidin in combination (Sigma)
- fungicidal agent, Fungizone(Sigma)

3.1.2 Seeding cells onto plates and dishes

When the proliferating cells reached ~70% confluency in the flask (typically 3-4 days), they were deemed ready for splitting and seeding into plates or dishes. This process was identical in all respects regardless of the cell type. All medium was warmed to ~37°C prior to use to protect the cells from any temperature differential.

Firstly, the proliferation medium was removed and the cells were washed twice with sterile PBS to remove the serum proteins and antiproteases which inhibit the trypsin. Then 4mL of trypsin was added to the flask and a gentle 2-3 minutes of agitation applied to augment detachment of the cells, which was verified microscopically, from the matrigel basement. The reaction was halted by the addition of

6 mL of 10% HS DMEM at which time the 10mL cell suspension was transferred to a 15mL Falcon tube and pelleted by centrifugation at ~3 000 x g for 5 minutes in a MSE Minor centrifuge. The supernatant was removed and discarded and the pellet thoroughly resuspended by pipetting in 1mL of 5% HS DMEM (differentiation) media containing antibacterial and fungicidal agents (Table 3.1).

From the cell suspension, 10μL was removed and mixed with trypan blue. The size of the cell pellet determined the volume of trypan blue used. Typically, 40-70μL would be sufficient to afford a satisfactory dilution and ensure an accurate representation of the total cell number. Ten microlitres of the trypan blue-cell mixture was then applied to a Neubauer haemocytometer and a cell count determined microscopically. Dead or injured cells, which take up the blue dye, were deemed not viable and therefore not included in the final total. The count was obtained by averaging the number of cells observed in four squares of the counting chamber. The concentration of cells/mL was derived using the formula:

$$\text{F1:} \quad \frac{\text{Number of viable cells in four squares}}{4} \times \text{dilution factor} \times 1 \times 10^4 = \text{cells / mL}$$

The multiplication constant $1x10^4$ is derived from the volume of each square, 0.1 mm deep and 1 x 1 mm in area, equating to $0.1mm^3$ (10^{-4}mL).

All vessels were seeded at a final cell density of 2×10^4 cells/$1.88mm^2$ which equates to the growth area of a single well in a 24 well plate. The number of cells/mL obtained from F1 was then divided by the total number of cells required to seed the vessel chosen as seen in F2, an example for a 24 well plate:

$$\text{F2:} \quad \frac{\text{cells / mL}}{24 \text{ wells} \times 2 \times 10^4 \text{ cells / well}} = \text{mL of cells removed and added to 12mL medium}$$

The 12mL of differentiation medium (Table 3.1) is calculated by the number of wells (24) multiplied by 500μL, the standard growth volume for a single well.

Prior to seeding, 50μg/mL poly-D-lysine was applied to the growth area of the plate and allowed to remain at room temperature for 1 hour before its removal and replacement with 100μg/mL Matrigel solution. This coating was incubated for ~1 hour at 37°C and the surplus removed immediately prior to seeding the trypsinised cells.

Typically, all remaining immortalised cells were returned to the flask for further proliferation and cultures were discarded after 3-4 passages to ensure the low level of non-myogenic cell types was kept to a minimum. Primary human cells that remained after the first trypsinisation were generally only passaged a second time before they were discarded.

3.1.3 Cryopreserving cells

To maintain cell stocks, low passage cultures were proliferated in a flask to ~70% confluency and then trypsinised as described in Section 3.1.2. After centrifugation, the medium was removed and the cells were diluted to a concentration of ~50 x 10^4 cells/mL in cold 10% HS DMEM or 10% HS HAM's F10 (Table 3.1). The agent DMSO was then added to a final concentration of 10% and the cell solution mixed thoroughly. Finally, 1mL of cell solution was quickly added to each sterile screw cap cryogenic tube. The tubes were placed into a pre-chilled (-20°C) controlled cooling chamber which was adjusted to -80°C for ~24 hours, after which time they were placed into liquid nitrogen for long term storage.

3.2 Transfection of cells

3.2.1 Transfection reagent comparison - nuclear fluorescence study

Transfection reagents are used to augment the transportation of the 2'OMeAOs into the cell nucleus, as this is where post-transcriptional processing occurs. Because several different cell lines were to be used in the transfection studies, it was necessary to determine the most suitable transfection reagent for each cell line.

Initially, a transfection reagent was tested in each cell line using M23D(+12-08)-FITC, a 5' fluorescein isothiocyanate (FITC)-labelled 2'OMeAO. M23D(+12-08)-FITC was based on a previously reported 2'OMeAO (without FITC) which was shown to induce skipping of exon 23 in the dystrophin gene in cultured C2C12 and primary mouse *mdx* myoblasts (Wilton et al., 1999). The addition of the fluorescein tag provided the opportunity to assess the ability of the transfection reagent to carry the 2'OMeAO into the cell cytoplasm and facilitate its nuclear uptake. Additionally, comparisons could be made to previously reported studies utilising

fluorescently labelled 2'OMeAOs in both mouse and human muscle cells (Dunckley et al., 1998; van Deutekom et al., 2001).

Each transfected well received 1µg (~266nM) of M23D(+12-08)-FITC complexed with one of the three transfection reagents assessed in this study, according to the protocols described below. The optimal ratios of carrier to M23D(+12-08)-FITC were determined by titrating the volume of transfection reagent against the standard 1µg of M23D(+12-08)-FITC. Nuclear fluorescence was evaluated at three or 24 hours post-transfection. The three hour time point was chosen, as this was when all transfecting complexes would typically be removed from the cells and replaced by differentiative medium. This would provide information about the efficiency of the reagent to complex with the M23D(+12-08)-FITC and then infiltrate the cell membrane within the three hour transfection period. The 24 hour time point was assessed as total RNA would be extracted from the cells in order to assay for any mRNA modification 24 hours following transfection. It was at this point that further localisation and persistence inside the nucleus of M23D(+12-08)-FITC could be evaluated.

3.2.1.1 Cell fixation

Cell fixation at both time points was identical. Three hours post-transfection, the medium in wells to be viewed 24 hours post-transfection was replaced with the relevant differentiative medium. In contrast, the short term wells were rinsed twice with PBS which was then removed before the addition of ice cold methanol. This was removed 60 seconds later and the cells allowed to air dry for 60 seconds before 500µL of PBS was added. Cells were visualised with an Olympus IX70 inverted microscope equipped with a U-RFL-T fluorescent burner. M23D(+12-08)-FITC was excited with a WB cube and the digital images were captured by an Olympus DP11 camera. The images were processed using the Adobe Photoshop 6.0 (for Macintosh) software.

Based on the results from each transfection, the optimal carrier and hence ratio of carrier to 2'OMeAO was established and adhered to throughout the project. For *H-2K* mouse cells and primary human cells, Lipofectin provided the maximum transfection with the minimal degree of cell loss. ExGen 500 however, was trialled late in the project as a potential 2'OMeAO carrier into the primary human cells to reproduce conditions reported by van Deutekom et al. (2001). This transfection agent was subsequently found to be less effective. Lipofectamine 2000 was found to be the best 2'OMeAO-delivery

agent for the transformed human DMD cell line. The protocol for transfection with each reagent, detailed below, is designed for duplicate well transfection in a 24 well plate.

3.2.2 Transfection reagents

3.2.2.1 Lipofectin

The optimal ratio was determined to be 2:1 (w:w) of Lipofectin to 2'OMeAO, within the range suggested by the manufacturer. Transfection was performed 72 hours after seeding to allow the myoblasts sufficient time to differentiate and form multinucleate myotubes.

Lipofectin and 2'OMeAO were diluted as two separate solutions each in 100µL of Opti-MEM. Lipofectin was incubated at room temperature for 45 minutes before being gently mixed with the 2'OMeAO and then incubated for a further 15 minutes at room temperature to allow the complexes to form and equilibrate. The final 1mL volume was made up by the addition of 800µL of Opti-MEM. The transfection medium was then gently mixed to ensure homogenicity before 500µL was added to each well. The cells were incubated at 37°C and 5% CO_2 / 95% air atmosphere for three hours, after which the transfection medium was replaced with 5% HS DMEM differentiative medium.

3.2.2.2 ExGen 500

ExGen 500 is the registered name for PEI (polyethyleneimine) and it was selected due to its reportedly low toxic effect and high efficiency of DNA delivery in human cells. Differentiation of the primary human myoblasts appeared to be slower than the mouse cells and so transfection of multinucleate myotubes was performed four days and 12 days following seeding in the exon 19 and exon 46 studies respectively. According to the nuclear accumulation of fluorescence in the preliminary study, 3.5 equivalents was observed to be optimal and was comparable to other reports (Dunckley et al., 1998; van Deutekom et al., 2001).

Transfection medium was prepared by diluting the 2'OMeAO in 150mM NaCl to a final volume of 100µL. PEI was then added to the mixture and immediately vortexed for 5 seconds, briefly centrifuged to gather the solution, and incubated at room

temperature for 15 minutes. The final 1mL volume was made up by the addition of 900µL of Opti-MEM, which was mixed by pipetting up and down before 500µL was added to each well. The cells were incubated at 37°C and 5% CO_2 / 95% air atmosphere for three hours after which the transfection medium was replaced with 5% HS DMEM differentiative medium.

3.2.2.3 Lipofectamine 2000

The optimal ratio was determined to be 3:1 (w:w) of Lipofectamine 2000 to 2'OMeAO which is within the range of 1:1 to 5:1 suggested by the manufacturer. Lipofectamine 2000 caused significant cell death when delivered to the mouse myotubes at ratios greater than 1:1 and with no greater nuclear uptake of the FITC-2'OMeAO complex. No toxic effect was observed in the case of the HDMD cells at the 3:1 ratio. However, presumably due to the immortalising process, these cells appear to be arrested in a mitotic state and most cells did not differentiate into mature myotubes. Therefore myoblast transfection was performed 72 hours post-trypsinisation.

Lipofectamine 2000 and 2'OMeAO were diluted as two separate solutions each in 100µL of Opti-MEM. Lipofectamine 2000 was incubated at room temperature for 15 minutes before being gently mixed with the 2'OMeAO and then incubated for a further 20 minutes at room temperature to allow the complexes to form and equilibrate. The final 1mL volume was made up by the addition of 800µL of Opti-MEM. The transfection medium was then gently mixed to ensure homogenicity before 500µL was added to both wells. The cells were incubated at 37°C and 5% CO_2 / 95% air atmosphere for 3 hours, after which the transfection medium was replaced with 5% HS DMEM differentiation medium.

3.3 Antisense Oligonucleotides

3.3.1 Nomenclature

During the course of this project, a nomenclature system was proposed by our laboratory as a means to identify the specific target to which a particular AO bearing that name was directed (Mann et al., 2002). This nomenclature provides information about the species in which the testing is undertaken, the exon at which the 2'OMeAO is directed and the exact annealing position (and hence length) relative to the acceptor or donor splice sites (Figure 3.1).

An addition to the published nomenclature is the prefix 'd' which was adopted only in this project. This prefix served to distinguish between PCR-grade DNA oligonucleotides (deoxy-AO) and the 2'-O-methylated RNA-like oligonucleotides with a full phosphorothioate backbone (2'OMeAOs) that were both directed at the same sequence.

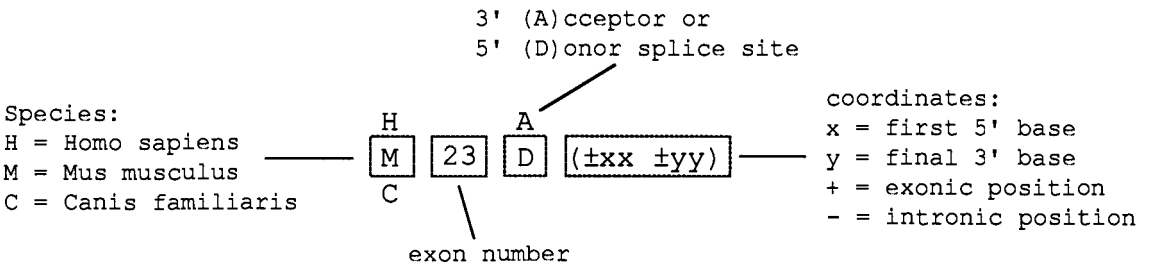

Figure 3.1 Schematic representation of 2'OMeAO nomenclature. Detailed is the systematic way in which all 2'OMeAOs were classified in this project. Note also that regions between species that bear 100% sequence homology are also acknowledged in the 2'OMeAO names' prefix ie. HM19A(+46+65) is directed at a wholly exonic sequence within both human and mouse exon 19. Figure taken with permission from Mann et al., 2002.

3.3.2 Antisense oligonucleotide design

In this study, all 2'OMeAOs designed to re-direct dystrophin pre-mRNA splicing in mouse or human cells incorporated the phosphorothioate backbone and a methyl group at the 2' hydroxyl position of the ribose moiety. The modified chemistry of the 2'OMeAO affords greater resistance to nuclease degradation within the cellular environment (Altmann et al., 1998), as well as preventing the recognition of the 2'OMeAO:RNA duplex by RNAseH as a target for destruction (Lavrovsky et al., 1997).

Initial experiments in the study were based on the 31mer 2'OMeAO reported by Takeshima et al. (1995), which would be described as HM19A(+35+65) under this nomenclature system. HM19A(+35+65) was directed at a putative exon splicing enhancer (ESE) and was able to induce the specific and effective removal of exon 19 from the mature transcript. Early 2'OMeAOs aimed to refine the 31 base region targeted by HM19A(+35+65). Furthermore, as the acceptor and donor splice sites play a vital role in the splicing process (and hence definition of exon boundaries), these exon 19 splice sites were also examined as potential targets for 2'OMeAO-induced exon removal.

Targeting and comparing each of these three sites formed a significant portion of the project, with the ultimate goal to determine the optimal target for 2'OMeAO-induced exon skipping. Consequently 2'OMeAO design was somewhat empirical in nature, necessitating a trial and error approach to determine the most effective motifs to which 2'OMeAOs should be directed.

Typically, directing 2'OMeAOs of varying lengths within the general confines of the splice sites was sufficient to induce the removal of the targeted exons. However, when this failed, a computational method, RESCUE-ESE (Relative Enhancer and Silencer Classification by Unanimous Enrichment, http://genes.mit.edu/burgelab/rescue-ese/) was employed to predict the likely positions of ESEs within the given sequences (Fairbrother, Yeh, Sharp & Burge, 2002).

3.3.3 Quality assay for 2'OMeAOs

The quality of all 2'OMeAOs used in this study was assessed by gel electrophoresis to confirm a satisfactory standard of synthesis. All exon 19 directed 2'OMeAOs save one, M19D(+02-18), were synthesised by Geneworks, Adelaide, South Australia. The remaining 2'OMeAOs including M19D(+02-18) and those directed at exons 20 to 25 and exon 46 were synthesised 'in-house' on an Expedite 8909 Nucleic Acid Synthesiser (Applied Biosystems) using a 1μmol thioate synthesis protocol.

The quality of each 2'OMeAO was confirmed by first diluting approximately 200ng of 2'OMeAO with 5μL of formamide loading buffer, heating to 94°C for 2min and then snap-chilling on ice. The 2'OMeAOs were then loaded onto a denaturing 20% polyacrylamide (acryl:bis ratio 19:1) TBE gel containing 7M urea and electrophoresed for up to 2 hours at 300V. In addition to the trityl outputs during synthesis, this assay satisfactorily validated the integrity of each 2'OMeAO and further verified the high standard of manufacture of the in-house synthesised 2'OMeAOs as compared to the commercially available molecules. Consequently, all 2'OMeAOs were generally deemed to be of a sufficiently high standard to proceed to cell transfections.

Table 3.2 Sequences of 2'OMeAOs used in this study. Upper and lower case characters represent exonic and intronic nucleotides respectively (silencer sequences abbreviated as Pu and Py (guggcaggguggu and cucucucu respectively) attached to M20D(+04-16) and the random 2'OMeAO are excepted).

Name	Sequence (shown 5' to 3')
HM19A(+35+65)	GCCUGAGCUGAUCUGCUGGCAUCUUGCAGUU
HM19A(+35+54)	UCUGCUGGCAUCUUGCAGUU
HM19A(+46+65)	GCCUGAGCUGAUCUGCUGGC
HM19A(+49+65)	GCCUGAGCUGAUCUGCU
HM19A(+52+65)	GCCUGAGCUGAUCU
HM19A(+32+45)	AUCUUGCAGUUUUC
HM19A(+46+57)	UGAUCUGCUGGC
M19A(-20+05)	AUGGCcugcagcaugagagcaaagg
M19D(+05-20)	aaucaacuucauguaauuacCAUUU
M19D(+02-18)	ucaacuucauguaauuacCA
H19A(-20+10)	GCUCUAUGGCcugcagcaugagagcaaaga
H19D(+10-15)	aacucguguaauuacCAUUCACCAU
Random	ccagaucggacgacgucaggacaaac
M23D(+12-8)-FITC	FITC-cggcuuacCUGAAAUUUU
M20D(+04-16)	aggaggaaaaccuuacCUUA
M20D(+04-16)-Pu	aggaggaaaaccuuacCUUA-guggcaggguggu
M20D(+04-16)-Py	aggaggaaaaccuuacCUUA-cucucucu
Pu-M20D(+04-16)	guggcaggguggu-aggaggaaaaccuuacCUUA
M20D(+08-12)	ggaaaaccuuacCUUACAAA
M20A(+23+47)	GUUCAGUUGUUCUGAAGCUUGUCUG
M20A(+140+164)	AGUAGUUGUCAUCUGUUCCAAUUGU
M21D(+04-16)	aaguguuuuuacuuacUUGU
M22D(+04-16)	ucaaauguccacagacCUGU
M22D(+08-12)	auguccacagacCUGUAAUU
M23D(+02-18)	ggccaaaccucggcuuacCU
M24D(+06-14)	gauacaaaucuuacUCUGCA
M24D(+08-12)	uacaaaucuuacUCUGCAUU
M24A(-10+15)	GGUUUUUAUGUGAUUcuggaauaaa
M24D(+10-15)	agauacaaaucuuacUCUGCAUUGU
M24A(+16+40)	CAACUUCAGCCAUCCAUUUCUGUAA
M24A(+78+102)	GAGCUGUUUUUUCAGGAUUUCAGCA
M25D(+06-14)	uaaacuagucauacCUGGCG
H46A(-07+13)	UUGUUCUUCUAGCcuggaga
H46A(+63+82)	GUUAUCUGCUUCCUCCAACC
H46A(+115+134)	GCUUUUCUUUUAGUUGCUGC
H46D(+02-18)	uugagaaaauaaaauuacCU

3.4 Total RNA preparation

The extraction and purification of total RNA from all cell lines was performed 24 hours post transfection. A cursory microscopic observation of the state of the cells was performed prior to harvesting and a comparison made against the untreated control. Though the subjective nature of the examination does not lend itself to any publishable data, an obvious trend of increased cell death with the highest 2'OMeAO concentration tested (correlating with the largest volume of transfection reagent) was observed.

RNA extraction was conducted under sterile conditions in a laminar flow biological cabinet. The differentiative medium was first removed and to each well of a 24 well plate was added 250µL of RNA Bee, an acid phenol RNA extraction formulation. A pipette tip was then used to disrupt and ensure thorough lysing of the cells. Duplicate wells were pooled to yield a starting volume of 500µL which was placed into a sterile 1.6mL microfuge tube.

To each tube was added 100µL of chloroform. This was vortexed thoroughly before incubation at 4°C for 5 minutes and centrifugation at 14 000 x g for 15 minutes at 4°C in a Beckman-Coulter Microfuge 18 Centrifuge. The resultant upper aqueous layer containing the RNA (250 - 280µL) was carefully removed to avoid disturbance of the interphase, and placed into a fresh RNAse-free 1.6mL tube containing 300µL of isopropanol. Each tube was vortexed thoroughly and incubated for 10 minutes at room temperature before pelleting the RNA by centrifugation at 14 000 x g for 15 minutes at 4°C. The supernatant was then removed and discarded and the pellet thoroughly resuspended in 50 µL of 300mM sodium acetate (pH 5.2) by vortexing, to facilitate removal of carry-over phenol and salts. The samples then each received 125µL of absolute ethanol, were vortexed and then incubated at -80°C for 10 minutes to enhance RNA precipitation before centrifugation at 14 000 x g for 15 minutes at 4°C. The supernatant was removed and the pellet was given a final wash by resuspending in 250µL 75% ethanol before centrifugation at 14 000 x g for 15 minutes at 4°C. After removing the supernatant, the RNA pellet was allowed to air dry at room temperature before thorough resuspension in 50µL of RNAse-free water and storage on ice for immediate use or at –20°C or –80°C for long term storage.

The quality and quantity of RNA samples was assessed by spectrophotometry on a Beckman DU650 spectrophotometer. A 1 in 20 dilution of RNA was prepared by mixing 5µL of RNA in 95µL of water and readings were taken at 260nm and 280nm to

estimate the purity and final yield. If further validation was required, 5μL of RNA was combined with glycerol loading buffer and electrophoresed through a 2% TAE agarose gel at 90V for ~ 2 hours.

3.5 Analysis of dystrophin mRNA

3.5.1 Reverse transcription and PCR amplification

To determine if any modification to the splicing pattern had been induced by the introduction of the antisense molecules, regions flanking the 2'OMeAO target site in dystrophin mRNA were subjected to reverse transcription (RT) with subsequent amplification of the cDNA strand by the polymerase chain reaction (PCR) method. Two RT-PCR systems were used in this project, the Titan One-tube RT-PCR system (Roche) and the *C. therm.* Polymerase One-step RT-PCR system (Roche). Each system contains several enzymes that allow the initial cDNA synthesis from the total RNA strand and then amplification of the region bounded by the sense and antisense cDNA strand primers. The Titan One-tube RT-PCR system was performed in a total reaction volume of 12.5μL and was used predominately throughout the project. The *C. therm.* system was employed only when it was necessary to duplicate conditions reported by van Deutekom et al. (2001) (see Chapter 6), and was performed in a total reaction volume of 20μL. The components of each reaction mix are described below in Tables 3.3 and 3.4, with primer sequences listed in Table 3.5.

Table 3.3 Component composition in a 12.5μL Titan One-tube RT-PCR reaction.

Reaction component	RNA	H_20	Buffer*	dNTP	DTT	Forward primer	Reverse primer	Enzyme mix
Reactant volume (μL)	varied	varied	2.5	0.5	0.625	0.75	0.75	0.25
Reactant final concentration	50ng / reaction	-	1x	200μM	5mM	3ng/μL	3ng/μL	-

* Supplied as a 5x preparation and diluted to yield a final concentration of 1.5mM magnesium chloride.

Table 3.4 Component composition in the 20μL *C. therm.* One-step RT-PCR reaction.

Reaction component	RNA	H_20	Buffer*	dNTP	DTT	DMSO	Forward primer	Reverse primer	RNAzin	Enzyme mix
Reactant volume (μL)	varied	varied	4.0	0.8	1.0	1.0	0.75	0.75	0.2	0.25
Reactant final concentration	50ng / reaction	-	1x	200μM	5mM	7%	3ng/μL	3ng/μL	20U	-

* Supplied as a 5x preparation and diluted to yield a final concentration of 2.5mM magnesium chloride in a single 20μL reaction.

Table 3.5 Forward and reverse primers used in RT-PCR reactions.

Name	Sequence (shown 5' to 3')	DS Number*
M1F	ATGCTTTGGTGGGAAGAAGTAG	2153
M13F	GCTTCAAGAAGATCTAGAACAGGAGC	1736
M17F	TGGAAACGGTAACTATGGTG	1600
H17F	CATGCTCAAGAGGAACTTCC	126
M20F	CAGAATTCTGCCAATTGCTGAG	2616
H42F	CACACTGTCCGTGAAGAAACGATGATG	212
M69F	GCACTTTAATTATGACATCTGCC	2187
M11R	GCTTTGTTTTTCCATGCTAGCTACCCT	JSR43#
M22R	CCTGATGCTACTCATTGTCTCC	2316
H25R	CTGAGTGTTAAGTTCTTTGAG	22
M26R	TTCTTCAGCTTGTGTCATCC	3658
M27R	AGTTCCTTTTTTAAGGCCTC	2494
H48R	CTGAACGTCAAATGGTCCTTC	3540
M79R	CTCTGCCCAAATCATCTGCC	2512

* Laboratory nomenclature; denotes DNA Synthesis number given to each primer (Geneworks).

This primer synthesised on site with an Expedite 8909 Nucleic Acid Synthesiser

The preparation for each RT-PCR reaction was essentially the same for each system. All components were thawed on ice and vortexed briefly before addition to a master mix. This contained sufficient reagent mixture for all RNA samples to be assayed, a negative control for the reaction itself and an 'extra sample'. The master mix was briefly vortexed and then aliquoted into 0.6mL thin walled tubes to await the addition of the RNA template. As standard throughout this project, 50ng of total RNA was added to each reaction mixture, except the reaction negative control which received

water. However, repetition of the conditions reported by van Deutekom et al. (2001) (see Chapter 6) required the addition of RNA to the reaction in amounts ranging from 5ng to 1000ng. The cycling conditions for each reaction are outlined in Tables 3.6 and 3.7.

Table 3.6 Cycling conditions for RT-PCR using the Titan One-tube RT-PCR system. Step 4 to step 6 cycled through 30 times after the initial cDNA strand denaturation.

Step 1	Reactant equilibration	2 minutes	25°C
Step 2	Reverse transcription	30 minutes	48°C
Step 3	Initial denaturation	2 minutes	94°C
Step 4	Subsequent denaturation	30 sec	94°C
Step 5	Primer annealing	1 minute	55°C
Step 6	Strand elongation	2 minutes	72°C

Table 3.7 Cycling conditions for RT-PCR using the *C. therm.* Polymerase One-step RT-PCR system. Step 4 to step 6 cycled through 20 times after the initial cDNA strand denaturation.

Step 1	Reactant equilibration	2 minutes	25°C
Step 2	Reverse transcription	30 minutes	62°C
Step 3	Initial denaturation	2 minutes	94°C
Step 4	Subsequent denaturation	45 sec	94°C
Step 5	Primer annealing	45 sec	60°C
Step 6	Strand elongation	1 minute	72°C

Reactions were performed on either a MJ PTC 100 or MJ Research mini thermal cycler, both equipped with a hot bonnet to provide more even temperature distribution, and eliminate the need for a mineral oil overlay.

3.5.2 Nested PCR amplification

When electrophoresed through a 2% agarose TAE gel as standard, RT-PCR (primary amplification) products were extremely difficult to visualise and hence an evaluation of the 2'OMeAO's ability to modify splicing patterns was difficult. This was not unexpected as dystrophin messenger RNA is reported to represent less than 0.01% of the mRNA in either human or mouse cardiac or skeletal muscle (Hoffman, Brown & Kunkel, 1987). Consequently, a second round of PCR amplification was performed on the primary template using a nested primer set. This ensured adequate representation of the dystrophin mRNA species present and increased the specificity of the reaction. The primer sequences are listed in Table 3.8 and components of the reaction mix are described in Table 3.9.

Table 3.8 Forward and reverse primers used in the nested secondary PCR reactions.

Name	Sequence (shown 5' to 3')	DS Number*
M1F	GTGGGAAGAAGTAGAGGACTG	2153
M17F	TGGAAACGGTAACTATGGTG	1600
H17F	GCAGATTACTGTGGATTCTG	123
M18F	GAAGCTGTATTACAGAGTTCTG	936
M20F	CAGAATTCTGCCAATTGCTGAG	2616
M20F	CCCAGTCTACCACCCTATCAGAGC	1803
M22F	AGTAGCATCAGGACGTGGATCC	2232
H44F	GCGATTTGACAGATCTGTTG	2495
H70F#	CATCAGGAGAAGATGTTCGAGAC	852
M10R	ACATCATTWGAAATCTCTCCTTG	2355
HM21R	GGCCACAAAGTCTGCATCCAG	1889
HM21R	TTGTCTGTAGCTCTTTCTC	2954
M23R	TGGGAGGAAAGTTTCTTCCAGT	1643
M24R	GAAAACATCAACTTCAGCCATCC	2233
H25R	GTCTCAAGTCTCGAAGCAAAC	124
M26R	CCTGCCTTTAAGGCTTCCTT	3657
M27R	CTATTTACAGTCTCAGTAAGG	2264
H47R	TTATCCACTGGAGATTTGTCTG	3540
M79R	CCAAATCATCTGCCATGTGG	405

* Laboratory nomenclature; denotes DNA Synthesis number given to each primer (Geneworks)

\# Human sequence specific primer used to amplify mouse cDNA had 2 mismatches (underlined)

Table 3.9 Component composition in a 50μL secondary nested PCR.

Reaction component	cDNA template	H_20	10x Buffer	dNTP	$MgCl_2$	Forward primer	Reverse primer	Tth plus polymerase
Reactant volume (μL)	1.0	37.4	5.0	1.0	4.0	0.75	0.75	0.1
Reactant final concentration	50ng / reaction	-	1x	200μM	2mM	3ng/μL	3ng/μL	0.55U

All reaction components were thawed on ice and vortexed briefly before addition to the master mix. To each 49μL of reaction mix, 1μL of primary amplification product was added as template. The study by van Deutekom et al. (2001) also reported a nested secondary PCR reaction, and while reaction components remained the same the cycling conditions were different as described in Tables 3.10 and 3.11 respectively.

Table 3.10 Cycling conditions for the secondary nested PCR using Tth plus polymerase. Step 2 to step 4 cycled through 25 times after the initial cDNA strand denaturation.

Step 1	Initial denaturation	2 minutes	94°C
Step 2	Subsequent denaturation	30 sec	94°C
Step 3	Primer annealing	1 min	55°C
Step 4	Strand elongation	2 min	72°C

Table 3.11 Cycling conditions for the secondary nested PCR using Tth plus polymerase. Step 2 to step 4 cycled through 32 times after the initial cDNA strand denaturation according to the protocol outlined by van Deutekom et al. (2001).

Step 1	Initial denaturation	2 minutes	94°C
Step 2	Subsequent denaturation	45 sec	94°C
Step 3	Primer annealing	45 sec	60°C
Step 4	Strand elongation	2 min	72°C

Typically, the last three steps cycled through 25 times after the initial cDNA strand denaturation (Table 3.10). However, cycling conditions reported by van Deutekom et al. (2001) were not the same and were adjusted accordingly (Table 3.11). Reactions were performed on either a MJ PTC 100 or MJ Research mini thermal cycler.

3.5.3 Agarose gel electrophoresis

Products from the second round of amplification were typically stored at –20°C or run directly on to a gel. Typically, 2.5µL of secondary PCR product was combined with glycerol loading buffer and electrophoresed through a 2% agarose TAE gel at 90V for ~ 2 hours, depending on the expected size of the amplified transcript fragment. All agarose gels incorporated a 100bp ladder molecular weight marker as a size standard. Initial experiments investigating exon 19 skipping were tailored to generate 1280bp unmodified (full length) amplicons after amplification across exons 13 to 21. Excision of dystrophin exon 19 (88 bp) would produce a smaller product which was difficult to discern from the full length product. The advantage of this assay was the minor size variation between the full length and shortened products which ensured similar amplification efficiencies for both. To increase the separation between these species, 3% agarose TAE gels were originally used. The increased resolving power of this system, however, also required a longer running time (~ 3 hours). Consequently, nested primers were designed to yield smaller products, that is, the relative size difference between the full length and skipped products was increased so that less time was required to electrophorese them through the gel while still maintaining a satisfactory separation.

On completion of the electrophoresis, the agarose gels were immersed in a 0.5µg/mL solution of ethidium bromide for ~10 minutes. The products were then visualised on an ultraviolet transilluminator and images recorded at a fixed resolution of 180dpi using a Kodak DC ID 2.0 digital gel documentation system.

3.5.4 Characterisation of 2'OMeAO-induced products

3.5.4.1 Amplicon isolation

Initial identification of each amplicon was performed visually relative to the 100bp size marker and compared with the transcript fragment length expected to be generated in the secondary nested PCR. However, to fully characterise the products of interest, each amplicon was isolated and reamplified using the bandstab technique (Wilton et al., 1997) or by complete band excision.

3.5.4.1.1 Bandstab procedure

The bandstab procedure was typically performed directly after observation of the products of interest. Using the UV transilluminator to visualise the bands in the gel, specific amplicons were pierced with a pipette tip which was then placed directly into a PCR tube containing a PCR reaction mixture as described by Wilton et al. (1997). This procedure was performed in duplicate to maximise eventual product recovery and was sometimes required when attempting to characterise products of low abundance. The product under investigation removed by the tip was thus used as template for a further 35 cycles of amplification under identical conditions as described in Tables 3.9 and 3.10, except that the annealing temperature was reduced to 50°C. The presence of the re-amplified product was confirmed by electrophoresis through a 2% agarose gel and visualised on a UV transilluminator.

3.5.4.1.2 Gel slice excision procedure

On occasions, the bandstab technique was unable to isolate a single product when the source contained several amplified transcript species that were smaller than the amplicon of interest. When this occurred, 45µL of the duplicate bandstab mixtures were electrophoresed through a 2% low melting point gel at 70V for ~3 hours. After staining in fresh ethidium bromide, the products, while being viewed on the UV transilluminator, were completely excised with a sterile scalpel with care taken to avoid removing excess agarose.

3.5.4.2 Amplicon purification

Amplicons derived through either the bandstab or gel slice excision procedures were purified using Qiaquick spin columns according to the manufacturer's instructions. The presence of the purified amplicon was confirmed by electrophoresis of a 5µL aliquot through a 2% agarose gel as described earlier. The remaining material was then stored at -20°C to await further analysis.

3.5.4.3 Amplicon sequencing

Following verification of purity and abundance, the amplicons of interest were placed into a sequencing reaction which incorporated the Big Dye Terminator chemistry (version 3). The components comprising the sequencing reaction mix are described in Table 3.12.

Table 3.12 Sequencing components and their proportions in a 10μL sequencing reaction. Template volume determined amount of water to be added. Forward or reverse primers were added at 50ng per reaction.

Reaction component	Big Dye (V3)	Big Dye buffer	Primer (F or R)	cDNA template	H_2O
Reactant volume (μL)	3.0	1.0	1.0	1-5μL	to 10μL

The sequencing reaction was always made up to a final volume of 10μL (with water if required). Both size and abundance of the purified product (estimated by band intensity on the gel), determined the amount to be added to the reaction as template. Based on the expected identity of the amplicon and also as a measure of congruity, 50ng of forward and reverse primer, in separate reactions, were chosen for sequencing of each template. Where possible, the primer selected for use in the sequencing reaction would be internal to the relevant primers used in the nested PCR. Primer sequences are listed in Table 3.13.

Table 3.13 Forward and reverse primers used in the sequencing PCR reactions.

Name	Sequence (shown 5' to 3')	DS Number*	Exon(s) skipped
H17F	GCAGATTACTGTGGATTCTG	123	Human 19
HM21R	TTGTCTGTAGCTCTTTCTC	2954	
M18F	GGATGTCGATATAACTGAACTTC	935	Mouse 19
HM21R	TTGTCTGTAGCTCTTTCTC	2954	
M19F	GCCATAGCACGAGAAAAAGCAG	2261	Mouse 20
M22R	CCTGATGCTACTCATTGTCTCC	2316	
M19F	CAGAATTCTGCCAATTGCTGAG	2616	Mouse 21
M23R	TGGGAGGAAAGTTTCTTCCAGT	1643	
M20R	CCCAGTCTACCACCCTATCAGAGC	1803	Mouse 22
M26R	CCTGCCTTTAAGGCTTCCTT	3657	
M21F	TCAGCTCTTCAGCCTCAAATTG	3737	Mouse 23
M26R	CCTGCCTTTAAGGCTTCCTT	3657	
M21F	TGAGGGCCAAAGAGAAAGAGC	783	Mouse 24
M26R	CCTGCCTTTAAGGCTTCCTT	3657	
M24F	TGTTTTCCTGAAAGAGGAATGG	2317	Mouse 25
M26R	TTCTTCAGCTTGTGTCATCC	3658	
H44F	GCGATTTGACAGATCTGTTG	2495	Human 46
H47R	TTATCCACTGGAGATTTGTCTG	3540	

* Laboratory nomenclature; denotes DNA Synthesis number given to each primer (Geneworks)

The 25 cycle sequencing PCR reaction detailed in Table 3.14 was performed on a MJ Research mini thermal cycler equipped with a hot bonnet to bypass the need for an oil overlay.

Table 3.14 Sequencing PCR reaction conditions. All sequencing reactions were performed on the same MJ Research mini thermal cycler for 25 cycles.

Step 1	Template denaturation	30 sec	94°C
Step 2	Primer annealing	30 sec	50°C
Step 3	Strand elongation	4 min 15 sec	60°C

Following the sequencing PCR reaction, non-template reactants were removed by ethanol precipitation. Template purification was performed at room temperature and commenced with the addition of 10µl of 600mM sodium acetate (pH 5.2) and 50µl absolute ethanol. The mix was then vortexed briefly prior to incubation for 15 minutes and centrifugation at 14 000 x g for 20 minutes in an Eppendorf 5415C centrifuge. The

supernatant was removed and the pellet resuspended in 250μL of 70% ethanol before centrifugation at 14 000 x g for 5 minutes. Finally, the supernatant was removed and the purified template allowed to air dry. Products were fractionated on an ABI 377 DNA Sequencer at the DNA sequencing facility, Centre for Neuromuscular and Neurological Disorders, by Ms. Lori Blechynden.

3.6 RNA binding assay

An RNA binding assay is an *in vitro* test of RNA fragment template amenability to hybridisation with antisense orientated DNA oligonucleotides (deoxy-AOs) directed at specific sequences. The assay was designed as a precursor to cell culture experiments as a means to increase target assessment throughput and reduce cost by bypassing the relatively lengthy cell culture process and expense of 2'OMeAO synthesis. When a deoxy-AO was able to demonstrate a high affinity for its target, it was selected for synthesis (in-house) as a standard 2'OMeAO and transfected into cells to assess its effect on the natural splicing process.

3.6.1 DNA isolation and purification

H2K *mdx* or primary human cells were proliferated in a 75cm^2 flask as described in Section 3.1.1 until they reached approximately 100% confluency, after which the cells were trypsinised as outlined in Section 3.1.2. After centrifugation, the supernatant was removed and the pellet resuspended thoroughly in 200μL PBS before being transferred to a sterile 1.6mL microfuge tube. All following steps, including cell lysis, RNA and protein removal and DNA precipitation were performed exactly as described in the Gentra Systems genomic DNA purification kit protocol for DNA isolation and purification from cultured cells. The purified genomic DNA was quantified and stored at -20°C to await downstream application.

3.6.2 Genomic DNA fragment synthesis incorporating a T7 promoter sequence

Purified mouse or human genomic DNA isolated from muscle cell cultures, was used as template in T7-PCR. The subsequent amplicons with the T7 promotor sequence incorporated became the template in an *in vitro* RNA transcription reaction. In an attempt to ensure an adequate approximation of secondary structure formation in the region under investigation, 300 - 400 bp of DNA sequence was selected as a template to be transcribed into RNA. Each DNA fragment would, if possible, contain the entire exon and >70 bases of intronic sequence both 5' and 3' of the exon. In situations where the exon was large and this was not possible, two fragments of ~350bp in length were selected to be synthesised, each incorporating only one splice site. The fragment length was determined by the position of the reverse primer and the forward primer which contained a 31 base T7 polymerase promoter sequence at the 5' end (Table 3.17). Reaction component composition and initial DNA fragment amplification conditions are outlined in Tables 3.15 and 3.16 respectively. All primers sequences are listed in Table 3.17.

Table 3.15 Component composition for a 25μL PCR reaction. Included was the template DNA at a final concentration of 4ng/μL and the ~60bp forward primer (includes T7 promotor sequence) at 2x that of the reverse primer which was only half the length.

Reaction component	DNA template	H_20	10x Buffer	dNTP	$MgCl_2$	Forward primer	Reverse primer	Tth plus polymerase
Reactant volume (μL)	varied	varied	2.5	0.5	2.0	1.0	0.5	0.5
Reactant final concentration	4ng/μL	-	1x	200μM	2mM	3ng/μL	3ng/μL	0.55U

Table 3.16 Cycling conditions for genomic DNA fragment amplification. Step 2 to step 4 cycled through 40 times after the initial DNA strand denaturation.

Step 1	Initial denaturation	2 minutes	94°C
Step 2	Subsequent denaturation	30 sec	94°C
Step 3	Primer annealing	1 min	55°C
Step 4	Strand elongation	2 min	72°C

Table 3.17 Forward and reverse primers used in the amplification of the genomic DNA fragments. Reverse primers are given in an antisense orientation in the 5' to 3' direction. The T7 polymerase promotor sequence is listed separately and is denoted as "**T7**" at the 5' position in each forward primer. Primers are based on exonic sequence unless prefixed with "Int" which indicates an intronic origin.

Name	Sequence (shown 5' to 3')	Exon Targeted	DS Number*
T7	GATCCTAATACGACTCACTATAGGGAACAGA	N/A	N/A
Int19T7F	**T7**GGTCATTGGTTTCCAGAGCATG		
20T7F	**T7**GGGTGTTAATGCTGAAAGTATCAG	20	3735
Int20R	CCAGAGTTTGCTTTGGCCCTCTTGC		3728
Int20T7F	**T7**CAGTATATGCAAAGTTTCAAAGTTAC	21	3729
Int21R	GATAGAGGGTTTAGCCTTGGG		3781
Int21T7F	**T7**GCTGACAAATTAGAAAAATATGACAG	22	3730
Int22R	CTTTACTTTTTCATTATTACCTTAAG		3731
Int23T7F	**T7**GCTACAATGAGACCTCCCTCAAAC	24	3786
Int24R	CCAAGAATGTGCTCAGGTACTGG		3787
Int24T7F	**T7**CATGTCGAATGTCATGATAAATGTATG	25	3775
Int25R	GTGTTTTGACAATATTTTCATAAAC		3776
Int45T7F	**T7**GGTTAACATCTTTTAAATTGC		3472
46T7F	**T7**AAGAACAAAAGAATATCTTGTC	46	3474
Int46R	GCAAGGAACTATGAATAACCT		3473

* Laboratory nomenclature; denotes DNA Synthesis number given to each primer (Geneworks).

Initially, the genomic DNA was amplified between the two primers in a 25μL PCR reaction for 40 cycles and the fragment electrophoresed through a 2% agarose gel as described earlier. Once synthesis of the correct size product was confirmed by visualisation on an UV transilluminator, two 50μL DNA amplification reactions were performed to increase the final yield of the product. After gel analysis of the second set of amplification products, the duplicate reactions were combined and purified on Qiaquick spin columns according to the manufacturer's instructions. The presence of the purified fragment was confirmed by electrophoresis through a 2% agarose gel.

3.6.3 *In vitro* RNA transcription

To produce an RNA fragment, the purified genomic DNA amplicons were used as template in an *in vitro* RNA transcription reaction using the Riboprobe® in vitro Transcription System (Promega) (Table 3.18). After addition of the DNA template, the reaction mixture was incubated at 37°C for 1 hour. A further 15 min incubation at 37°C with 1μL DNase I ensured the removal of the DNA template before the synthetic RNA was extracted and purified as described in Section 3.4. The purified RNA was quantified, diluted to 50ng/μL and stored at -20°C.

Table 3.18 Component composition in a 20μL *in vitro* RNA transcription reaction.

Reaction component	DNA template	H_20	Transcription buffer*	rNTP	DTT	RNAzin	T7 RNA polymerase
Reactant volume (μL)	varied	varied	4.0	4.0	2.0	1.0	1.0
Reactant final concentration	~300ng / reaction	-	1x	200μM	10mM	40U	20U

* Supplied as a 5x preparation and diluted to yield a final concentration of 1.2mM magnesium chloride in a single 20μL reaction.

3.6.4 Target hybridisation and bandshift detection

To estimate deoxy-AO affinity to the target sequence, varied amounts of each deoxy-AO (sequence information given in Table 3.19) were added to a hybridisation reaction containing a constant 50ng of the synthetic RNA, 2μL of 2x hybridisation buffer and water to a final volume of 4μL. The reactants were incubated for 30 minutes at 37°C before being combined with glycerol loading buffer and electrophoresed through an 8% polyacrylamide TBE gel at 200V for approximately 3 hours under non-denaturing conditions. The gel was then placed into a SYBR gold stain followed by visualisation of the reactants on a UV transilluminator. As the secondary structure of the RNA fragment could be altered when a deoxy-AO annealed, the complexed and uncomplexed RNA were often discerned as separate bands. The complexed band was separated from the unbound RNA band, thus inducing a 'bandshift'.

The degree of bandshift induced was given a rating between 0 and 4, where a 0 rating indicated no bandshift (equivalent to the RNA alone control) and a rating of 4 corresponded to 100% bandshift. A deoxy-AO was required to score a rating of at least 2 (equivalent to approximately 50% bandshift) when present at 5ng per reaction to be considered suitable for synthesis as a 2'OMeAO for further evaluation in cell culture.

Figure 3.2 Non-denaturing polyacrylamide gel demonstrating the varied degrees of bandshift induced by deoxy-AOs. Five nanograms of deoxy-AO was added to 50ng of RNA fragment.

Table 3.19 Sequences of deoxy-AOs used in this study. Upper and lower case characters represent exonic and intronic nucleotides respectively.

Name	Sequence (shown 5' to 3')	DS
dM20A(-18+02)	CTctacaaagaaaaccaaaa	3849
dM20A(-16+04)	CCCTctacaaagaaaaccaa	3850
dM20A(-14+06)	CACCCTctacaaagaaaacc	3851
dM20A(-12+08)	AACACCCTctacaaagaaaa	3852
dM20A(-15+10)	TTAACACCCTctacaaagaaaacca	3875
dM20A(-10+15)	CAGCATTAACACCCTctacaaagaa	3876
dM20D(+02-18)	gaaggaggaaaaccttacCT	3720
dM20D(+04-16)	aggaggaaaaccttacCTTA	3721
dM20D(+06-14)	gaggaaaaccttacCTTACA	3722
dM20D(+08-12)	ggaaaaccttacCTTACAAA	3723
dM20D(+10-15)	ggaggaaaacattacCTTACAAATT	3854
dM20D(+10-20)	tggaaggaggaaaacattacCTTACAAATT	3853
dM21D(+02-18)	aaaagtgtttttacttacTT	3784
dM21D(+04-16)	aagtgtttttacttacTTGT	3782

* Laboratory nomenclature; denotes DNA Synthesis number given to each primer (Geneworks).

Table 3.19 continued.

Name	Sequence (shown 5' to 3')	DS
dM21D(+06-14)	gtgtttttacttacTTGTCT	3783
dM21D(+08-14)	gtttttacttacTTGTCTGT	3785
dM22D(+02-18)	attcaaatgtccacagacCT	3724
dM22D(+04-16)	tcaaatgtccacagacCTGT	3725
dM22D(+06-14)	aaatgtccacagacCTGCAA	3726
dM22D(+08-14)	atgtccacagacCTGTAATT	3727
dM24A(-16+04)	CCCTctacaaagaaaaccaa	3850
dM24A(-14+06)	CACCCTctacaaagaaaacc	3851
dM24A(-12+08)	AACACCCTctacaaagaaaa	3852
dM24A(-15+10)	TTATGTGATTctggaataaaaaagc	3877
dM24A(-10+15)	GGTTTTTATGTGATTctggaataaa	3878
dM24D(+02-18)	atcagatacaaatcttacTC	3788
dM24D(+04-16)	cagatacaaatcttacTCTG	3789
dM24D(+06-14)	gatacaaatcttacTCTGCA	3790
dM24D(+08-12)	tacaaatcttacTCTGCATT	3774
dM24D(+10-20)	tcatcagatacaaatcttacTCTGCATTGT	3859
dM24D(+15-10)	caaatcttacTCTGCATTGTTTGAG	3860
dM25D(+02-18)	gaattaaactagtcatacCT	3777
dM25D(+04-16)	attaaactagtcatacCTGG	3778
dM25D(+06-14)	taaactagtcatacCTGGCG	3779
dM25D(+08-12)	aactagtcatacCTGGCGGC	3780
dH46A(-13+07)	TTCTAGCctggagaaagaag	3598
dH46A(-11+09)	tctttctccagGCTAGAAGA	3599
dH46A(-09+11)	tttctccagGCTAGAAGAAC	3600
dH46A(-07+13)	tctccagGCTAGAAGAAC	3646
dH46A(+28+47)	AGAATTTCAAAGAGATTTAA	3611
dH46A(+63+82)	GGTTGGAGGAAGCAGATAAC	3445
dH46A(+83+103)	ATTGCTAGTATCCCACTTGAA	3612
dH46A(+115+134	GCAGCAACTAAAAGAAAAGC	3446
dH46A(+111+125	AAGAGCAGCAACTAA	3613
dH46D(+04-16)	CAAGgtaattttattttctc	3601
dH46D(+06-14)	GTCAAGgtaattttattttc	3602
dH46D(+08-12)	AAGTCAAGgtaattttattt	3603
dH46D(+08-14)	AAGTCAAGgtaattttattttc	3647

* Laboratory nomenclature; denotes DNA Synthesis number given to each primer (Geneworks).

Chapter 4 – Targeting exon 19: 2'OMeAOs directed at exon splicing enhancers

In 1991, Matsuo and colleagues reported a 52bp deletion in exon 19 of the dystrophin gene. It was concluded that this deletion was responsible for the abnormal processing of the DMD Kobe allele (missing exon 19) found in the 16 year old patient with DMD (Matsuo et al., 1990) as the resultant mature transcript was out-of-frame. This was despite the fact that the consensus acceptor and donor splice sites of exon 19 were untouched. In 1995, Takeshima et al. investigated the role of the deleted sequence in exon 19. Using a minigene transcription product, which included the wild-type exon 19 in a HeLa cell nuclear extract, they demonstrated that the region missing in the DMD Kobe allele was necessary for exon 19 definition. By directing a 2'OMeAO at a 31 base region within the 'deleted' sequence, the authors were able to inhibit intron 18 splicing and thereby prevent exon 19 inclusion in the mature RNA. A follow-up study by Pramono et al. (1996) was undertaken in human lymphoblastoid cells using a DNA version of the 2'OMeAO used in the Takeshima et al. (1995) study. This antisense ODN, directed at the ESE (ERS) of exon 19, was able to alter the dystrophin pre-mRNA splicing in these cells such that exon 19 was excluded.

The focus of this section of the project was to further define the exonic motif targeted by the 31mer in the previous studies (Takeshima et al., 1995; Pramono et al., 1996). To achieve this aim, 2'OMeAOs were systematically designed to various portions of the 31bp region of exon 19 to identify crucial motifs involved in definition of the exon. Three transfection reagents were evaluated to determine which would deliver the 2'OMeAO to the cell nucleus most effectively in *H-2K* normal and *mdx* mouse muscle cells, and in primary human and HDMD muscle cells.

4.1 Transfection reagent optimisation

To determine the most effective vehicle for 2'OMeAO delivery in *H-2K* mouse, normal primary human and human DMD cells, the transfection reagents Lipofectin, Lipofectamine 2000 and ExGen 500 were evaluated. These reagents were assessed at two time points, 3 hours and 24 hours post-transfection, for their ability to deliver a fluorescently-labelled 2'OMeAO, M23D(+12-08)-FITC (Table 3.2) to the cell nucleus. All transfections were performed with a standard 300nM (~1μg) final 2'OMeAO concentration in serum-free Opti-MEM media and according to the manufacturer's instructions. M23D(+12-08)-FITC was designed to target the donor splice site of exon 23 in the dystrophin gene (Mann et al., 2001). The same FITC-labelled 2'OMeAO was used in this study to ensure reproducibility and to determine the best reagent for transfection of human cells. Based on the assumption that the nuclear uptake of M23D(+12-08)-FITC is not sequence dependent, its utility was still relevant in this project. As localisation of the fluorescent tag to the nucleus, the site of pre-mRNA transcription, is the final outcome measure, coupling FITC to M23D(+12-08) simply gives the fluorescent tag 'directions' specific to the dystrophin gene.

4.1.1 Transfection of *H-2K* mouse muscle cells with M23D(+12-08)-FITC

Three ratios of Lipofectin:2'OMeAO, 1:1, 2:1, and 5:1 (weight:weight) were evaluated in mouse cells. After three hours, cytoplasmic fluorescence in both *H-2K* normal and *mdx* cell lines appeared to be weak and diffuse throughout the cell at each ratio tested with no preferential nuclear accumulation observed. After 24 hours, however, nuclear fluorescence was observed in approximately 100% of cells when the 2'OMeAO was complexed with Lipofectin at a ratio of 2:1 (Figure 4.1), with a minimal increase in both fluorescence and cell death at a ratio of 5:1. Transfection at a 1:1 ratio resulted in less uptake compared to the optimal 2:1 ratio (results not shown). No fluorescence was detected in the untreated cells or those cells that received Lipofectin alone at a sham 300nM concentration (2µg/500µL). When 300nM of the uncomplexed M23D(+12-08)-FITC was delivered to the cells, only a weak and diffuse cellular fluorescence was observed in both cell lines after three hours. This signal, however, was no longer detectable after 24 hours and was not observed in the nucleus.

Based on these results and previous success with this reagent (Mann et al., 2001; Mann et al., 2002), all *H-2K* cells used in this project were transfected at a ratio of 2:1 of Lipofectin:2'OMeAO because of cell death, high efficiency and low volume of usage per transfection.

Lipofectamine 2000 and ExGen 500 were also assessed and each displayed differing abilities to deliver M23D(+12-08)-FITC to the nuclei of the mouse myoblasts. Three ratios of Lipofectamine 2000:2'OMeAO, 1:2, 1:1 and 2:1 were tested. The lower ratios were chosen as previous experience in our laboratory with this reagent had indicated that higher doses were associated with punctate cytoplasmic structures (fluorescent aggregates) and greater cell damage. At both time points transfection efficiency was high, with ~100% of cells demonstrating some degree of fluorescence, although very little accumulation of the 2'OMeAO was observed specifically in the nucleus. However, the intensity of the signal throughout the cell appeared to be slightly higher than comparable ratios of Lipofectin and 2'OMeAO (results not shown). The 1:1 ratio of Lipofectamine 2000:2'OMeAO was considered to be optimal for this reagent. However, considering the degree of cell death and the apparent lack of localisation to the nucleus, Lipofectamine 2000 was not used to transfect mouse cells in this project.

The third reagent assessed, ExGen 500, was tested late into the project as a potential replacement for Lipofectin. Three equivalents of ExGen 500 to 2'OMeAO, 2,

3.5 and 5 were evaluated. A diffuse cellular fluorescence was detected after three hours which then became predominantly localised to the nucleus 24 hours post-transfection. While the highest ratio was associated with only a minor toxic reaction, small fluorescent aggregates were observed across the well (Figure 4.2), possibly indicating a maximal uptake of the complex. Due to the reduced toxicity and aggregates, the ratio of 3.5eq of ExGen 500 to 1μg 2'OMeAO was deemed optimal for transfecting the *H-2K* cells. These observations were consistent with those reported previously (Dunckley et al., 1998; van Deutekom et al., 2001).

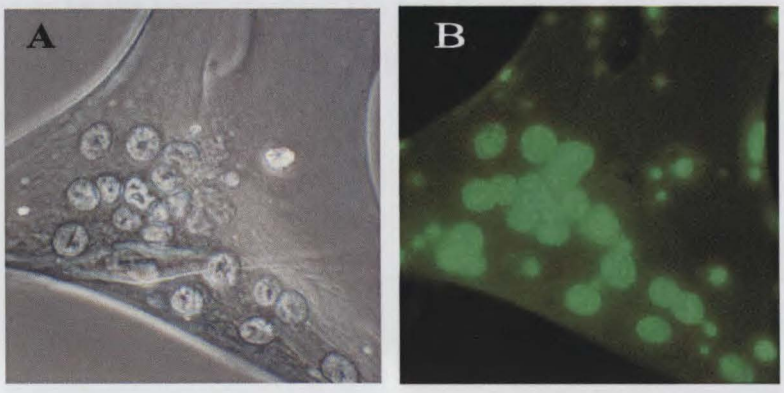

Figure 4.1 Phase contrast and fluorescent photographs taken 24 hours after *H-2K mdx* mouse myotubes were transfected with M23D(+12-08)-FITC. Typically, cells were allowed to differentiate for 72-96 hours before transfection (A). Strong nuclear fluorescence (B) could be detected 24 hours post-transfection when Lipofectin was complexed with M23D(+12-08)-FITC at the optimal ratio of 2:1. (40x magnification).

4.1.2 Transfection of human muscle cells with M23D(+12-08)-FITC

The results observed from the fluorescent studies using Lipofectin and Lipofectamine 2000 in the primary human cells were similar to those obtained in the mouse cells. However, in primary human cells transfected with Lipofectin, the nuclear localisation was not as distinct after 24 hours compared to the mouse cells. Lipofectamine 2000 was again found to be associated with increased cell death, and despite comparable transfection efficiency, was excluded due to its more toxic nature. Therefore all experiments involving 2'OMeAO-induced exon 19 skipping (section

4.3.2.1) in primary human cells were performed with Lipofectin at a 2:1 ratio of Lipofectin:2'OMeAO, the reagent (and ratio) deemed most effective for inducing exon 23 skipping in the same primary human cell line (pers. comm. C. Mann). When the opportunity to reproduce the previously reported 2'OMeAO-induced skipping of exon 46 in human cells arose, ExGen 500 was, however, selected as the transfection reagent based on the protocol outlined by the authors (van Deutekom et al., 2001).

As observed in the mouse cell transfection experiments, ExGen 500 was able to efficiently deliver M23D(+12-08)-FITC to the cell nucleus after 24 hours. Interestingly, the fluorescent aggregates but not cell death were observed to increase with an increase in the amount of ExGen 500. Again, the ratio of 3.5eq to 1μg of M23D(+12-08)-FITC was considered to be the point at which the signal intensity was strongest with minimal fluorescent aggregate accumulation (Figure 4.2), consistent with the findings of van Deutekom et al. (2001).

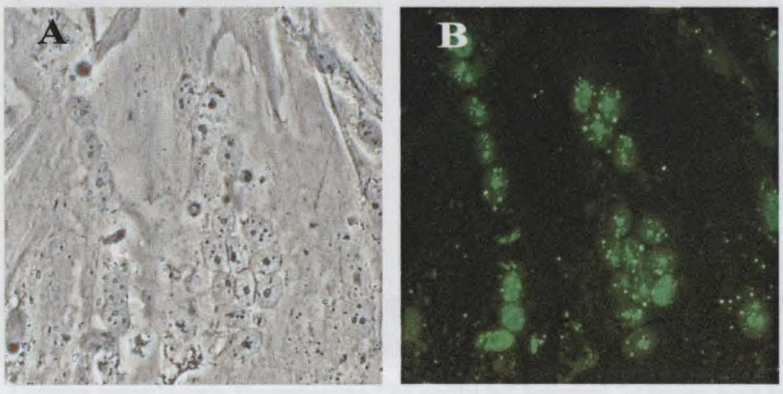

Figure 4.2 Phase contrast and fluorescent photographs taken 24 hours after primary human myotubes were transfected with M23D(+12-08)-FITC. Typically, cells were allowed to differentiate for 96 hours before transfection (A). When M23D(+12-08)-FITC was delivered to the cell uncomplexed with ExGen 500, a weak and diffuse cellular fluorescence was observed 3 hours later but not after 24 hours (not shown). However, strong nuclear fluorescence (B) could be detected 24 hours post transfection when 3.5 eq of ExGen 500 was complexed with ~1μg of M23D(+12-08)-FITC. Note the low level of fluorescent aggregates outside the cells (10x magnification).

Fluorescent studies in the immortalised HDMD cells were less pronounced than those obtained in the three cell lines previously tested. Furthermore, distinct nuclear localisation of M23D(+12-08)-FITC was very rarely observed, regardless of the carrier. Therefore, as no reagent appeared to have a toxic effect on the cells, higher ratios of carrier to 2'OMeAO were tested. The greatest difference was seen with Lipofectamine 2000. While a 5:1 ratio (weight:weight) of carrier to 2'OMeAO resulted in 20-30% cell death after 24 hours, a 3:1 ratio resulted in minimal or no cell death and an increase in the uptake of the fluorescent molecule. Also, as was seen with the ExGen 500 transfections in the primary human cells, the increase in both ExGen 500 and Lipofectamine 2000 was associated with an increase in fluorescent aggregates (Figure 4.3)

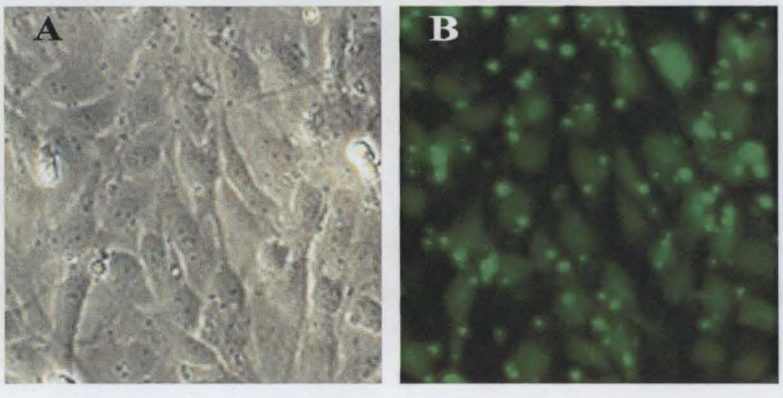

Figure 4.3 Phase contrast and fluorescent photographs taken 24 hours after HDMD myotubes were transfected with M23D(+12-08)-FITC. Typically, cells were allowed to differentiate for 72 hours before transfection (A). Diffuse cytoplasmic fluorescence (B) could be detected 24 hours post-transfection when Lipofectamine 2000 was complexed with M23D(+12-08)-FITC at a ratio of 3:1 (weight:weight). Further increasing the ratio of the carrier to the 2'OMeAO did not increase signal intensity, only fluorescent aggregates and cell death (10x magnification).

4.2 Quality assay of 2'OMeAOs directed at the exon 19 ESEs

At the onset of this study, the first and second generation 2'OMeAOs were synthesised by Geneworks. However, our group acquired access to an Expedite 8909 Nucleic Acid Synthesiser (Applied Biosystems) and commenced synthesising all subsequent 2'OMeAOs in-house. For comparison and to ensure the continued quality of all succeeding 2'OMeAOs, 200ng of each 2'OMeAO from Geneworks and 200ng of

each 2'OMeAO synthesised in-house were resuspended with formamide loading buffer and electrophoresed through a denaturing polyacrylamide gel (Figure 4.4). In addition to the monitoring of the trityl signal at the end of each coupling during synthesis, this assay satisfactorily validated the integrity of each 2'OMeAO used to induce exon 19 skipping.

Figure 4.4 Each 2'OMeAO targeting the exon 19 ESE in this study was run on a denaturing polyacrylamide gel to assess the standard of synthesis. As apparent yields varied, 2'OMeAO concentrations were adjusted and re-evaluated by spectrophotometry prior to cell transfection

4.3 Induction of exon 19 skipping across species using 2'OMeAOs directed at the ESE

4.3.1 Exon 19 skipping in mouse muscle cells

Our initial experiments to induce dystrophin exon 19 skipping were undertaken using the conditionally immortalised normal *H-2K* mouse muscle cell line which can be induced to fuse and express normal dystrophin (Morgan et al., 1994). However, the dystrophin mRNA would be out-of-frame when exon 19 is removed, as an amber stop codon 43 bases into exon 20 is created (Figure 4.5) and, as a consequence, no dystrophin can be produced. Therefore, detection of the exon 19 deleted message was anticipated to be more difficult relative to the normal message, due to a high turnover arising from nonsense mediated decay mechanisms (Maquat, 1995). Based on the results of these early investigations, it was hypothesised that the *H-2K*

mdx cell line may represent a better model with which to assess 2'OMeAO-induced exon skipping in the dystrophin gene, as this dystrophin mRNA carries a nonsense mutation in exon 23 and should be metabolised at a similar rate to the 2'OMeAO induced, out-of-frame transcripts missing exon 19.

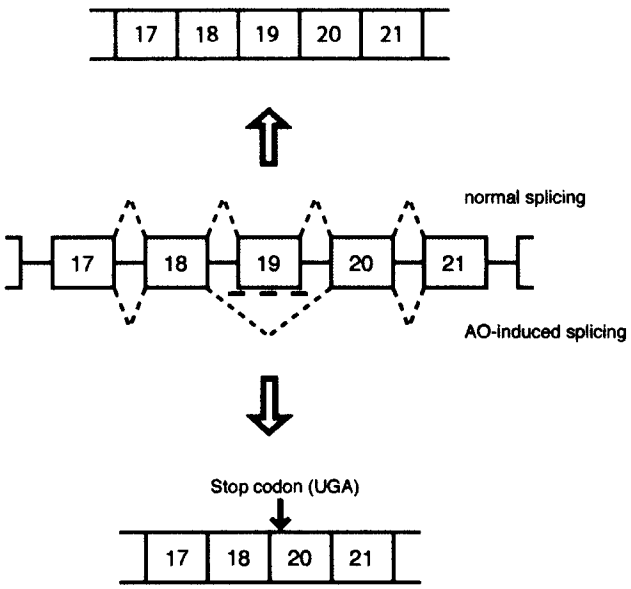

Figure 4.5 Schematic representation of normal and 2'OMeAO-induced splicing patterns. Normal splicing (indicated by broken lines above the exons) removes the introns (single horizontal lines) and retains each exon to produce a mature RNA (not drawn to scale). The 2'OMeAO-induced splicing (2'OMeAOs indicated by small bold horizontal lines, modified splicing indicated by broken lines below the exons) prevents recognition of the targeted exon. The transcript missing the entire exon 19 is out-of-frame and a termination signal (arrow) occurs at the 15th codon into exon 20 (Errington, Mann, Fletcher & Wilton, 2003).

4.3.1.1 *H-2K* normal muscle cells

The 2'OMeAO HM19A(+35+65) (Table 3.2 and Figure 4.8), originally described by Takeshima et al. (1995), was the first 2'OMeAO tested to provide a necessary starting point for the project. Myotube transfections were performed by complexing HM19A(+35+65), at a standard dose of 300nM, with Lipofectin at the optimised ratio of 2:1 Lipofectin:2'OMeAO (weight:weight) as described earlier. Total RNA was extracted from pooled duplicate wells 24 hours post-transfection and purified for analysis of the dystrophin gene transcripts. The RNA was then reverse transcribed

into cDNA with subsequent amplifications between nested primers flanking exon 19. Only two transcript fragments separated by gel fractionation were detected - the larger 759bp product corresponding to the full-length amplicon (includes exon 19) and the shorter 671bp product corresponding to the transcript species missing exon 19 (Figure 4.6).

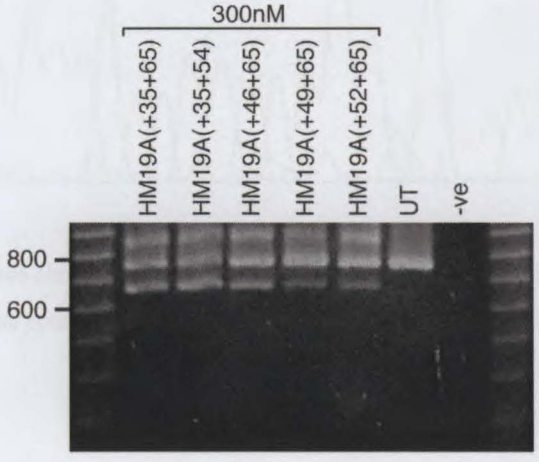

Figure 4.6 Exon 19 skipping induced by 1st, 2nd and 3rd generation 2'OMeAOs in *H-2K* normal mouse mRNA. RT-PCR analysis of RNA harvested 24 hours after cultured myotubes were transfected with 2'OMeAOs at 300nM. The full-length product spanning exons 17 to 21 is 759 bases long and the shorter product is missing 88 bases due to the precise removal of exon 19. The smeared larger bands above the full-length products are due to heteroduplex formation, as it is not seen in the untreated lane where there are no shorter products. Subsequent secondary PCRs were performed with a more internal reverse primer which greatly reduced formation of heteroduplexes.

To confirm the exact nature of the exonic arrangements arising from the 2'OMeAO-induced splicing modification, both products were isolated and directly sequenced to confirm their predicted identities (Figure 4.7). It was concluded that HM19A(+35+65) had indeed induced the precise removal of dystrophin exon 19 from the normal *H-2K* mouse mRNA.

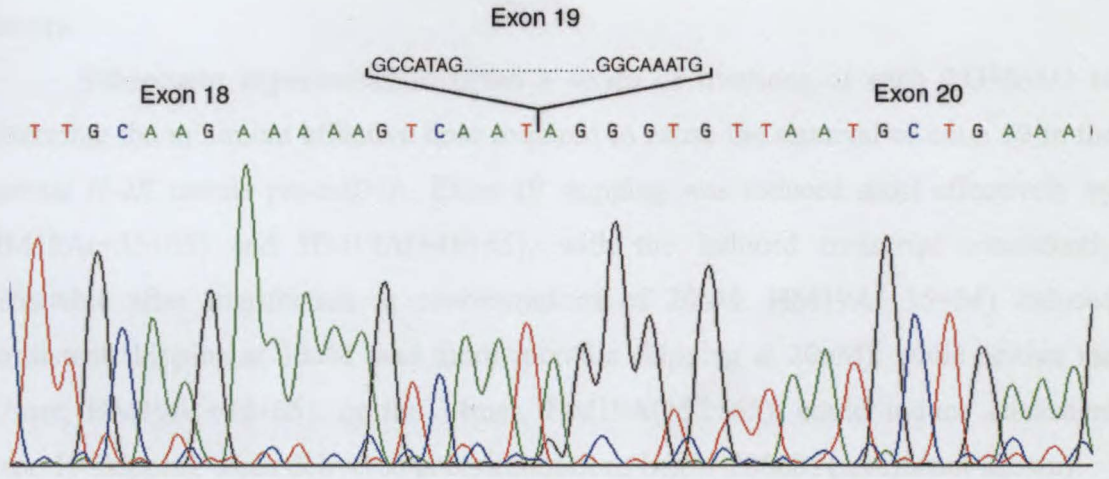

Figure 4.7 DNA sequence chromatogram of the PCR products across the junction of dystrophin exons 18 and 20, indicating precise removal of exon 19. The junction of exons 18 and 19 and exons 19 and 20 are shown for comparison.

We subsequently designed two shorter overlapping 2'OMeAOs within HM19A(+35+65), HM19A(+35+54) and HM19A(+46+65), as the second generation of 2'OMeAOs to further define the crucial region(s) of this ESE (Table 3.2 and Figure 4.8). Separate 300nM dose transfections of H2K normal muscle cells were performed, and a gel analysis of the subsequent RT-PCR fragments revealed that both HM19A(+35+54) and HM19A(+46+65) were also able to induce precise and consistent exon 19 skipping (Figure 4.6).

A third generation of 2'OMeAOs was designed to assess a likely minimum threshold for 2'OMeAO length as well as to refine the putative ESE-like motif. These two 2'OMeAOs, HM19A(+49+65) and HM19A(+52+65), are 17- and 14mers respectively directed at sequences within the region previously targeted by HM19A(+46+65) (Table 3.2 and Figure 4.8). This region was chosen based on a marginally but consistently stronger product induced by HM19A(+46+65) as compared to HM19A(+35+54), initiating speculation that the motif involved in exon 19 recognition and inclusion in the mature mRNA may reside in this region. Transfection with HM19A(+49+65) and HM19A(+52+65) at a final concentration of 300nM was sufficient for the 14mer to induce very similar levels of exon 19 skipping as the 17mer (Figure 4.6). However, the induced products appeared less abundant when compared to that induced by the parent 2'OMeAO, implying either a possible restriction for

2'OMeAO length or that only part of the crucial region had been blocked from splicing factors.

Subsequent experiments involved a series of titrations of each 2'OMeAO to determine the minimum effective dose required to cause the removal of exon 19 in the normal *H-2K* mouse pre-mRNA. Exon 19 skipping was induced most effectively by HM19A(+35+65) and HM19A(+46+65), with the induced transcript consistently detectable after transfection at concentrations of 20nM. HM19A(+35+54) induced consistent skipping at 30nM (and more sporadic skipping at 20nM), while neither the 17mer, HM19A(+49+65), or the 14mer, HM19A(+52+65), could induce consistent exon 19 skipping when delivered at concentrations below 200nM (results not shown).

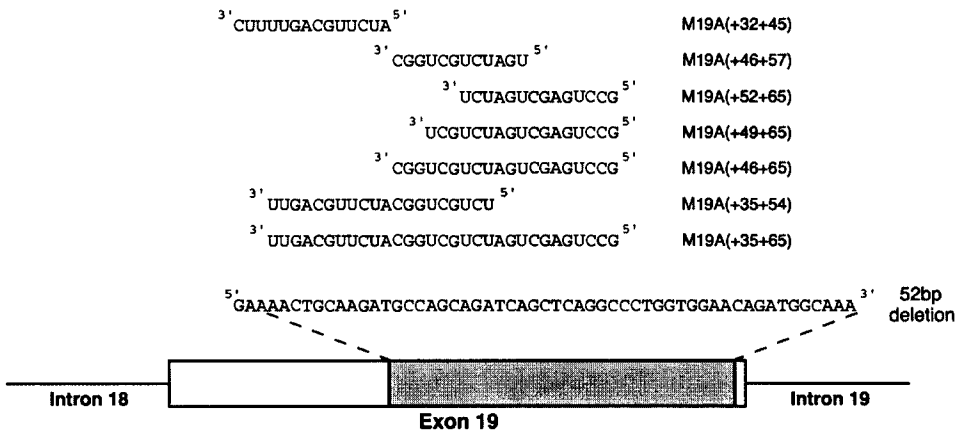

Figure 4.8 Schematic representation of the annealing sites for 2'OMeAOs to dystrophin pre-mRNA inside the 52bp deletion within exon 19. The putative ESE (shaded region in exon 19) was targeted by the first, second, third and fourth generation 2'OMeAOs (sequences shown 3' - 5') The nucleotide sequence of exon 19 within the ESE in mouse and human dystrophin genes was identical, allowing the application of each 2'OMeAO across species (Errington et al., 2003).

4.3.1.2 *H-2K mdx* muscle cells

The next series of experiments was conducted in the transformed *H-2K mdx* muscle cell line, as it was anticipated that the turnover rate of both natural and 2'OMeAO-induced transcripts would be similar and therefore provide a better estimate of the relative degree to which the 2'OMeAOs affect splicing patterns. Separate duplicate transfections were performed by complexing Lipofectin at 2:1 with either the first, second or third generation 2'OMeAOs, HM19A(+35+65), HM19A(+35+54), HM19A(+46+65), HM19A(+49+65) and HM19A(+52+65) (Table 3.2) at a standard dose of 300nM, as described earlier. Twenty-four hours after transfection, total RNA was extracted and purified and RT-PCR of the relevant dystrophin transcripts conducted. Agarose gel analysis of the amplified transcripts revealed that 2'OMeAO-induced exon 19 skipping appeared to be stronger in *mdx* cell cultures at the 300nM transfection concentration (Figure 4.9) than that detected in normal mouse cells. Again, only two transcript fragments were observed, the full-length 759bp product and the 671bp exon 19 deleted product.

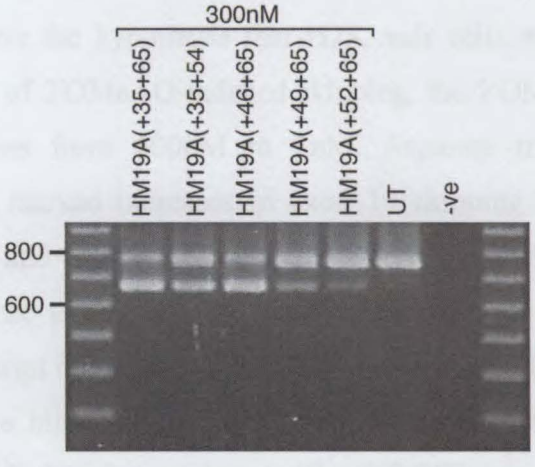

Figure 4.9 Agarose gel image of exon 19 skipping induced by 1st, 2nd and 3rd generation 2'OMeAOs at a final transfection concentration of 300nM. Skipped transcripts appeared to be more easily detected in the *mdx* cell line.

The two 2'OMeAOs HM19A(+32+45) and HM19A(+46+57) were tested only in the *mdx* cells (Table 3.2 and Figure 4.8). These represent the fourth and final generation of 2'OMeAOs designed to assess the sensitivity of the two polypurine stretches identified by Pramono et al. (1996) as targets for 2'OMeAO-induced exon 19 skipping. HM19A(+32+45) was directed at a 14 base region commencing 2 bases upstream from the 5' end of HM19A(+35+54). We hypothesised that the crucial region lay partially in the overlap between HM19A(+35+54) and HM19A(+46+65), and that a 2'OMeAO directed to block the 5' sequence targeted by HM19A(+35+54) would be less likely to induce exon 19 skipping. Conversely, the 12mer HM19A(+46+57), the shortest 2'OMeAO used in the study, was directed at the overlap and was expected to induce exon 19 skipping, assuming it could bind at sufficient strength to displace the competing splicing factors. Transfections with these 2'OMeAOs at a final concentration of 300nM resulted in the precise and reproducible removal of exon 19 by HM19A(+46+57). HM19A(+32+45) was unable to reliably induce exon 19 skipping (Figure 4.10).

4.3.1.2.1 Titration of 2'OMeAOs directed at the exon 19 ESE

In order to prove the hypothesis that H2K *mdx* cells were a better model for determining efficiency of 2'OMeAO-induced skipping, the 2'OMeAOs were tested at a range of concentrations from 600nM to 5nM. Separate transfections with each 2'OMeAO resulted in marked increases in exon 19 skipping between the minimum concentration required and 100nM. However, 2'OMeAO transfection concentrations of 600nM, the highest dose tested, generally resulted in only marginal increases in the level of induced transcript compared to that induced by a 2'OMeAO at 100nM (Figure 4.10). Furthermore, the highest transfection concentration of 600nM was never able to cause 100% exon 19 skipping as detected by RT-PCR, presumably because some full-length mRNA would be present prior to the transfection. Moreover, an increase in the concentration of the 2'OMeAO (with a concomitant rise in the amount of Lipofectin), was associated with an increase in the degree of cell damage after transfection.

A dosage effect was clearly evident with all 2'OMeAOs tested. HM19A(+35+65), HM19A(+46+65) and HM19A(+35+54) all induced precise and reproducible exon 19 skipping when delivered at concentrations as low as 5nM (Figure

4.10A-C), compared to the minimum transfection concentration of 20nM required for the same effect in the normal *H-2K* cells. HM19A(+49+65) and HM19A(+52+65) were again judged less efficient than the first and second generation 2'OMeAOs based on their ability to induce skipping at 50nM (Figure 4.10D,E). This, however, still represented a four-fold decrease in the minimum concentration required to consistently detect skipping induced in the normal cells, supporting the use of *H-2K mdx* muscle cells as the preferred model for assessing 2'OMeAO-induced exon skipping. Previously, HM19A(+32+45) could not consistently induce exon 19 skipping at 300nM and transfections with this 2'OMeAO at 600nM could only induce low levels of skipping (Figure 4.10F). However, the shortest 2'OMeAO tested in this study, HM19A(+46+57), was able to induce the specific removal of exon 19 at 100nM (Figure 4.10G).

Experimental controls included transfection with a random sequence 2'OMeAO at 600nM, which had similar base composition to M19A(-20+05) (Table 3.2), an uncomplexed 2'OMeAO, HM19A(+35+65), also at 600nM, and Lipofectin alone at a mock concentration of 600nM (~4µg/500µL). In all three cases, no skipping of exon 19 was ever detected (Figure 4.10A).

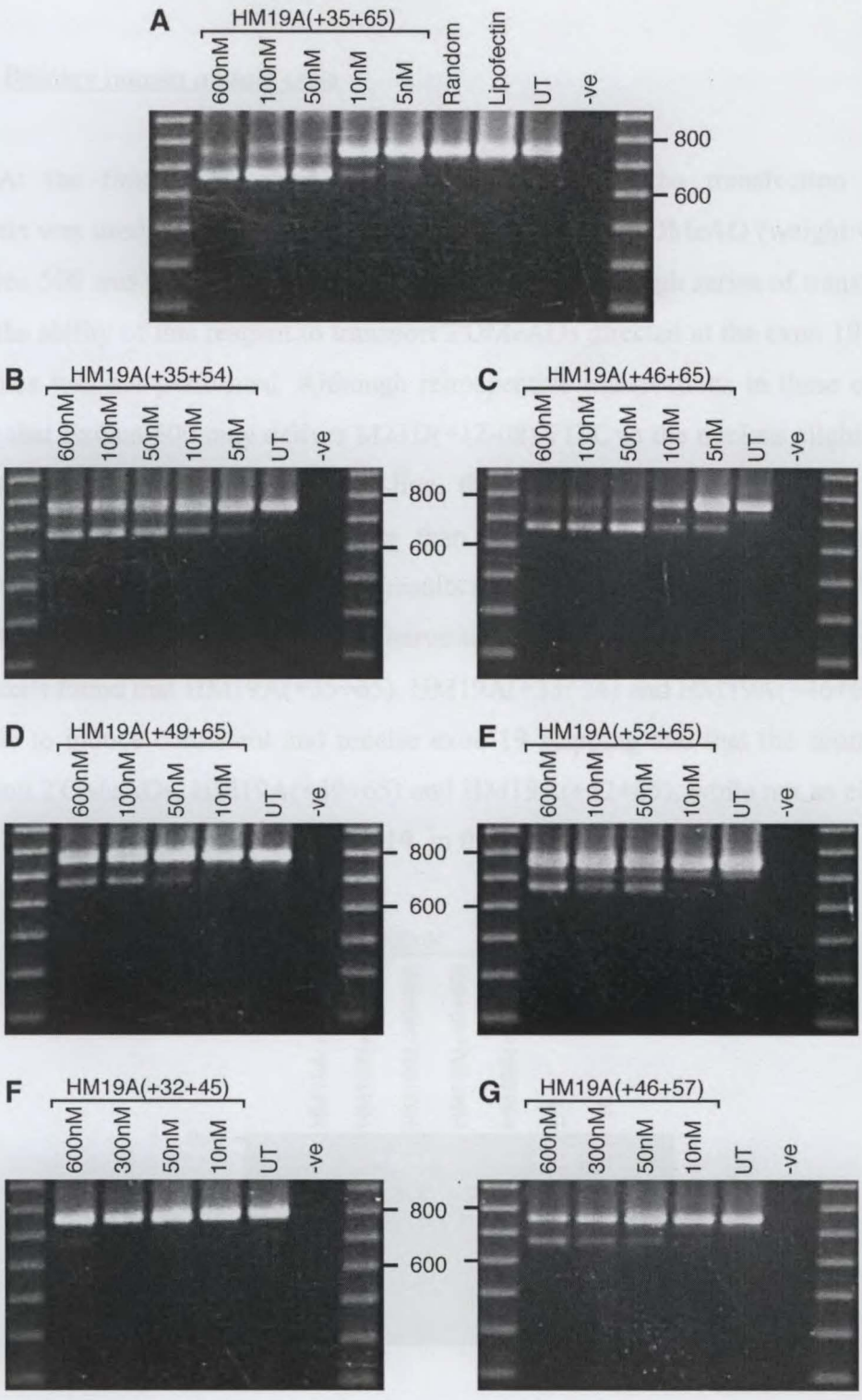

Figure 4.10 Agarose gel images of titrated 2'OMeAOs directed at exon 19. A 2'OMeAO consisting of a random arrangement of a similar base composition to HM19A(-20+05), as well as Lipofectin only, were used as controls in panel A.

4.3.2 Exon 19 skipping in human muscle cells

4.3.2.1 Primary human muscle cells

At the time these experiments were conducted, the transfection reagent Lipofectin was used at the optimised ratio of 2:1 Lipofectin:2'OMeAO (weight:weight). As ExGen 500 was evaluated only late in the project, a thorough series of transfections testing the ability of this reagent to transport 2'OMeAOs directed at the exon 19 ESE or splice sites was not performed. Although retrospective transfections in these cells did indicate that ExGen 500 may deliver M23D(+12-08)-FITC to the nucleus slightly more efficiently in the primary human cell line, the 2'OMeAO-induced exon 19 deleted product at no stage appeared stronger than its counterpart induced by the same 2'OMeAOs complexed with Lipofectin (results not shown).

RT-PCR analysis of the RNA harvested from 2'OMeAO-transfected primary human cells found that HM19A(+35+65), HM19A(+35+54) and HM19A(+46+65) were each able to induce consistent and precise exon 19 skipping and that the shorter third generation 2'OMeAOs, HM19A(+49+65) and HM19A(+52+65), while not as effective, could still prevent the inclusion of exon 19 in the final transcript (Figure 4.11).

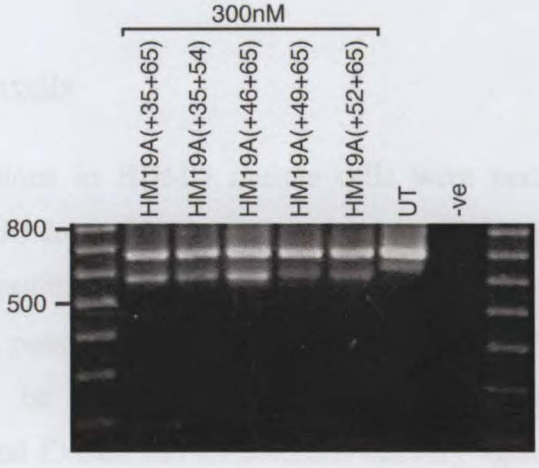

Figure 4.11 Agarose gel image of exon 19 skipping induced by 1st, 2nd and 3rd generation 2'OMeAOs when transfected into primary human cells at a final dose of 300nM.

Titrations to determine a minimum concentration at which skipping could be detected found that HM19A(+35+65), HM19A(+35+54) and HM19A(+46+65) could each induce the consistent removal of exon 19 at a concentration of at least 200nM. However, the shorter 2'OMeAOs, HM19A(+49+65) and HM19A(+52+65), required a final transfection concentration of no less than 300nM for the same reproducible effect (results not shown).

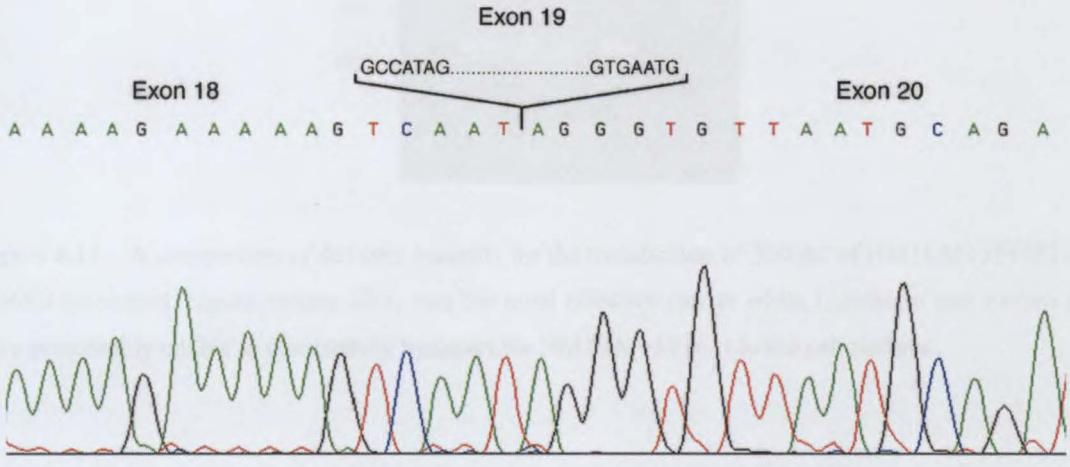

Figure 4.12 DNA sequence chromatogram of the PCR products across the junction of human dystrophin exons 18 and 20, indicating precise removal of exon 19.

4.3.2.2 HDMD muscle cells

Initial transfections in HDMD muscle cells were performed by complexing Lipofectin with a 300nM dose of 2'OMeAO at the optimised ratio in mouse cells of 2:1 (weight:weight). The resulting induced transcripts were difficult to detect and were only observed at low levels, possibly indicating that delivery of the 2'OMeAO to the nucleus of these cells may be a limitation. Subsequent experiments also evaluated Lipofectamine 2000 and ExGen 500 as potential delivery agents for the fluorescently labelled 2'OMeAO, M23D(+12-08)-FITC. It was found that Lipofectin at 2:1 (carrier:2'OMeAO), Lipofectamine 2000 at 3:1 (carrier:2'OMeAO), and ExGen 500 at 4 equivalents were the optimal ratios for each carrier molecule to 2'OMeAO, with the least degree of cytotoxicity or excess extracellular aggregates. Furthermore, in a directly comparable experiment, 300nM of HM19A(+35+65) was transfected separately using each of the delivery agents at their optimised ratio (or equivalents). We found that Lipofectamine 2000 at a ratio of 3:1 (weight:weight) was the only reagent able to

efficiently deliver the 2'OMeAO and result in a comparatively stronger exon 19 deleted product detected by RT-PCR (Figure 4.13).

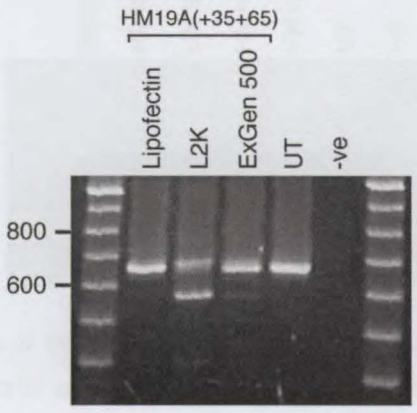

Figure 4.13 A comparison of delivery reagents for the transfection of 300nM of HM19A(+35+65) into HDMD myoblasts. Lipofectamine 2000 was the most effective carrier while Lipofectin and ExGen 500 were presumably unable to consistently transport the HM19A(+35+65) to the cell nucleus.

Following these findings, each first, second and third generation 2'OMeAO directed at the exon 19 ESE was transfected into the HDMD cells at a final concentration of 300nM complexed with Lipofectamine 2000. Twenty-four hours post-transfection, the RNA was harvested and assayed for the presence of the exon 19 deleted transcript. HM19A(+35+65), HM19A(+35+54) and HM19A(+46+65) were all able to induce the precise and repeatable removal of exon 19. HM19A(+49+65) and HM19A(+52+65), however, were found to be less efficient as judged by their extremely limited ability to induce exon 19 skipping in these cells at a concentration of 300nM (Figure 4.14).

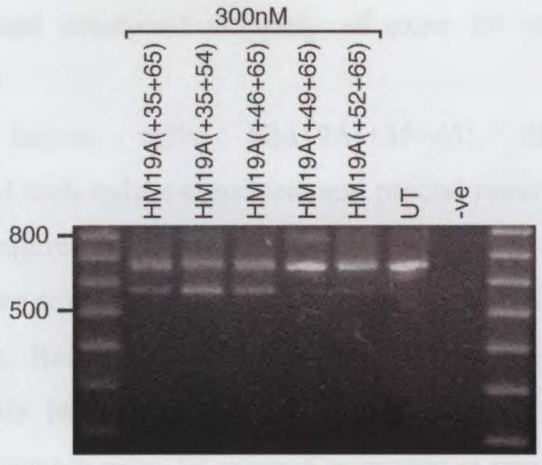

Figure 4.14 Agarose gel image of exon 19 skipping induced by 1st, 2nd and 3rd generation 2'OMeAOs when transfected into HDMD cells at a final concentration of 300nM. The skipped transcript was consistently detected, but was weaker than that observed in the normal primary cell line.

4.4 Summary

Optimisation of transfection conditions for each cell type was performed, resulting in the selection of Lipofectin at a ratio of 2:1 (Lipofectin:2'OMeAO) for transfection in *H-2K* mouse and primary human muscle cells. In HDMD cells, however, Lipofectamine 2000 at a ratio of 3:1 (Lipofectamine 2000:2'OMeAO) was the only reagent able to efficiently deliver the 2'OMeAO.

In normal *H-2K* mouse cells, exon 19 skipping was induced most effectively by HM19A(+35+65) and HM19A(+46+65), as the induced transcript could still be detected at a transfection concentration of 20nM. HM19A(+35+54) was also very effective, inducing consistent exon 19 skipping at 30nM. The shorter 2'OMeAOs, HM19A(+49+65) and HM19A(+52+65), were not as efficient, requiring concentrations of at least 200nM to achieve consistent exon 19 removal.

The same hierarchy of 2'OMeAO effectiveness was observed in the *H-2K mdx* muscle cells. However, the exon 19 skipped transcript could still be detected when the 2'OMeAOs were at lower transfection concentrations. HM19A(+35+65), HM19A(+46+65) and HM19A(+35+54) could each induce exon 19 skipping at 5nM, and HM19A(+49+65) and HM19A(+52+65) induced detectable exon 19 skipped transcripts at 50nM. In addition, it was demonstrated that the 14mer, HM19A(+32+45), designed within HM19A(+35+54), was very ineffective at inducing exon 19 skipping, even at a concentration of 600nM. However, a 12mer, HM19A(+46+57), was capable

designed within HM19A(+35+54), was very ineffective at inducing exon 19 skipping, even at a concentration of 600nM. However, a 12mer, HM19A(+46+57), was capable of inducing precise and consistent skipping of exon 19 when at a transfection concentration of 50nM.

In primary human cells, HM19A(+35+65), HM19A(+35+54) and HM19A(+46+65) could each induce consistent and precise removal of exon 19 at lower concentrations than required to achieve the same result with HM19A(+49+65) and HM19A(+52+65). These concentrations, however, were up to 40-fold greater than those used in the *mdx* cells. Results for HDMD cells were similar, except that skipped products were generally less abundant and HM19A(+49+65) and HM19A(+52+65) could not induce a detectable exon 19 skipped transcript at transfection concentrations comparable to that used in the primary human cells.

4.5 Discussion

4.5.1 Transfection reagents and cell lines

Cationic lipids have been used to enhance cellular uptake and activity of 2'OMeAOs in cell culture. One such formulation, Lipofectin, has been used as a transfection reagent for 2'OMeAOs in primary *mdx*, *H-2K mdx* and C2C12 mouse myoblasts (Mann et al., 2001; Wilton et al., 1999). Since it has been suggested that no single cationic application is optimal for all uses (Bennett, 1998), a comparison of Lipofectin with another reagent, Lipofectamine 2000, was undertaken to ensure optimal transfection conditions for each of the four cell lines to be evaluated in the current study. In addition, a 2001 study by van Deutekom and colleagues successfully employed ExGen 500 as a transfection reagent in mouse and human cells. At this time, evaluation of the 2'OMeAOs targeted to exon 19 had been completed, so ExGen 500 was investigated retrospectively, with the analysis thought to be of interest for the remaining experiments and future studies.

In optimising 2'OMeAO transfection conditions, it was found that the different transfection reagents evaluated had varying degrees of efficiency in different muscle cell lines. This is consistent with the observation that the ability of different cell types to

take up oligonucleotide molecules or liposomes varies to a large degree (Galderisi, Cascino & Giordano, 1999; Gao & Huang, 1995). This may be related to the size of the particle to be internalised and differences in the levels of endocytic activity between the different cell types (Gao & Huang, 1995). The particle size of 2'OMeAO-liposome complexes (lipoplexes) varies, and appears to be dependent on a combination of the cationic liposome formulation used and the final concentration of the lipoplex (Gao & Huang, 1995). The results presented in this thesis emphasise the necessity for optimising 2'OMeAO delivery for each cell type.

In *H-2K* mouse myoblasts, Lipofectin at a ratio of 2:1 appeared to be an effective transfection reagent, as nuclear fluorescence was observed in approximately 100% of cells at 24 hours post-transfection, and cell death was not observed, consistent with previous reports (Mann et al., 2001; Wilton et al., 1999). In contrast, *H-2K* cells transfected with Lipofectamine 2000 complexed with M23D(+12-08)-FITC did not exhibit the same degree of distinct nuclear localisation and displayed fluorescent aggregates when higher ratios of Lipofectamine 2000 to 2'OMeAO were used. Interestingly, these same aggregates were observed following transfection with high doses of ExGen 500. Cells transfected with this reagent showed predominant nuclear localisation of the fluorescent 2'OMeAO at 24 hours post-transfection and there was no toxic reaction at the optimal dose of 3.5eq, consistent with observations reported previously (Dunckley et al., 1998; van Deutekom et al., 2001).

It is unclear why cells transfected with ExGen 500 or Lipofectamine 2000 at doses required to achieve significant nuclear localisation were observed to have fluorescent aggregates at 24 hours post-transfection. These cytoplasmic structures could represent the internalised 2'OMeAO-liposome complexes (lipoplexes) within endosomes or lysosomes (Bennett, 1998). Their presence may be related to the amount of time the lipoplexes spend in the endosome, determined by the differing mechanisms of action of the reagents. For example, the DOPE component of Lipofectin is thought to function by reducing the aggregation of complexes and facilitating the release of the 2'OMeAO from the endosome after internalisation (Zelphati & Szoka, 1996). While DOPE is also one of the constituents of Lipofectamine 2000, it represents a lower proportion of the liposome formulation compared to Lipofectin. As the efficiency of the cytoplasmic release is determined by the DOPE content of the liposomes (Gao & Huang, 1995), it can be assumed that Lipofectin would be more efficient in releasing

the 2'OMeAO. ExGen 500 has been suggested to act by buffering the acidic endosomal environment, thereby protecting the 2'OMeAO until it is released into the cytoplasm by subsequent endosomal swelling and rupture (Boussif et al., 1995; Kichler, Leborgne, Coeytaux, & Danos, 2001). It is therefore possible that the aggregates observed in cells transfected with Lipofectamine 2000 or ExGen 500 simply represent a slower escape from the endosome, delaying the passive diffusion of the 2'OMeAO to the nucleus. Thus, improved nuclear localisation may have been observed 48 hours post-transfection, similar to that reported by Dunckley et al. (1998).

While there were no differences in M23D(+12-08)-FITC uptake for any of the transfection reagents between the *H-2K* normal and *mdx* cells, results did differ between primary human and HDMD cells. In the primary human cells, Lipofectin at a ratio of 2:1 was found to be the most effective reagent, although the fluorescence was observed to be more diffuse throughout the cell (and less localised to the nuclei) compared to that observed in mouse cells. Lipofectamine 2000, at the ratio required to achieve a comparable degree of nuclear localisation, again resulted in high levels of cell death. ExGen 500 performed most effectively at 3.5 eq, consistent with the findings of van Deutekom et al. (2001) for human muscle cells. In contrast, HDMD cells required higher doses of each delivery reagent to achieve efficient fluorescent 2'OMeAO transfection, with Lipofectamine 2000 proving to be the best carrier at a ratio of 3:1. Interestingly, this ratio was associated with a much lower level of cell death than that observed in *H-2K* mouse and primary human cells when transfected with the same concentration of Lipofectamine 2000, again highlighting the importance of optimising transfection conditions for each cell type.

4.5.2 Exon 19 skipping in *H-2K* normal and *mdx* muscle cells

Our initial attempts to induce dystrophin exon 19 skipping were undertaken using the conditionally immortalised normal *H-2K* mouse myoblast cell line. However, in unaffected cells, dystrophin mRNA missing exon 19 is out-of-frame and would be subject to nonsense mediated decay (Maquat, 1995). Therefore, detection of the exon 19-deleted message was anticipated to be more difficult relative to the more stable wild-type mRNA. Based on the results of these early investigations, it was hypothesised that a better estimate of the extent of skipped and full-length transcript could be

achieved using the *H-2K mdx* cell line, where both natural and 2'OMeAO-induced dystrophin transcripts should be metabolised at comparable rates.

As anticipated, a higher abundance of exon 19 skipped transcripts was detected in the 2'OMeAO-transfected *H-2K mdx* muscle cells, as compared to those detected in the *H-2K* normal muscle cells that had been transfected with the same concentration of 2'OMeAO. For both cell lines, the same transfection reagent was used and the nuclear fluorescence observed was identical at each ratio and at each time point tested. This would suggest that the difference in stability and metabolism of the endogenous and 2'OMeAO-induced skipped transcripts is a more likely explanation than the efficiency of the transfection process.

Although 2'OMeAO efficiency differed between *H-2K* normal and *mdx* muscle cells, the pattern of efficiency of individual 2'OMeAOs was very similar. This study investigated the effect of several 2'OMeAOs in both cell lines. The first generation 2'OMeAO evaluated, HM19A(+35+65), originally designed by Takeshima et al. (1995), was able to consistently induce the efficient and precise removal of exon 19. However, a study by Pramono et al. (1996), reported that an antisense oligodeoxynucleotide version of HM19A(+35+65) was able to induce 100% exon 19 skipping 24 hours after transfection in normal human lymphoblastoid cells. The present project was unable to induce exon 19 removal from all transcripts in either mouse or human muscle cells. This discrepancy may be due in part to the difference in levels of dystrophin expression in each cell type. Human lymphoblastoid cells are known to produce very low levels of dystrophin mRNA by illegitimate transcription (Chelly et al., 1988), and we have previously shown that a 2'OMeAO could induce 100% exon skipping in myoblast cultures where there were also low levels of dystrophin expression (Wilton et al., 1999). However, the same 2'OMeAO was less effective in *H-2K* muscle cells, where much higher levels of dystrophin are synthesised (Mann et al., 2001).

Perhaps more significant is the difference in the chemistry of the antisense agents utilised. DNA:RNA duplexes are cleaved by RNaseH (Furdon, Dominski & Kole, 1989). Therefore, the selection of a DNA AO in the Pramono et al. (1996) study could have biased their assay, as any full-length message may have been degraded through RNaseH activity, leaving only the induced transcripts missing exon 19 to be detected by RT-PCR. Subsequent studies from this same group using a dystrophic primary human muscle cell line deleted for exon 20 did not report the same high level

of induced in-frame transcript using 2'OMeAO chemistry (Takeshima et al., 2001). Finally, normal dystrophin mRNA has an estimated half life of some 16 hours (Tennyson et al., 1995), so even if 2'OMeAO-induced exon skipping was 100% efficient soon after transfection and nuclear uptake, some full-length mRNA would be expected to remain in the cytoplasm after 24 hours.

The main focus of this section of the project was to attempt to refine the ESE motif within dystrophin exon 19. ESEs are thought to play a critical role in correct splice site selection through cross-exon interactions between splicing factors bound to the 3' and 5' splice sites (Reed, 1996), perhaps promoting the use of nearby weak splice sites (Coulter, Landree & Cooper, 1997; Tanaka et al., 1994; Watakabe et al., 1993). Disruption of an ESE can lead to partial or complete exon skipping (Liu, Cartegni, Zhang & Krainer, 2001a), either through alterations in secondary structure (Cartegni, Chew & Krainer, 2002; Watakabe et al., 1993) or disruption of sequences crucial for recognition by splicing factors such as SR proteins. These proteins are thought to recruit components of the general splicing machinery (Black, 1995; Reed, 1996). It has been suggested that targeting exonic sequences with 2'OMeAOs may result in more efficient and specific exon skipping than targeting splice sites, as there is less disruption to the splicing process; the exon is simply not marked for inclusion (van Deutekom & van Ommen, 2003).

The hierarchy of 2'OMeAO efficacy followed a similar pattern in each cell line. However, the *H-2K mdx* myoblasts will be discussed in greater depth as this cell line represented the best molecular model for 2'OMeAO-induced exon skipping. Exon 19 was initially targeted for 2'OMeAO-induced skipping by the first generation 31mer HM19A(+35+65). This 2'OMeAO, directed at a region containing two ESE-like polypurine stretches (GCAAGA and AGCAGA - Pramono et al., 1996; Takeshima et al., 1995), could induce consistent and precise exon 19 skipping at very low concentrations (5nM). Subsequently, a second generation of two overlapping 20mers was designed to the upstream and downstream portions of this region to determine which (if either) was more significant to the splicing process. The downstream HM19A(+46+65) was consistently more efficient than the upstream HM19A(+35+54), based on the relative abundance of exon 19 skipped transcripts. Although secondary structure has been suggested as a limiting factor in hybridisation (Crooke, 1999; Dagle & Weeks, 2001) and therefore 2'OMeAO-induced exon skipping, the 31mer was able to

induce exon skipping at the same level of efficiency as the downstream 20mer. Therefore, it is doubtful that the difference between the performance of the two second generation 2'OMeAOs was due to accessibility to their respective targets. A second consideration is that the annealing potentials of the two 20mers differed. As the annealing temperature (T_m) increases with higher G/C content, it is possible that the upstream 20mer annealed less efficiently than its downstream counterpart, as the G/C contents were 50% and 65% respectively. Both 2'OMeAOs should still anneal efficiently at 37°C, so it is likely that the motif crucial for splicing enhancement of exon 19 resides in the downstream region targeted by HM19A(+46+65).

Consequently, the third generation of 2'OMeAOs was designed within the downstream 20mer to further define the ESE motif. An additional aim was to assess a likely minimum threshold for 2'OMeAO length, as indicated by the ability of the 2'OMeAO to hybridise under cellular conditions and to carry out the desired effect (Dagle and Weeks, 2001). The 17mer, HM19A(+49+65) induced exon 19 skipped products of higher abundance than that induced by the 14mer, HM19A(+52+65), however both were less efficient compared to the first and second generation 2'OMeAOs. Since the T_m of the 2'OMeAO:pre-mRNA complex decreases with a concomitant decrease in length, shorter 2'OMeAOs may have lower affinity to the target sequence at 37°C (Agrawal, 1992; Crooke, 1999). Thus the reduced length of the 17mer and 14mer may have resulted in a diminished level of affinity to their target sequences, particularly since the G/C contents of these two 2'OMeAOs (59% and 57% respectively) were actually higher than that of the more efficient upstream 20mer. Alternatively, the lower abundance of the exon 19-skipped transcripts may indicate that the 17mer and 14mer were targeted too far downstream and were no longer blocking the ESE from splicing factors as effectively as the longer 2'OMeAOs.

It is possible that the crucial region is at least partly within the area overlapped by the two 20mers but extends more into the downstream portion of the exon. This could account for the more efficient skipping induced by HM19A(+46+65) compared to the upstream 20mer, and the ability of the 17mer and 14mer to induce precise skipping of exon 19, albeit at low levels, despite the reduced length.

To test the hypothesis that the region crucial for exon inclusion lay within the overlap of the two 20mers, a fourth generation consisting of two 2'OMeAOs were designed and evaluated in *H-2K mdx* cells. Consistent with this hypothesis, a 14mer

HM19A(+32+45), targeted to the 14 bases commencing two nucleotides upstream of the overlap, was unable to induce reliable exon 19 skipping, even at a final transfection of 600nM. The targeted region included the upstream purine-rich ESE-like motif identified previously (Figure 4.8; Pramono et al., 1996; Takeshima et al., 1995). However, although ESEs commonly occur in purine-rich or A/C-rich regions (Coulter, et al., 1997; Tanaka et al., 1994), it has been noted that many natural sequences that are ESE-like do not function as ESEs unless they occur in an appropriate context (Liu et al., 1998). It is unlikely that the inefficiency of this 2'OMeAO could be due to secondary structure as the 31mer and upstream 20mer targeting the same area were efficient in inducing exon 19 skipping. The difference between these 2'OMeAOs was that the regions targeted by HM19A(+35+65) and HM19A(+35+54) also included the downstream polypurine ESE-like motif, whereas HM19A(+32+45) did not (Figure 4.8; Pramono et al., 1996; Takeshima et al., 1995). Decreased length, while a possible factor, is also unlikely to explain the failure of HM19A(+32+45) to induce efficient exon skipping as the 14mer, HM19A(+52+65), directed at the downstream region, was successful. Interestingly, the G/C content of the region targeted by HM19A(+32+45) was 36%, the lowest of the 2'OMeAOs tested. A reduction in annealing temperature resulting from the combination of decreased length and lower G/C content could partially account for the inefficiency of this 2'OMeAO. A likely additional factor could be that the sequence targeted, despite containing a region which resembled an ESE, was not as important to exon inclusion as the region containing the downstream motif. In addition, the 12mer HM19A(+46+57), which was directed at the downstream motif, was able to induce consistently precise skipping of exon 19, although less effectively than the 14mer HM19A(+52+65) and 17mer HM19A(+49+65). This suggests that although the shorter length of this 2'OMeAO may have reduced its annealing temperature, a motif crucial for exon 19 inclusion was contained within the target sequence. Whether the 2'OMeAO-induced skipping of exon 19 was effected by alterations in secondary structure or by disruption of sequences crucial for recognition by splicing factors remains unclear.

4.5.3 Exon 19 skipping in primary human and HDMD muscle cells

The 31 base region of exon 19 containing the putative ESEs was homologous in mouse and human cells, allowing the 2'OMeAOs directed at this region to be tested on both species. In primary human and HDMD cells, the hierarchy of 2'OMeAO efficacy followed a similar pattern to that observed in the mouse cells, as discussed previously (Section 4.5.2). Compared to the mouse cells, however, the 2'OMeAOs were not as efficient in human cells, requiring higher concentrations to achieve consistent exon 19 skipping. This was particularly evident in the HDMD cell line. The differences between the level of 2'OMeAO-induced exon 19 skipped transcripts between the normal cell lines and the cell lines with dystrophin gene mutations may be partly due to the variation in turn over rates of natural and exon 19 skipped products (Maquat, 1995). However, the differences in 2'OMeAO-induced skipping efficiency between primary human and *H-2K* normal mouse cells (unaffected cell lines), or between HDMD and *H-2K mdx* cells (affected cell lines), may not be attributable to variations in transcript turnover rates as the natural and skipped transcripts should be metabolised at similar rates in each case.

The reason for the apparent disparity in the expected abundance of exon 19 skipped transcript detected in the human and mouse cells is unclear. It is possible that there are differences in target site accessibility between species or that the ESEs in the human exon 19 were not as significant to exon inclusion as those in the mouse exon 19. It has been suggested that ESEs promote the use of nearby weak splice sites (Coulter et al., 1997; Tanaka et al., 1994; Watakabe et al., 1993). However, the strength of the exon 19 acceptor and donor splice sites in human (93% and 76% respectively) and mouse (91% and 78% respectively), are very similar (Senapathy, Shapiro & Harris, 1990), which should indicate a similar reliance on ESEs or other enhancers. The difference in ability to detect the induced transcript at lower transfection concentrations between mouse and human cells is more likely to be due to differences in efficiency of 2'OMeAO delivery to the nucleus, consistent with the results of the fluorescence studies (Section 4.1.2).

It has been noted that primary cells are typically more sensitive to the effects of antisense oligonucleotides than transformed cells (Baker et al., 2001). This may partially account for the decreased efficiency of the 2'OMeAOs in HDMD cells compared to the primary human cells. However, this did not appear to limit the

performance of 2'OMeAOs in the transformed *H-2K* cell lines, which supports the efficiency of the transfection process as the major limiting factor in the performance of the 2'OMeAOs in human cell lines. Although it is possible that further optimisation of the transfection process may have yielded more efficient 2'OMeAO-induced skipping of exon 19, this study has demonstrated that the direction of 2'OMeAOs to ESEs is a viable approach to the modification of splicing in human cells.

Chapter 5 - Targeting exon 19: 2'OMeAOs directed at the acceptor and donor splice sites

Previously, studies involving the 2'OMeAO-induced removal of exon 23 in the *mdx* mouse involved targeting the acceptor or donor splice sites (Dunckley et al., 1998; Mann et al., 2001; Wilton et al., 1999). These splice sites were obvious targets as ESEs are often ill- defined, but characterised by purine-rich regions within an exon. However, it has been suggested that the targeted 2'OMeAO-induced removal of an exon may be more specific if these exonic motifs are employed (van Deutekom et al., 2001). In the previous chapter, it was shown that the ESE was intimately involved with the precise definition of exon 19. Therefore, the next logical step was to evaluate the splice sites of exon 19 as potential targets for the specific removal of this exon in mouse and human dystrophin pre-mRNA.

Furthermore, the effect of targeting multiple sites with combinations of 2'OMeAOs was investigated to determine if the 2'OMeAO-induced removal of exon 19 could be enhanced while maintaining its specificity.

Finally, to ensure specificity of the antisense activity of the 2'OMeAOs, two further assays were undertaken. First, mismatched 2'OMeAOs directed at the acceptor and donor splice sites in mouse and human cells were assessed for their ability to induce exon 19 skipping. Second, additional screens were performed to determine whether the splicing patterns in other regions of the dystrophin gene transcript were affected by the 2'OMeAOs directed at exon 19.

5.1 Quality assay of 2'OMeAOs directed at the exon 19 splice sites

All but one 2'OMeAO of the five designed to target the splice sites of exon 19 in either mouse or human cell lines were part of the third generation of 2'OMeAO design synthesised by Geneworks. M19D(+02-18), was designed to be a refined version of M19D(+05-20) (a third generation 2'OMeAO synthesised 'in-house'). However, to maintain consistency, all 2'OMeAOs targeting splice sites were subject to the same quality check. As described earlier, ~200ng of each 2'OMeAO was complexed with formamide loading buffer and electrophoresed through a denaturing polyacrylamide gel (Figure 5.1). In most cases the 2'OMeAO integrity was confirmed to be relatively high with a predominant single band indicating the full length 2'OMeAO. Furthermore, the

quality of M19D(+02-18) validated the acceptable standard of manufacture of the 'in-house' synthesised 2'OMeAOs compared to those commercially available, although the yield was lower than expected and subsequently corrected prior to evaluation in cell culture.

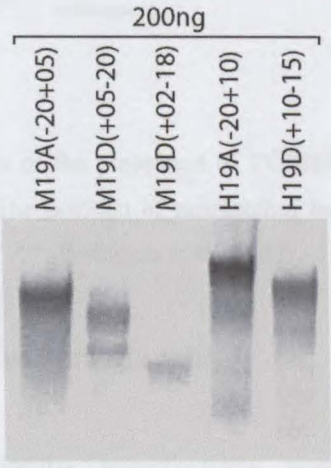

Figure 5.1 Each 2'OMeAO targeting the splice sites for both mouse and human dystrophin exon 19 was run on a denaturing polyacrylamide gel to assess the standard of synthesis. As apparent yields varied, 2'OMeAO concentrations were adjusted and evaluated by spectrophotometry prior to cell transfection.

5.2 Induction of exon 19 skipping across species using 2'OMeAOs directed at the splice sites

As exon 19 removal had only been attempted by directing 2'OMeAOs at the ESEs, it was necessary to evaluate the splice sites as possible targets for exon skipping. Earlier investigations by our group involved the 2'OMeAO-induced removal of exon 23 by targeting the donor splice site (Mann et al., 2001; Wilton et al., 1999). Attempts to repeat the work reported by another group that induced the non-specific removal of exons 22-30 by directing 2'OMeAOs at the acceptor site (Dunckley et al., 1998), however, were not successful (Mann et al., 2001; Wilton et al., 1999). In this study we designed 2'OMeAOs to target either the acceptor or donor splice sites and wished to compare these regions to the ESE targeted earlier. The choice to direct the 2'OMeAOs at mostly intronic sequence was based on the early findings of our group which found the more exonic sequences in the donor splice site region to be less effective at inducing exon 23 skipping (Mann et al., 2001; Mann et al., 2002; Wilton et al., 1999) (Figure 5.2).

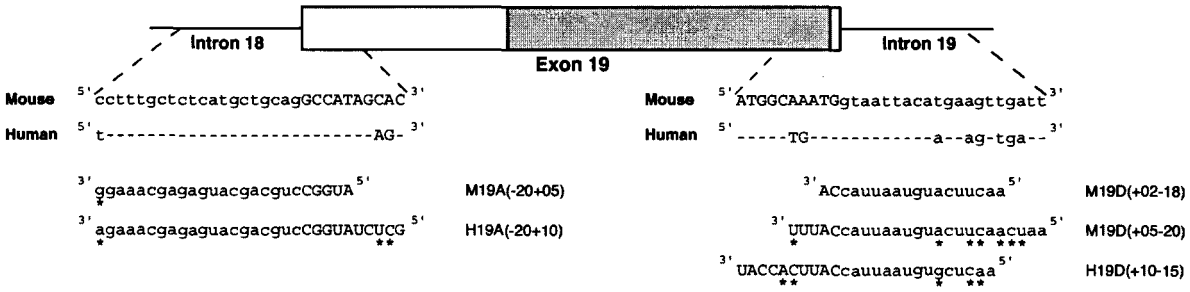

Figure 5.2 Schematic representation of the placement of 2'OMeAOs targeting the mouse and human splice sites of dystrophin exon 19. The position of mismatches between species sequence and species specific 2'OMeAOs are indicated by " * " (Errington et al., 2003).

5.2.1 Exon 19 skipping in mouse muscle cells

All *H-2K* mouse myotube transfections were performed by complexing Lipofectin at the ratio of 2:1 Lipofectin:2'OMeAO (weight:weight) with each 2'OMeAO at a standard dose of 300nM. Total RNA was extracted from pooled duplicate wells 24 hours post-transfection and purified for analysis of the dystrophin gene transcripts by RT-PCR.

5.2.1.1 *H-2K* normal muscle cells

Initial experiments assessed only one 25mer 2'OMeAO directed at each splice site M19A(-20+05) or M19D(+05-20) (Table 3.2 and Figure 5.2). In the *H-2K* normal cells, the donor site appeared to be the more amenable target, as M19D(+05-20) would induce a consistently stronger exon 19 skipped transcript compared to M19A(-20+05) (Figure 5.3). In fact, analysis of the minimum effective dose for both 2'OMeAOs revealed that transfection of M19D(+05-20) at a final concentration of 100nM could still induce exon 19 skipping, whereas M19A(-20+05) could not consistently remove exon 19 when the transfection concentration was below 300nM (results not shown). It should also be noted that at no time did transfections with M19A(-20+05) or M19D(+05-20) induce the removal of any other exons, nor did their presence initiate any aberrant splicing at cryptic splice sites. Exon 19 removal was always found to be precise, with exon 18 joined exactly to exon 20 (Figure 4.7).

5.2.1.2 *H-2K mdx* muscle cells

Based on the results from the *H-2K* normal muscle cell transfections with M19A(-20+05) and M19D(+05-20), it was anticipated that the exon 19 skipped transcript would be easier to detect in *mdx* muscle cells due to nonsense mediated decay of both wild-type and 2'OMeAO-induced messages at similar rates. Initial experiments in the *H-2K mdx* cells demonstrated more abundant exon 19 deleted transcript fragments following transfection with the splice site-directed 2'OMeAOs M19A(-20+05) and M19D(+05-20) at 300nM (Figure 5.3). The natural (full length) *H-2K mdx* transcripts appeared to be less abundant when compared to the normal intact transcript. As some degree of full length *H-2K mdx* transcript would be expected to be present before the 2'OMeAO was added to the cells, these results suggest that the 2'OMeAO-induced skipping of exon 19 in the *H-2K mdx* cells was very efficient, particularly when the donor site was targeted.

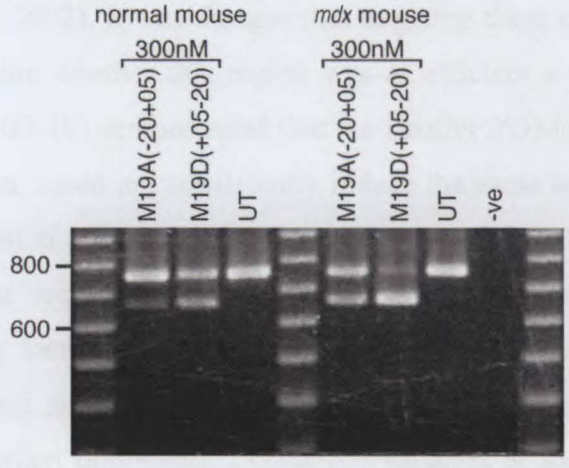

Figure 5.3 Comparison of exon 19 skipping induced by 2'OMeAOs directed at the acceptor or donor splice site in *H-2K* normal and *mdx* mouse mRNA. RT-PCR analysis of RNA harvested 24 hours after cultured myotubes were transfected with 2'OMeAOs at 300nM. Shortened transcripts appeared to be moderately more abundant in the *mdx* cell line. The full-length product spanning exons 17 to 21 is 761 bases long and the shorter product is missing 88 bases due to the precise removal of exon 19.

A titration of M19A(-20+05) and M19D(+05-20) demonstrated that both 2'OMeAOs were consistently able to induce the shortened transcript when transfected at a dose as low as 10nM, although the abundance of the induced transcript was slightly higher in cells transfected with the donor site-directed 2'OMeAO. This was despite the apparent lower quality of M19D(+05-20) compared with M19A(-20+05) (Figure 5.1), demonstrating that the shorter bands, which still contain the same sequence as the full length 2'OMeAO, do not compromise the ability of the 2'OMeAO to induce efficient exon skipping. Interestingly, the lowest effective concentration for either splice site-directed 2'OMeAO was only 5nM more than that required by the best 2'OMeAOs directed at the ESE. This effect was not seen in normal mouse cells which further validates the use of *mdx* muscle cells to assess 2'OMeAO effectiveness *in vitro*.

As the sequence targeted by M19D(+05-20) appeared to be the most sensitive to 2'OMeAO-induced exon skipping, M19D(+02-18) was designed to determine if the original target region could be further refined. This 2'OMeAO was directed at the same exon:intron coordinates which had proved efficient for 2'OMeAO-induced skipping of exon 23 (Mann et al., 2002). It was thought that targeting these coordinates in exon 19 could help to determine whether this region was as efficient a target in other exons. Titrations of M19D(+02-18) demonstrated that the smaller 2'OMeAO, while targeting a highly sensitive region, could not consistently induce the same level of skipping as the parent 2'OMeAO when at a final transfection concentration of 10nM (Figure 5.4). This may indicate that the sequences not obstructed were important for exon boundary definition by splicing factors, or that the longer 2'OMeAO could anneal at a higher efficiency and displace splicing factors more effectively. Interestingly, the opposite effect was reported when optimising 2'OMeAOs directed at the donor splice site of exon 23 (Mann et al., 2002). Efficient exon 23 skipping was induced using a 25mer but the motif targeted was refined by directing a smaller 20mer within the same region, suggesting that there may be specific motifs recognised by the spliceosome for individual exons or that there were differences in secondary structure which affected the ability of the 2'OMeAOs to anneal to the target sites.

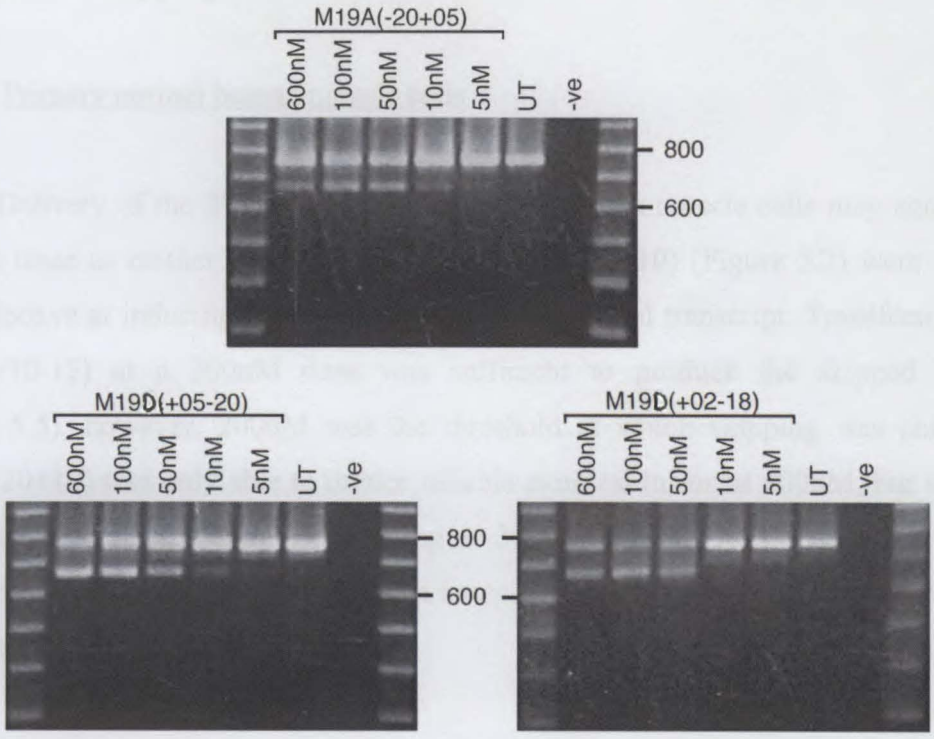

Figure 5.4 Titration of 2'OMeAOs directed at the acceptor or donor splice site of exon 19 skipping in *H-2K mdx* mouse mRNA. The smaller M19D(+02-18) directed at the donor splice site was less effective than its parent but was still consistent and completely specific.

5.2.2 Exon 19 skipping in human muscle cells

5.2.2.1 Primary normal human muscle cells

Delivery of the 2'OMeAOs in the primary human muscle cells may again have been an issue as neither H19D(+10-15) nor H19A(-20+10) (Figure 5.2) were deemed very effective at inducing exon 19 removal from the final transcript. Transfection with H19D(+10-15) at a 300nM dose was sufficient to produce the skipped product (Figure 5.5), however, 200nM was the threshold at which skipping was consistent. H19A(-20+10) was only able to induce reliable exon exclusion at 600nM, but was able on occasion to induce exon 19 skipping at 300nM (Figure 5.5), suggesting that the human acceptor splice site was the least amenable target for human exon 19 removal, similar to that of the mouse.

Figure 5.5 Exon 19 skipping induced by 2'OMeAOs directed at the acceptor or donor splice site in primary human muscle mRNA. RT-PCR analysis of RNA harvested 24 hours after cultured myotubes were transfected with 2'OMeAOs at 300nM. The full-length product spanning exons 17 to 21 is 668 bases long and the shorter product is missing 88 bases due to the precise removal of exon 19.

5.2.2.2 HDMD muscle cells

HDMD myoblasts were transfected with either H19A(-20+10) or H19D(+10-15) at 300nM complexed with Lipofectamine 2000 at a 3:1 ratio. RT-PCR analysis of the transcripts showed a similar pattern to that seen in the primary human cells. While the exon 19 skipped transcripts were of much lower abundance in the less reliable HDMD

cells, the donor site usually appeared to be the more amenable of the two targets to antisense modification (Figure 5.6).

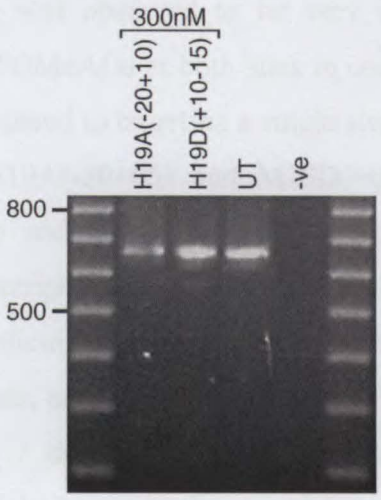

Figure 5.6 Agarose gel image of exon 19 skipping in HDMD muscle cells. Each splice site-directed 2'OMeAO was transfected into the cells at a final concentration of 300nM. The skipped transcript was consistently detected but also weaker than that observed in the unaffected primary cell line.

The shorter transcript fragment was isolated from the gel by the bandstab procedure (Wilton et al., 1997b) and analysed by direct sequencing. The identity of the 668bp product was confirmed to be exon 18 joined precisely to exon 20, again verifying the specific action of each splice site-directed 2'OMeAO to induce precise exon 19 skipping in HDMD myoblast mRNA (Figure 4.12).

5.3 Targeting multiple sites

When targeting either the ESE or splice sites of dystrophin exon 19, the 2'OMeAO-induced skipping was observed to be very effective in some cells. We therefore tested if directing 2'OMeAOs at both sites in combination would enhance the action of the 2'OMeAOs compared to targeting a single site.

HM19A(+35+65), M19A(-20+05) and M19D(+05-20) were transfected into *mdx* myotubes individually and at the concentration equating to the threshold of detection of the induced transcript by our standard RT-PCR assay. Each 2'OMeAO was added to target the three splicing motifs according to the 4 possible combinations; acceptor and donor splice sites, acceptor splice site / ESE, ESE / donor splice site and acceptor splice site / ESE / donor splice site. In these combinations, the final concentration was the sum of the concentrations used for each individual 2'OMeAO.

Twenty-four hours post-transfection, RNA was extracted and analysed by RT-PCR. When transfected singly, the shortened product was barely visible on the gel relative to the natural product. However when added to the cells together, each combination appeared to have a synergistic effect. Furthermore, targeting all three sites in concert seemed to elicit a degree of skipping greater than the sum of all three 2'OMeAOs singly (Figure 5.7). This may indicate that adding low doses of 2'OMeAOs that block each motif, rather than high doses of a 2'OMeAO which targets a single splicing motif, may be preferable.

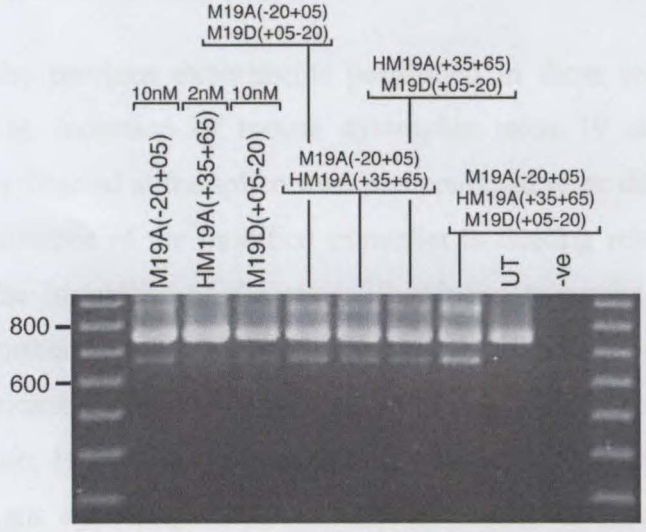

Figure 5.7 Exon 19 skipping induced by targeting multiple sites with 2'OMeAOs. Singly HM19A(+35+65) was transfected at 2nM, M19A(-20+05) at 10nM and M19D(+05-20) at 10nM. Alone, each could barely induce exon 19 skipping but in combination the level of skipped product increased.

5.4 Mismatched 2'OMeAOs

As one of the essential antisense controls, it was necessary to investigate potential nonspecific effects of 2'OMeAO mismatches on the ability to remove exon 19 from the mature transcript. Unlike the exonic region bounded by HM19A(+35+65), target sequence homology between the human and mouse genes was not conserved at the acceptor and donor splice sites. This allowed some mismatched controls (Stein & Krieg, 1994) when the 2'OMeAOs H19A(-20+10) and H19D(+10-15) were transfected into mouse cells and M19A(-20+05) and M19D(+05-20) were transfected into the human cells (Figure 5.2).

5.4.1 Human-specific 2'OMeAOs directed at mouse pre-mRNA

H19A(-20+10), the 2'OMeAO directed at the human intron 18 acceptor splice site, extended 5 nucleotides further into the exon than M19A(-20+05). H19A(-20+10) differed from the mouse sequence by 3 nucleotides, one at the 3' end and the other two at the penultimate and antepenultimate bases of the 5' end, thereby providing perfect sequence homology between bases -19 and +07. The 2'OMeAO H19D(+10-15), which is directed at the human intron 19 donor splice site, has 5 mismatches but is identical to the mouse sequence from bases +04 to –09 (Figure 5.2).

5.4.1.1 *H-2K* normal muscle cells

Based on the previous experiments performed in these cells using perfectly matched 2'OMeAOs, induction of mouse dystrophin exon 19 skipping by human specific 2'OMeAOs directed at the splice sites was predicted to be difficult to detect. As shown earlier, persistence of the modified transcript is fleeting relative to the natural message, due to the instability of the exon 19 skipped transcript through nonsense mediated decay. Furthermore, the number of mismatches with the target sequence was expected to significantly decrease the 2'OMeAO's annealing potential. Consistent with this expectation, H19D(+10-15) was not able to induce the removal of exon 19, despite the donor site appearing to be the more amenable of the two splice sites to 2'OMeAO manipulation with the mouse-specific 2'OMeAO (Section 5.2.1.1., Figure 5.8). However, exon 19 skipping was consistently detected in cells transfected with H19A(-20+10) at a final concentration of 600nM, and sporadically at a final

concentration of 300nM. This could be due to the longer region (26 bases) of perfect homology between this 2'OMeAO and its target region.

Figure 5.8 Human specific 2'OMeAOs directed at normal *H-2K* mouse pre-mRNA. Both 2'OMeAOs were transfected separately at 600nM and 300nM and RNA extracted 24 hours later. RT-PCR analysis across the region targeted by H19A(-20+10) could detect only a low level of exon 19 skipping. H19D(+10-15) was unable to induce the removal of exon 19 on every attempt.

5.4.1.2 *H-2K mdx* muscle cells

As observed earlier in the transfected *mdx* cultures, a higher level of the dystrophin mRNA transcript missing exon 19 was detected relative to the full length transcript. Despite the mismatches in the 2'OMeAO sequence, H19A(-20+10) was occasionally able to induce exon 19 skipping in *mdx* cultures at a transfection concentration of 50nM, but only consistently when delivered at 100nM (Figure 5.12). While H19D(+10-15) could induce the sporadic and very weak excision of exon 19 at several of the concentrations tested, it could not consistently induce skipping even at a final transfection concentration of 600nM (Figure 5.9).

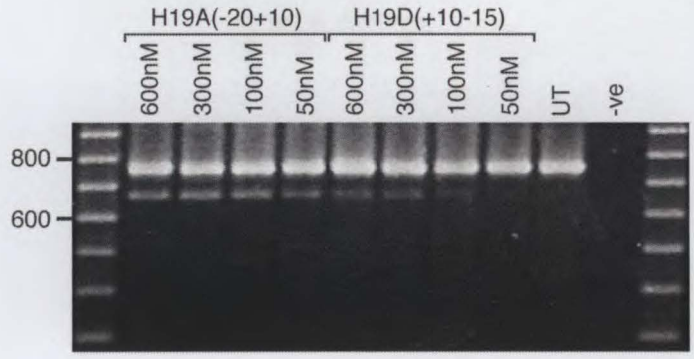

Figure 5.9 Agarose gel image of mismatched human 2'OMeAOs transfected into *mdx* mouse cells. As observed in the normal cells, the acceptor site directed 2'OMeAO, H19A(-20+10) was better able to induce exon 19 skipping than H19D(+10-15), which targeted the donor splice site.

5.4.2 Mouse-specific 2'OMeAOs directed at human pre-mRNA

Two mouse-specific 2'OMeAOs, M19A(-20+10) and M19D(+05-20), were tested in both primary human and HDMD cells. M19A(-20+05) was directed at the mouse intron 18 acceptor splice site, extended 5 nucleotides less into exon 19 than did H19A(-20+10) and differed from the human sequence by only the last 3' nucleotide, thus providing 96% perfect sequence homology. M19D(+05-20) was the same length as its human-specific homologue but extended 5 nucleotides further into intron 19 and had 7 mismatches.

5.4.2.1 Primary human muscle cells

Transfection of the primary human myoblasts with the mouse-specific 2'OMeAOs did not yield any unexpected results. M19A(-20+05) induced a consistent, low level of exon 19 skipped transcript of similar abundance to that induced by the human-specific 2'OMeAO, H19A(-20+10), when delivered at a final concentration of 600nM. However, H19A(-20+10) was still able to induce sporadic exon 19 skipping when transfected at 300nM, whereas the mismatched 2'OMeAO did not. It is difficult to say at this point if it was the additional 6 homologous bases or the single nucleotide mismatch in M19A(-20+05) that would explain the marginal difference in efficacy. No skipping, specific or aberrant, was detected in the RNA from primary human cells transfected with the seven base mismatched M19D(+05-20) even at a final concentration of 600nM.

Figure 5.10 Mouse-specific 2'OMeAOs transfected into primary human myoblasts. RT-PCR analysis of the RNA extracted from human muscle cultures after separate 600nM transfections with either M19A(-20+05) or M19D(+05-20). Only the 2'OMeAO directed at the acceptor site, M19A(-20+05), could induce a detectable exon 19 skipped transcript.

5.4.2.2 HDMD muscle cells

Previous experiments in these cells with human-specific 2'OMeAOs directed at the splice sites showed a similar but weaker pattern to that observed in the primary cell line. This was also the case when the HDMD cells were transfected with the mismatched 2'OMeAOs. The exon 19 skipped product induced by M19A(-20+05) at 600nM was less abundant and less reproducible than that seen in the unaffected primary cell line, and M19D(+05-20) was never able to induce a detectable exon 19 skipped transcript.

5.5 Specificity of 2'OMeAO action throughout the dystrophin transcript

Additional tests to assess the disruption of splicing patterns in other regions of the dystrophin transcript were undertaken using total RNA from 2'OMeAO treated *mdx* cells which had previously shown exon 19 skipping. These regions included exons 1 to 10, 20 to 26 and 70 to 79. No other splicing patterns were consistently generated, other than the removal of exon 19 (Figure 5.11).

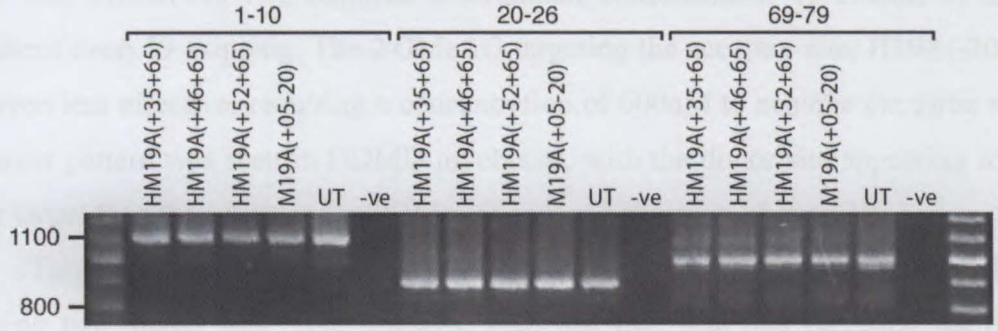

Figure 5.11 2'OMeAOs targeted to exon 19 do not alter dystrophin processing in other regions of the gene transcript. Each lane represents RNA preparations pooled from 4 separate transfection experiments in which the RNA had been extracted from either untreated or 2'OMeAO treated cultures shown to have skipped exon 19. Apart from occasional sporadic alternatively processed transcripts (eg shorter product in the untreated sample, exons 1-10), no consistent rearrangements in dystrophin processing were detected. (Errington et al., 2003).

5.6 Summary

Exon 19 skipping induced by splice site-directed 2'OMeAOs was precise and very efficient. Transfection studies in *H-2K* normal muscle cells revealed that the donor site appeared to be a more amenable target for 2'OMeAO-induced skipping of exon 19. In *H-2K mdx* cells, both M19A(-20+05) and M19D(+05-20) were effective at concentrations as low as 10nM. An attempt to refine the highly efficient M19D(+05-20) by designing a smaller 2'OMeAO within the same region was not successful, as M19D(+02-18) proved to be less effective.

In primary human muscle cells transfection with the 2'OMeAO targeting the donor site, H19D(+10-15), required a minimum concentration of 200nM to induce consistent exon 19 skipping. The 2'OMeAO targeting the acceptor site, H19A(-20+10), was even less effective, requiring a concentration of 600nM to achieve the same effect. A similar pattern was seen in HDMD myoblasts, with the donor site appearing to be a better target than the acceptor for 2'OMeAO-induced skipping of exon 19.

Targeting multiple splicing motifs in *H-2K mdx* myotubes revealed that targeting two motifs was more effective than just one, and that targeting the donor, acceptor and ESE appeared to have a greater effect than the sum of that induced by all three 2'OMeAOs individually.

Transfection of the *H-2K* normal and *mdx* muscle cells with the human-specific 2'OMeAO directed at the acceptor splice site was able to induce exon 19 skipping, despite the three mismatched bases. Conversely, this effect could not be induced by transfection of the mouse cells with the mismatched donor site-directed 2'OMeAO. The same outcomes were observed with mismatched 2'OMeAO transfections in the human cells.

Finally, a screen of several regions of the dystrophin gene transcript including the 3' and 5' ends was undertaken. No other splicing patterns were consistently generated, other than the specific removal of exon 19.

5.7 Discussion

The acceptor and donor splice sites flanking exon 19 were evaluated as potential targets for 2'OMeAO induced skipping of that exon. The efficient 2'OMeAO-induced skipping of dystrophin exon 23 by targeting the donor splice site has been reported (Mann et al., 2001; Mann et al., 2002). Attempts to remove that exon with 2'OMeAOs directed at the acceptor site have been unsuccessful, possibly due to secondary structures in this region restricting accessibility of the 2'OMeAO to that target. Furthermore, additional skipping of adjacent exons was observed when the exon 23 donor splice site was blocked (Mann et al., 2001; Mann et al., 2002; Wilton et al., 1999). It has been suggested that targeting internal exonic motifs may result in more specific exon skipping (van Deutekom et al., 2001). By targeting 2'OMeAOs to the splice sites of exon 19, it was possible to compare the efficiency and specificity of skipping induced to that induced by targeting the ESEs.

5.7.1 Exon 19 skipping in *H-2K* mouse muscle cells

In *H-2K* normal and *mdx* cells the 2'OMeAO M19D(+05-20), directed at the donor splice site of exon 19, appeared to consistently induce more exon 19 skipped transcript than M19A(-20+05), which was directed at the acceptor splice site. It is important to note that the skipping observed with either 2'OMeAO was reliable and precise. Compared to the *H-2K* normals, skipping was consistently stronger in the *mdx* cells, again most likely due to the relative rates of turn over of the natural and exon 19 skipped products in the two cell lines (Maquat, 1995).

In an attempt to refine the donor splice site motif, the 20mer M19D(+02-18) was designed within M19D(+05-20). An 2'OMeAO, M23D(+02-18), directed to the corresponding bases of exon 23, had improved the efficiency of skipping compared to a 25mer targeting the same region (Mann et al., 2002). However, this effect was not observed when exon 19 was targeted, as the shortened product was considerably less abundant than that induced by M19D(+05-20). The T_m of a duplex decreases as its length decreases (Agrawal, 1992; Crooke, 1999). This may account for the lower activity of the shorter M19D(+02-18) relative to the parent 25mer, through a reduction in affinity to the target sequence or less effective competition with splicing factors. However, this does not account for the difference in the level of activity between

M19D(+02-18) and M23D(+02-18). It is possible that the five bases no longer obstructed by M19D(+02-18) were important for exon 19 donor splice site function, or perhaps that secondary structures played a comparatively more significant role in accessibility of the exon 23 donor splice site. Interestingly, the G/C content of the sequence targeted by M23D(+02-18) was 60%, twice that of M19D(+02-18) at 30%. As the annealing temperature increases with G/C content, this may also have contributed to the higher efficiency of the exon 23-directed 20mer.

5.7.2 Exon 19 skipping in human muscle cells

In the primary human cells, neither 2'OMeAO targeting the splice sites of exon 19 induced very efficient skipping. The donor site-directed H19D(+10-15) did induce precise removal of exon 19 but at higher concentrations than required in mouse cells. A similar pattern was observed in HDMD muscle cells, in that the exon 19 skipped transcript induced by the 2'OMeAO targeted to the donor site was of greater abundance than that induced by the 2'OMeAO targeted to the acceptor site. In both cases, although the skipping of exon 19 was precise and specific, it was significantly weaker than that observed in either the primary human cells or the mouse cells. Compared to the primary cells, the relative rates of transcript turnover should result in the exon 19 skipped transcript being easier to detect in the HDMD cells. As this was not reflected in the results, it appears that transfection efficiency may have been a limitation in these cells.

There are several possible explanations for the differences in efficiency of exon 19 skipping observed in the human and mouse cells. It could be that the splice sites are less significant to exon 19 inclusion in humans, perhaps relying more on the activity of ESEs or other splicing enhancers. However, the similarity of exon 19 splice site strengths between human and mouse (Senapathy et al., 1990), and the results of 2'OMeAOs targeting ESEs in exon 19, suggest that this is unlikely (Section 4.5.2). Another possible reason is that secondary structures in these regions may differ between the species, which could influence accessibility to the splice sites (Crooke, 1999; Dagle & Weeks, 2001). Additionally, it is not known whether there are differences in the general splicing machinery between mouse and man which may have an effect on competition for the targeted site. However, as transfection of the human cells was observed to be less efficient than that of the mouse cells (Section 4.1.2), limitation in delivery of the 2'OMeAO is again the most likely reason for the difference in abundance

of induced transcripts detected in the two species. While it has been demonstrated that the targeting of splice sites with 2'OMeAOs is a feasible approach to the specific modification of splicing in human cells, further optimisation of transfection conditions, including the evaluation of additional reagents, may result in improved efficiency of exon skipping.

5.7.3 Targeting multiple sites

Targeting either the ESE or the splice sites of dystrophin exon 19 resulted in similarly effective 2'OMeAO-induced skipping in *H-2K mdx* cells. However, a study targeting the same motifs of exon 23 demonstrated significantly disparate results, as neither the acceptor splice site nor an ESE-like motif proved to be amenable to 2'OMeAO-induced exon skipping (Mann et al., 2001; pers. comm. C. Mann). Furthermore, a study by Ito and colleagues (2001) investigated the extent to which internal exon sequences in three dystrophin exons influence splicing and how they compare to the 3' consensus splice sites of these exons. The significance of each of these motifs to splicing varied between exons, and there appeared to be no obvious relationship between splice site strength and the presence of ESEs (Ito et al., 2001). Based on the results of these studies, it is highly likely that more than one motif may need to be targeted to achieve efficient exon skipping if there is not a predominant strong or controlling site, and it may be difficult to predict which motif to target based only on the strength of the consensus splice site sequences. It has been reported that targeting a combination of splicing motifs, such as both splices sites, can improve the efficiency of skipping (De Angelis et al., 2002).

This approach was tested in *H-2K mdx* mouse muscle cells, as the results of the previous chapter suggested that this cell line may represent a better molecular model for determining the efficacy of 2'OMeAO-induced skipping in the dystrophin gene than the other models evaluated. The 31mer HM19A(+35+65), and the two splice site-directed 25mers, M19A(-20+05) and M19D(+05-20), were transfected into *H-2K mdx* myoblasts in each of the four possible combinations. Each combination of two 2'OMeAOs induced an exon 19 skipped transcript of higher abundance than that induced by individual 2'OMeAOs, consistent with the findings of De Angelis et al. (2002). Of these combinations, that of the two 2'OMeAOs directed to the splice sites appeared to induce the most effective removal of exon 19. However, the combination of all three

2'OMeAOs resulted in a significant increase in the abundance of the exon 19 skipped product compared to the paired combinations, and at a final concentration of only 22nM. The abundance of this shorter product was similar to that induced by each of the three individual 2'OMeAOs at final concentrations of 50nM. This suggests that adding low doses of 2'OMeAOs to block each motif rather than high doses of a single 2'OMeAO may be preferable, particularly since it may result in a lower level of cell damage associated with the transfection reagent used. This approach may be particularly useful when excluding exons which prove resistant to 2'OMeAOs targeting a single motif.

5.7.4 Effects of mismatched 2'OMeAOs in mouse and human cells

Mismatched AOs represent a useful control for the demonstration of target hybridisation specificity through changes in both composition and secondary structure (Stein & Krieg, 1994). Homology between the human and mouse sequence at the acceptor and donor splice sites is not maintained, thereby allowing mismatched 2'OMeAOs to be evaluated between species. Two human-specific splice site-directed 2'OMeAOs were transfected into mouse cells. Although the three mismatches within H19A(-20+10) appeared to reduce its binding affinity (as indicated by the increased 2'OMeAO concentration required to induce consistent skipping of exon 19), the 26 consecutive homologous bases were adequate to induce consistent skipping at a final concentration of 600nM. As there were three mismatched bases at the ends of H19A(-20+10) (Figure 5.2), they would not have destabilised the duplex to the same degree as would be expected to result from the presence of internal mismatches (Woolf, Melton & Jennings, 1992).

The fact that a 26 base sequence successfully hybridised to the mouse pre-mRNA despite three flanking mismatches is not a particular concern, as a specified sequence 26 nucleotides in length is unlikely to occur more than once in the human genome (Agrawal, 1992; Branch, 1996). However, as the length of a 2'OMeAO increases, there is a seemingly paradoxical decrease in specificity. This is because longer 2'OMeAOs contain many nested internal sequences of sufficient length to hybridise to non-targeted pre-mRNA sequences (Stein, 2001; Woolf et al., 1992). It has been demonstrated in *Xenopus* oocytes that sequences as short as 10 bases can cause antisense effects (Woolf et al., 1992), and even the 12mer evaluated in this study,

HM19A(+46+57), was able to induce consistent exon 19 skipping. In addition, H19D(+10-15), with five mismatches to the analogous mouse sequence and only 13 bases of straight homology, was able to induce exon 19 skipping, albeit sporadic and weak, at 600nM. This was despite having mismatches more internal to the 2'OMeAO compared to H19A(-20+10). The fact that the donor site appears to be more amenable to 2'OMeAO activity may have contributed to the level of skipping induced by the mismatched 2'OMeAO. It has been estimated statistically that a specific 13 base sequence may occur over 40 times in the human genome (Branch, 1996). Based on these results, it is theoretically possible that the 30mer H19A(-20+10) could hybridise with a number of unintended sites, although the secondary structures of these regions would be expected to differ from that of the intended target. It has been demonstrated that the structure of mRNA has a significant effect on antisense activity (Vickers, Wyatt & Freier, 2000), and that variations in accessibility will result in some mRNA sequences being more susceptible to non-specific hybridisation than others (Branch, 1996), which may be the case for the donor site of exon 19. It is unknown how many flanking mismatches would be required to sufficiently alter secondary conformation of the 2'OMeAO or to reduce binding affinity such that non-specific hybridisation would be avoided.

A similar pattern was seen in the human cells transfected with two mouse-specific 2'OMeAOs. M19A(-20+05), with only one mismatch and 24 bases of straight homology, consistently induced exon 19 skipping at 600nM in human cells. Not unexpectedly, this mismatched 2'OMeAO proved almost as efficient as the human specific 2'OMeAO, H19A(-20+10). It is difficult to discern whether the marginal decrease in efficacy observed with the mismatched 2'OMeAO would be due to the single mismatch or the decreased length of the 2'OMeAO, at 25 rather than 30 bases. M19D(+05-20), with 7 mismatches and 13 bases of straight homology, did not induce exon 19 skipping in human cells, even at a final concentration of 600nM. This 2'OMeAO had the same number of internal consecutive homologous bases but two more mismatches with the human sequence compared to H19D(+10-15) when directed against mouse cells. It is possible that the lack of 2'OMeAO activity in the human cells could be due to the secondary structure alterations induced by the additional two mismatches; however, as transfection conditions appeared to be a limiting factor in these cells, it was expected that any skipping induced would be weaker in comparison to that observed in the *H-2K mdx* cells. Determining the relative contribution of these

factors would require further evaluation of the effects of number and position of mismatches in 2'OMeAOs of various lengths.

The mismatched 2'OMeAOs were demonstrated to have a reduced annealing potential, reflecting their weakened biological function, and supporting the conclusion that their effect is mediated by a true antisense mechanism (Stein & Krieg, 1994). Additionally, these data demonstrate that the high 2'OMeAO concentrations (≥1μM), often used in other studies, may have the potential for the non-specific removal of untargeted exons in other genes that contain splicing motifs homologous to small stretches within the 2'OMeAO. The fact that some skipping was induced, despite the presence of mismatched bases, is a safety concern for non-specific effects. These results highlight the importance of optimising 2'OMeAOs so that lower concentrations can be used, thus reducing the likelihood of non-specific effects.

5.7.5 Specificity of 2'OMeAO action throughout the dystrophin transcript

To evaluate the specificity of antisense effects to the targeted region of the dystrophin gene, RT-PCR was performed across exons 1-10, 20-26 and 70-79 on pooled RNA samples extracted from 2'OMeAO-treated and untreated cultures. Four 2'OMeAOs were selected for evaluation: HM19A(+35+65), HM19A(+46+65), HM19A(+52+65) and M19D(+05-20). For each of the 2'OMeAOs, it was demonstrated that exon 19 skipping was absolutely specific to the target sequence, at least in the target gene examined here. There was no loss of adjacent exons, and splicing patterns elsewhere in the dystrophin gene transcript did not appear to be altered by the treatment. Although this does not preclude the possibility of non-specific activity elsewhere in the genome, these results are encouraging. As the 31mer, HM19A(+35+65), and the 25mer, M19D(+05-20), are significantly longer than the 16 to 20 bases recommended to minimise non-specific effects (Stein, 2001), there is the concern that these longer 2'OMeAOs will contain multiple short sequences capable of non-specific hybridisation (Stein, 2001; Woolf et al., 1992). However, this effect was not observed in the regions of the dystrophin gene included in this assay. The 14mer, HM19A(+52+65), was shorter than the recommended length, as a specified sequence of 14 nucleotides would be expected to occur more than once in the human genome (Agrawal, 1992; Branch, 1996). Although it is possible that this 2'OMeAO would be capable of annealing to sites other than the intended target, this was not observed in other regions of the dystrophin gene.

Although this assay screened only certain regions of the dystrophin mRNA, the positive results indicate the reduced likelihood that these 2'OMeAOs would induce non-specific effects, and strengthen the observation that targeting the dystrophin exon 19 splice sites produces the same high degree of specificity as targeting the ESE.

Chapter 6 - Results from targeting exon 46

Van Deutekom and colleagues reported the 2'OMeAO-mediated removal of dystrophin exon 46 from the gene transcript in both mouse and human myotubes (van Deutekom et al., 2001). They proposed that 2'OMeAO-induced skipping of this exon would restore the reading frame in ~7% of patients with DMD. Furthermore, their work demonstrated that at least 75% of 2'OMeAO-transfected DMD patient myotubes were expressing correctly localised dystrophin as a result of the removal of exon 46. The study by van Deutekom et al. (2001) directed a series of overlapping 2'OMeAOs at polypurine-rich exonic regions, but omitted targeting the splice sites. We considered it would also be important to assess exon 46 splice sites as possible targets for 2'OMeAOs to compare the efficiency of re-directing splicing.

6.1 Quality assay of 2'OMeAOs directed at exon 46

Prior to myotube transfection, all exon 46 directed 2'OMeAOs were subject to quality control assessment. As described earlier, approximately 200ng of each 2'OMeAOs was electrophoresed through a denaturing polyacrylamide gel (Figure 6.1). Only 'in-house', Expedite 8909 (Applied Biosystems) synthesised 2'OMeAOs were used in this part of the study and all were found to be of a sufficiently high quality to proceed to cell transfections.

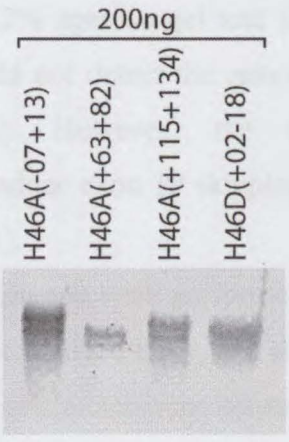

Figure 6.1 Each 2'OMeAO targeting exon 46 was run on a denaturing polyacrylamide gel to assess the standard of synthesis. As apparent yields varied, 2'OMeAO concentrations were adjusted prior to transfection.

6.2 Transfection of primary human cells with 2'OMeAOs directed at exon 46

Initial experiments attempted to reproduce the results of van Deutekom et al. (2001) and, as such, all procedures outlined in that study were adhered to. The 2'OMeAO hAON 8 (nomenclature used by van Deutekom et al.) was, however, renamed H46A(+115+134) (Figure 6.2 and Table 3.2) according to our nomenclature system (Mann et al., 2001), and selected as the first 2'OMeAO to be evaluated. Exon 46 skipping was reported to be most efficient when targeting this region in both normal and dystrophic human cells. In addition, we designed another 20mer 2'OMeAO, H46D(+02-18), to anneal to the donor splice site of exon 46 to allow comparison of the motifs as 2'OMeAO-induced exon skipping targets. A 1:1 mixture of the two 2'OMeAOs was included in the assay to assess any combined effect, and an exon 19 2'OMeAO, HM19A(+35+65), was included as an experimental positive control.

Primary normal human cells were seeded onto collagen coated plates and allowed to differentiate into myotubes over 12 days in a low-serum (5% horse serum) medium. Transfections were conducted in the absence of serum for 3 hours after complexing 2'OMeAOs at a final concentration of 1000nM with ExGen 500 at 3.5eq. At 24 hours post-transfection, total RNA was extracted from the myotube cultures and purified. RT-PCR was performed on 1000ng of RNA using human dystrophin specific primers, encompassing exons 17 to 21 and exons 44 to 47, to screen for the skipping of exons 19 and 46 respectively. After a secondary round of PCR amplification, the fragments were separated on a 2% agarose gel and viewed by UV transillumination. Under these conditions, we could not detect the removal of exon 46 from the mature transcript (data not shown). However, the transfection positive control, HM19A(+35+65), was able to induce exon 19 skipping at a level achieved in previous experiments (refer to Figure 4.11).

A further series of experiments were performed in which various experimental parameters were addressed sequentially. Firstly, the substrate collagen was substituted for matrigel, a well established cell attachment substrate. Also, the time for myotube differentiation was varied between 4 and the reported 12 days. In addition, Lipofectin and Lipofectamine 2000 were tested as 2'OMeAO delivery reagents and the 2'OMeAO final transfection concentrations were also varied to maximise cell survival. Furthermore, RT-PCR conditions were adjusted, where various amounts of RNA were

used as template to minimise possible carry-over of inhibitory contaminants from the RNA extraction procedure. The standard Titan one tube RT-PCR reaction kit was also used to compare reverse transcription capabilities. Under no circumstances was exon 46 skipping detected, whereas the positive control HM19A(+35+65), delivered at a final concentration of 300nM with any transfection reagent, was consistently able to induce exon 19 skipping.

6.3 Attempting exon 46 removal with second generation 2'OMeAOs

6.3.1 RNA binding assay (RBA)

Based on the failure of the initial experiments to induce exon 46 skipping, an assay to assess DNA AO (deoxy-AO) binding to its target RNA was designed. Briefly, a 413 base T7 transcribed RNA fragment (fragment 1) containing the desired target sequence was placed into a hybridisation reaction with a deoxy-AO (see Section 3.6) for 30 minutes at 37°C and separated on an 8% polyacrylamide gel for 3 hours. Hybridisation of the deoxy-AO to the target RNA sequence was assessed by visualisation of the SYBR gold stained complexes by UV transillumination. The efficient annealing of the deoxy-AO to the RNA fragment should induce a conformational change, resulting in altered migration of the complex through the polyacrylamide gel, relative to the unbound RNA. The resultant separation of the two species was visualised as two bands, where the duplex band was 'shifted' from the unbound RNA band. To determine the most amenable targets by this assay, a titration of each deoxy-AO against a constant 50ng of RNA was performed. The deoxy-AO that was still able to induce a bandshift which scored a rating of at least 2, (Figure 3.2) when added at 5ng per reaction, was deemed suitable for synthesis as a 2'OMeAO.

A total of 14 deoxy-AOs were tested in this fashion: five targeting regions within exon 46, four targeting the acceptor site and five targeting the donor site. Of the exonic deoxy-AOs, three were directed at regions targeted by van Deutekom et al. (2001) and two were directed at other motifs (Figure 6.2). Results of the RBA for all 14 deoxy-AOs are summarised in Table 6.1.

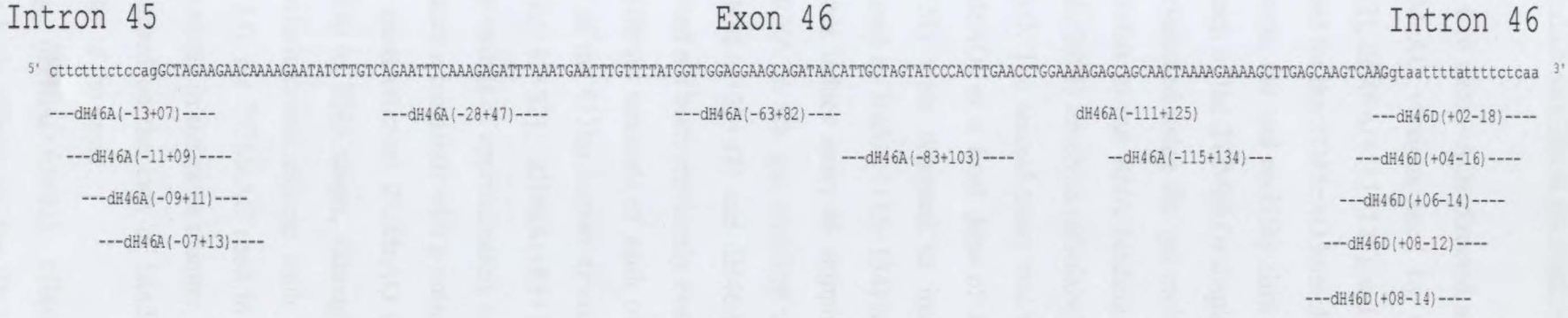

Figure 6.2 Schematic illustration of annealing sites for deoxy-AOs to a section of the 413 base human dystrophin RNA fragment including exon 46. The exonic sequence is in upper case and the intronic sequences are in lower case (sequences are given 5' - 3'). The annealing sites are indicated by the broken lines flanking the deoxy-AO. The deoxy-AOs, dH46A(+63+82), dH46A(+111+125) and dH46A(+115+134) are DNA versions of the 2'OMeAOs described by van Deutekom, et al. (2001).

6.3.1.1 Deoxy-AOs directed at the exon 46 ESE

Of the five deoxy-AOs directed at motifs within exon 46, three were selected from the 2'OMeAO versions used by van Deutekom et al. (2001). We designed dH46A(+63+82), dH46A(+111+125) and dH46A(+115+134) based upon the levels of efficacy reported for the 2'OMeAO homologues by van Deutekom and colleagues using two different tests, the 'gel mobility shift assay' and myotube transfection. This group reported that each of the 2'OMeAOs displayed a high affinity for radiolabelled exon 46 targets when evaluated using the gel mobility shift assay; an RNA:2'OMeAO binding affinity test similar to our RNA binding assay. However, the reported protocol (van Deutekom et al., 2001) involved radiolabelling of the RNA fragment before the addition of the 2'OMeAO. The second assay was the standard transfection of human myotubes with the 2'OMeAOs at a final dose of 1000nM. In their study, H46A(+63+82) and H46A(+115+134) were reported to induce exon 46 skipping with the skipping efficiency induced by H46A(+115+134) being reproducibly highest. H46A(+111+125), however, did not induce exon 46 skipping despite its apparent high affinity for the radiolabelled RNA in the gel mobility shift assay. In our study, an additional two deoxy-AOs, dH46A(+28+47) and dH46A(+83+103), were designed to target exonic regions which had not been previously evaluated.

Two different amounts of each of the five deoxy-AOs, 200ng and 5ng, were added to 50ng of the 413bp human dystrophin mRNA fragment spanning exon 46. At 200ng, dH46A(+63+82), dH46A(+83+103) and dH46A(+111+125) all induced bandshifts with ratings of approximately 4. At the same concentration, dH46A(+28+47) was able to induce a bandshift with a rating of only 2. Surprisingly, dH46A(+115+134), the reportedly most efficient 2'OMeAO (van Deutekom et al., 2001) was apparently unable to bind to its RNA target, although it is possible that it did anneal but did not result in a conformational change such that a bandshift was induced. Furthermore, H46A(+115+134), the 2'OMeAO used in the initial cell transfection experiments, was retrospectively tested in the same manner. This 2'OMeAO also did not appear to anneal to the target, based on the lack of bandshift, possibly indicating a limitation in the predictive ability of the assay.

At 5ng, dH46A(+63+82), dH46A(+83+103) and dH46A(+111+125) each demonstrated a high affinity for the RNA target with bandshift ratings of 3, 2, and 2 respectively. dH46A(+28+47), however, did not achieve a bandshift at this lower

concentration (Table 6.1). Based on these results, dH46A(+63+82) was selected for synthesis as a 2'OMeAO for subsequent transfection into the normal primary human muscle cells.

6.3.1.2 Deoxy-AOs directed at the exon 46 splice sites

Annealing experiments with the deoxy-AOs directed at the exon 46 splice sites indicated that the acceptor site for this exon may be the more amenable of the two for 2'OMeAO binding. A bandshift rating of 2 was induced by dH46A(-13+07) and dH46A(-07+13) while dH46A(-11+09), dH46A(-09+11) could only achieve a bandshift rating of 1 (Table 6.1). Based on the fact that dH46A(-07+13) was the only deoxy-AO to induce a bandshift with a rating of 4 at 200ng, it was selected for synthesis as a 2'OMeAO for subsequent evaluation in cell culture.

The donor splice site was deemed a poor target for 2'OMeAO-induced exon removal as only two deoxy-AOs were able to induce a bandshift. When 5ng of these deoxy-AOs, dH46D(+06-14) and dH46D(+08-12), were added to the target, each was only able to induce a bandshift which rated less than 1 (Table 6.1).

6.3.1.3 ESE- and donor- directed deoxy-AOs targeting a shorter RNA fragment

A second smaller RNA fragment (fragment 2) was designed to determine if the length of the RNA fragment was a factor in allowing access to the target sequence by the less effective deoxy-AOs. This could partly account for the difference in RNA binding ability observed between the deoxy-2'OMeAO, H46A(+115+134), evaluated in this study and the 2'OMeAO tested by van Deutekom et al. (2001). Fragment 2 was 286 bases long and did not include the 127 bases of 5' sequence in fragment 1. Due to the promising results obtained with the deoxy-AOs directed at the acceptor site, we decided to truncate the 5' end entirely, rather than remove sequence from both ends.

6.3.1.3.1 Deoxy-AOs directed at the ESE

Although 5ng of dH46A(+63+82) was able to induce a similar level of bandshift when annealed to fragment 2 as compared to that induced when annealed to fragment 1, a dramatic increase in deoxy-AO-induced bandshift was observed for dH46A(+115+134). Where previously no shift could be detected when 200ng was added to fragment 1, 5ng of dH46A(+115+134) added to fragment 2 induced a bandshift with a rating of 3. However, as already shown, this result did not correlate with the initial transfection experiments, emphasising the possibility that the modified secondary or tertiary structures formed in this system may not provide a realistic indication of the situation in cells. This is not surprising as this *in vitro* binding assay lacks the muscle specific nuclear proteins present *in vivo*, and the target RNA transcript is not being continually transcribed as would be found *in vivo*. No significant difference was induced by 5ng of dH46A(+83+103) using fragment 2 as target, where a bandshift rating of 2 was achieved compared to the same rating with fragment 1. Hybridisation of 200ng of the deoxy-AO dH46A(+28+47) to the target sequence could induce a bandshift which rated 2 but 5ng produced no detectable shift, indicating that access to this region may not be possible in the system due to secondary or tertiary conformations.

6.3.1.3.2 Deoxy-AOs directed at the donor splice site

The donor splice site on fragment 2 also appeared to be a poor target. H46D(+02-18), (a 2'OMeAO), dH46D(+04-16) and dH46D(+08-14) each failed to anneal to their respective targets, even when added at 200ng. However, while a bandshift was evident when either dH46D(+06-14) or dH46D(+08-12) were added to fragment 2 at 200ng each, both appeared to induce bandshifts which rated less than 1 when added at 5ng. This degree of bandshift still falls well below the bandshift rating of 2 arbitrarily selected for a deoxy-AO to progress to subsequent evaluation in cell culture.

Table 6.1 Estimated amounts of RNA fragment bound and induced to 'shift' due to a conformational change, given as a rating, where 0 represents no bandshift and 4 represents a complete bandshift (Figure 3.2).

deoxy-AO tested	Bandshift rating after exposure to varied amounts of deoxy-AO(ng)			
	Fragment 1 (413nt)		Fragment 2 (286nt)	
	200ng	5ng	200ng	5ng
dH46A(-13+07)	3	2	-	-
dH46A(-11+09)	3	1	-	-
dH46A(-09+11)	3	1	-	-
dH46A(-07+13)	4	2	-	-
dH46A(+28+47)	2	0	2	0
dH46A(+63+82)	4	3	4	3
dH46A(+83+103)	3	2	4	2
dH46A(+111+125)	4	2	4	2
dH46A(+115+134)	0	0	4	3
dH46D(+02-18)	0	0	0	0
dH46D(+04-16)	0	0	0	0
dH46D(+06-14)	3	1	0	0
dH46D(+08-12)	3	1	0	0
dH46D(+08-14)	0	0	0	0

6.3.2 Exon 46 skipping in primary human muscle cells

Primary normal human cells were seeded on to matrigel coated plates and allowed to differentiate into myotubes over 4 days in a low-serum (5% horse serum) medium. A parallel series of myotube transfections were conducted in the absence of serum for 3 hours, after complexing the second generation 2'OMeAOs at a final concentration of 1000nM with ExGen 500 at 3.5eq or with Lipofectin at 2:1 (weight:weight). At 24 hours post-transfection, total RNA was extracted from the myotube cultures. Reverse transcription was performed on 1000, 200, 50 and 5ng of RNA followed by 30 cycles of amplification across dystrophin exons 19 or 46 using human specific primers. After a secondary round of PCR amplification of 25 cycles, the cDNA transcript fragments were electrophoresed through a 2% agarose gel and viewed by UV transillumination. Dystrophin exon 46 skipping was induced at marginally lower levels compared to that reported by others (Aartsma-Rus et al., 2002; van Deutekom et

al., 2001). However, the very weak and inconsistent exon 46-deleted transcript fragments were detected in the mRNA of myotubes transfected with H46A(-07+13) and H46A(+63+82) and complexed with Lipofectin but not ExGen 500 (Figure 6.3). Furthermore, RT-PCR using 50 and 5ng of RNA template provided the only detectable dystrophin exon 46-skipped transcript fragments observable as a 478bp product, 148bp shorter than the 620bp full length transcript fragment generated across exons 44 and 47.

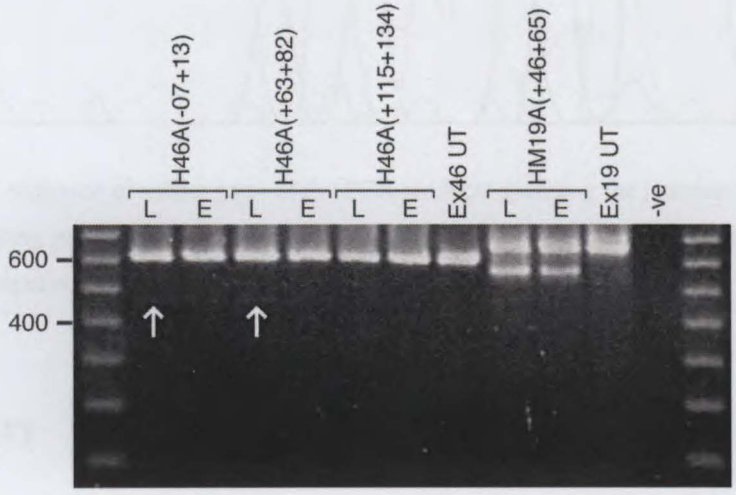

Figure 6.3 Agarose gel image demonstrating a very weak 478bp product corresponding to dystrophin exon 46 skipping. Only H46A(-07+13) and H46A(+63+82) were able to induce the removal, albeit inconsistent, of exon 46 at a final transfection concentration of 1000nM and complexed with Lipofectin at 2:1. The positive control, HM19A(+46+65), was able to induce exon 19 skipping when delivered complexed with either Lipofectin at 2:1 or ExGen 500 at 3.5 equivalents.

Confirmation of the identity of both amplicons was established after isolation and direct sequencing of each product (Figure 6.4). H46A(+115+134) was unable to induce exon 46 removal that could be detected by our assay. Furthermore, such was the inconsistency of exon 46 removal that subsequent experiments involving transfection of 2'OMeAO combinations such as H46A(-07+13) with H46A(+63+82) or H46A(-07+13) with H46A(+115+134) were unable to reproduce the removal of exon 46. However, HM19A(+46+65), a second generation 2'OMeAO targeting exon 19, was able to induce the consistent removal of exon 19 under every condition tested (Figure 6.3) indicating that there should be no limitation in delivery of the 2'OMeAO to the cell nucleus.

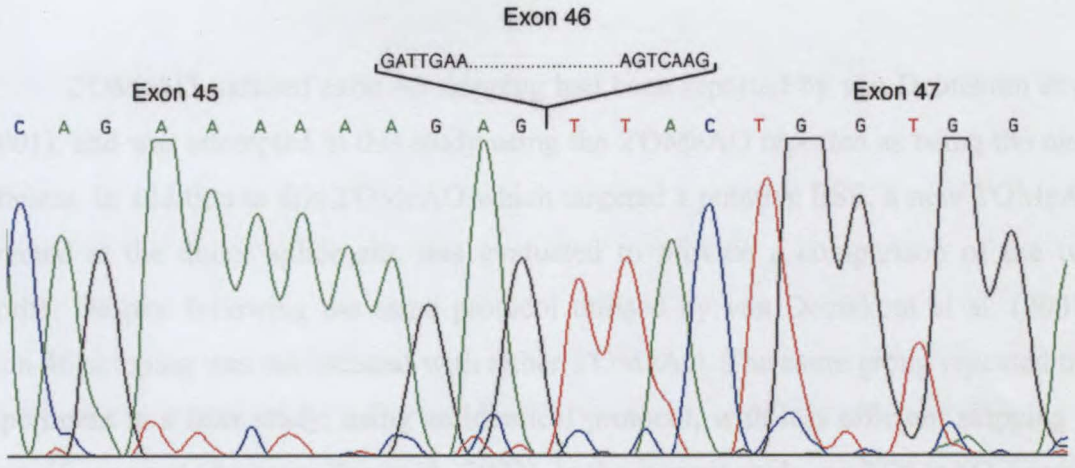

Figure 6.4 DNA sequence chromatogram of the PCR products spanning the junction of dystrophin exons 45 and 47, indicating precise removal of exon 46. The junction of exons 45 and 46 and exons 46 and 47 are shown for comparison.

6.4 Summary

Skipping of exon 46 in primary normal human cells proved difficult. The RBA was limited in its ability to identify amenable sites for 2'OMeAO annealing and activity. Very weak and inconsistent exon 46 skipping was seen in normal primary human myotubes transfected with H46A(-07+13) and H46A(+63+82). No skipping was observed following transfection with H46A(+115+134), and combinations of these three 2'OMeAOs were ineffective in increasing the level of exon 46 skipping. The transfection process was excluded as a limiting factor, as an exon 19 positive control 2'OMeAO was successful in inducing exon 19 skipping under the same conditions.

6.5 Discussion

2'OMeAO-induced exon 46 skipping had been reported by van Deutekom et al. (2001), and was attempted in this study using the 2'OMeAO reported as being the most efficient. In addition to this 2'OMeAO which targeted a putative ESE, a new 2'OMeAO directed at the donor splice site was evaluated to provide a comparison of the two motifs. Despite following the same protocol utilised by van Deutekom et al. (2001), exon 46 skipping was not induced with either 2'OMeAO. The same group repeated this experiment in a later study, using an identical protocol, with less efficient skipping of exon 46 reported (Aartsma-Rus et al., 2002). In the current study, an 2'OMeAO directed at the exon 19 ESE was included as a positive control, and was able to induce exon 19 skipping, which suggested that the limitation was not in the transfection process. Attempts to identify a limitation in the protocol by modifying each variable, from type of cell attachment substrate to the amount of RNA template in RT-PCR, were unsuccessful.

At this point an assay was implemented to test the potential of a 2'OMeAO to anneal to its target sequence. This was to facilitate the screening of a larger number of potential 2'OMeAOs using PCR grade DNA homologues (deoxy-AOs) against RNA fragments. Such screening is desirable because the testing of multiple oligonucleotides (20 - 50) in cells is usually required for the discovery of just a few active antisense sequences (Lebedeva & Stein, 2001; Matveeva et al., 1998). Deoxy-AOs are less expensive to synthesise because they do not require the chemical modifications necessary to protect 2'OMeAOs from nuclease degradation in the cellular environment.

A similar assay was employed by van Deutekom et al. (2001) to detect bound and unbound RNA. In their study, the shift induced by the deoxy-AOs that had bound to a radiolabelled RNA fragment was detected, whereas in this report the gel was simply stained with SYBR gold. Fourteen deoxy-AOs were tested by this method, three of which, H46A(+63+82), and H46A(+111+125) and H46A(+115+134), were the 2'OMeAOs reported as showing a high affinity for the radiolabelled exon 46 RNA fragment in the study by van Deutekom and colleagues. The other 11 deoxy-AOs were spread across two more regions within exon 46 and the acceptor and donor splice sites.

Furthermore, the annealing potential of these deoxy-AOs was evaluated using two different length RNA fragments to assess deoxy-AO access to different length RNA. The two fragments used, at 413 and 286 bases long, were both longer than the

164 base fragment used by van Deutekom et al. (2001). As the conformation of the fragments could be different, it was necessary to determine if the length of the RNA fragment was a factor in allowing access to the target sequence and hence the difference observed between the deoxy-AOs trialed in this study and those used by van Deutekom and colleagues. Significant differences were found between the two fragments for several of the deoxy-2'OMeAOs (Table 6.1), confirming that fragment length can affect the ability of a deoxy-AO to anneal, presumably through alterations in secondary structure. It was considered likely that the shorter fragment would less accurately reflect *in vivo* conditions, and it is probable that even the longer fragment would be insufficient to mimic secondary structures existing in full-length RNA. A further consideration is that synthetic assays lack certain significant features of the cellular environment, such as hnRNPs or other splicing factors (Matveeva et al., 1998; Moore, Query & Sharp, 1993), which could affect binding of the 2'OMeAO through competition for the target site.

Of the 14 deoxy-AOs directed against splicing motifs in the long RNA fragment, the two which demonstrated the strongest affinity to their targets, dH46A(+63+82) and dH46A(-13+07), were then synthesised as 2'OMeAOs for subsequent evaluation in cell culture. Interestingly, 200ng of dH46A(+115+134) apparently failed to induce a detectable bandshift in every trial, despite being the DNA homologue of the 2'OMeAO which induced the strongest exon 46 skipping in the study by van Deutekom et al. (2001). However, when tested against the second smaller RNA fragment, as little as 5ng of dH46A(+115+134) was able to induce a bandshift. This highlights the potential effect of fragment length on the ability of a deoxy-AO to anneal to its target, and therefore the importance of fragment length on the validity of the RBA as a predictor of 2'OMeAO activity.

Another interesting finding was that the two donor site-directed deoxy-AOs, dH46D(+06-14) and dH46D(+08-12), appeared to anneal to their targets while dH46D(+02-18) and dH46D(+04-16) did not, despite targeting regions only two or four bases further into the intron. In addition, dH46D(+08-14) also did not appear to induce a bandshift, despite incorporating the sequences targeted by the two deoxy-AOs, dH46D(+06-14) and dH46D(+08-12), which had successfully induced bandshifts. While secondary structure of the fragment may have played a role, particularly with the downstream deoxy-AOs, it is also possible that the apparently unsuccessful deoxy-AOs did anneal to their targets but that this hybridisation did not result in a conformational

change sufficient to induce a bandshift. For this reason, RNase H digestion assays may be a useful adjunct to the RBA in predicting the ability of a 2'OMeAO to anneal to its target, in that this method does not rely on conformational change to detect binding of the deoxy-AO (Matveeva et al., 1998).

In evaluating the three selected 2'OMeAOs in cell culture (the two chosen as a result of the RBA as well as the original H46A(+115+134) previously tested), a variety of transfection protocols were employed. Under previously reported conditions (ExGen 500 as the transfection agent, allowing cells to differentiate for 12 days and using 1000ng of RNA as template in RT-PCR) (van Deutekom et al., 2001), none of the 2'OMeAOs tested induced exon 46 skipping. However, using the protocol which had been successful for exon 19 skipping in both human and mouse cells (Lipofectin as the transfection agent, allowing cells to differentiate for four days and using 50ng or 5ng of RNA as template in RT-PCR) resulted in the induction of exon 46 skipping by H46A(-07+13) and H46A(+63+82) when delivered at a final transfection concentration of 1000nM. These results demonstrate that binding to a target sequence, as indicated by a bandshift, does not necessarily guarantee antisense activity in cellular conditions. This was also seen in the study by van Deutekom et al. (2001), as only four of the five 2'OMeAOs which induced a shift in the gel mobility assay induced skipping of exon 46. It is possible that using the *in vitro* methods currently available, exon skipping can only be reliably predicted by biological assays, rather than in a synthetic environment using fragments of RNA.

In the current study, skipping of exon 46 was eventually achieved by targeting either the acceptor splice site or an internal exonic sequence, although this was a different site to the putative ESE targeted by van Deutekom et al. (2001). A study which examined the nucleotide sequences of dystrophin exons 43, 46 and 53 for splicing enhancer activity was unable to identify any sequences in exon 46 which enhanced splicing when inserted into *Drosophila* doublesex pre-mRNA (Ito et al., 2001). This was despite some of these sequences being purine-rich, leading the authors to conclude that exon 46 lacks a significant splicing enhancer sequence. It was suggested that the strength of the 5' and 3' splice sites (which had splice site scores of 97.3% and 85.6% respectively) may have been adequate to promote correct splicing, or that the flanking introns may contain splicing enhancers (Ito et al., 2001). It is also possible that the skipping of exon 46 in the study by van Deutekom et al. (2001) was achieved through disturbance of the RNA secondary structure induced by the binding of the 2'OMeAO,

rather than the target sequence being an actual ESE (van Deutekom & van Ommen, 2003). Whatever the mechanism, the reasons for the difference in results reported by van Deutekom and colleagues and those obtained in the current study are not clear.

One difference between the protocols employed in the two studies may partially explain the discrepancy in results. The 2'OMeAOs used in the study by van Deutekom et al. (2001), were all 5'-fluorescein (FAM)-labelled and originated from a different source to those used in this report. A study by Mann et al. (2001) reported that a 20mer 2'OMeAO with a 5'-fluorescein tag (FITC) was highly efficient in removing exon 23 as compared to the unlabelled 2'OMeAO of the same sequence. In addition, a 25mer 2'OMeAO (unlabelled) directed at the same region, but extending five bases further into intron 23, was found to induce efficient skipping. It was suggested that the 5' fluorescent tag extended the displacement properties of the 2'OMeAO further into intron 23 than the unlabelled 20mer, possibly obstructing sequences important for splicing. This was confirmed by the efficient skipping induced by 2'OMeAOs which were subsequently designed to extend further into this intronic region (Mann et al., 2002). It is therefore conceivable that the FAM label may have had a similar effect on the exon skipping reported by van Deutekom et al. (2001). The extended length of H46A(+115+134) in the van Deutekom study compared to the unlabelled 2'OMeAO used in this study may have resulted in the blocking of sequences upstream of the targeted region. It is possible that these sequences are involved in the efficient recognition of exon 46. In addition, 2'OMeAOs are eventually degraded by nucleases, predominantly by a 3' to 5' exonuclease activity, regardless of 2'OMe modifications (Agrawal 1999). It is possible that the 2'OMeAOs employed by van Deutekom and colleagues (2001) were able to persist longer in the cellular environment because of some level of protection conferred by the fluorescent moiety, thereby facilitating nuclear uptake of the 2'OMeAO. Furthermore, it has been reported that oligodeoxynucleotides carrying a fluorescent tag were observed to have comparatively greater stability inside cells than their untagged counterparts (Politz, Taneja & Singer, 1995). It is likely that similar differences exist between tagged and untagged 2'OMeAOs.

Chapter 7 – Results from targeting exons 19-25

The focus of this project was to evaluate several pre-mRNA motifs as potential sites for blockade by 2'OMeAOs, to induce the specific removal of the targeted exon. The final aspects of the project sought to apply the knowledge gained regarding target selection, to assess the possibility of multiple exon removal as is seen in protein studies on naturally occurring revertant fibres. These rare dystrophin-positive fibers occur singly, or in clusters, and may represent up to 10% of the total muscle fibre population (Sherratt et al., 1993). Furthermore, their very existence coupled with a reported increase in number with age (Hoffman et al., 1990) suggests there may be some selective advantage at play, perhaps indicating an attempt to compensate for nonsense or frameshift mutations in the dystrophin gene. We therefore hypothesised that utilising the 2'OMeAO-induced removal of a specific block of exons to mimic an intrinsic biological phenomenon may produce a more natural or functional revertant dystrophin and thereby provide a more effective therapy in the long term. The minimum number of naturally skipped exons has been reported as being as low as five (Wilton et al., 1999). This group has detected several of these rare revertant transcripts, one of which was missing dystrophin exons 21 to 25, and more significant to this project, one which was missing exons 19 to 25 (Wilton et al., 1999). We therefore attempted to induce multiple exon skipping as observed in revertant transcripts in *H-2K mdx* mouse muscle cells. We anticipated that initial experiments would determine the best target for the 2'OMeAO-induced removal of each exon individually, and subsequent experiments would then apply the best 2'OMeAOs in combination to induce multiple exon skipping.

7.1 RNA binding assay

The RNA binding assay was used to evaluate the splice sites of each exon as potential targets for its 2'OMeAO-induced removal. Pre-mRNA fragments of between 329 and 390 bases were transcribed, comprising regions of the acceptor and donor splice sites and the flanking intronic sequences of each exon to be evaluated.

Each fragment was synthesised using DNA isolated from *H-2K mdx* mouse muscle cells as template in the *in vitro* T7 transcription reaction (Section 3.6.3). After quantifying the purified RNA fragments by spectrophotometry, 50ng was placed into

individual hybridisation reactions with each of the relevant deoxy-AOs to assess their ability to anneal to their specific target and induce a bandshift.

Initial experiments were performed by adding 200ng of each deoxy-AO to the hybridisation reactions. Following the preliminary evaluation, the amount of each deoxy-AO was titrated against 50ng of RNA to determine which target might be most amenable to deoxy-AO hybridisation. Assessment of the degree of bandshift was made subjectively, based on the difference between the RNA alone control (bandshift rating of 0) and complete bandshift (bandshift rating of 4).

For ease of presentation, findings from the RBA with deoxy-AOs directed to pre-mRNA fragments comprising exons 21, 22 or 25 will be reported first, as the results were similar. Exons 20 and 24, which required the evaluation of additional target sites to achieve exon skipping, will be described in the subsequent sections.

Exon 23 skipping in the *H-2K mdx* mouse has previously been reported (Mann et al., 2002; Mann et al., 2002; Wilton et al., 1997a). Therefore, RNA binding studies were not performed as the motif targeted by the previously described M23A(+02-18) (Mann et al., 2002) has been shown to be highly effective at inducing the removal of exon 23.

7.1.1 Target selection for exons 21, 22 and 25

RNA fragments of 383, 340 and 380 bases representing exons 21, 22 and 25 respectively were synthesised in a cell-free assay to assess four deoxy-AOs designed to target the donor splice site of each exon. For each exon, all four deoxy-AOs tested were able to induce a bandshift rating of 4 at 200ng. The deoxy-AOs were titrated to determine the lowest effective dose. The results of the binding assay for all twelve deoxy-AOs are summarised in Table 7.1.

Even when added at 5ng, all four deoxy-AOs targeting exon 21 achieved a bandshift rating of at least 2, demonstrating the possible high amenability of the donor site for 2'OMeAO-induced exon skipping. As a lower dose of 2.5ng of dM21D(+04-16) was still sufficient to induce a strong bandshift, scoring a rating of 3, it was selected for testing in cell culture.

Following titration of the deoxy-2'OMeAOs targeting exon 22, dM22D(+04-16) appeared to bind most efficiently as 0.5ng was still sufficient to induce a complete bandshift. One nanogram of either dM22D(+08-12) or dM22D(+06-14) was enough

to induce a bandshift which scored a rating of 2, whereas the same dose of dM22D(+02-18) resulted in a bandshift rating of only 1. Of the deoxy-AOs screened, dM22D(+04-16) was selected to be synthesised as an 2'OMeAO for trial in cell cultures due to its apparent high annealing potential and dM22D(+08-12), four bases further into the exon, was evaluated as a comparison.

Subsequent titrations of the amount of deoxy-AO available to anneal to the exon 25 pre-mRNA fragment found that both dM25D(+08-12) and dM25D(+06-14) were able to induce moderate bandshifts (rating of 2) when as little as 2.5ng was added. Moving the deoxy-AOs just 2 or 4 bases more into the intron markedly decreased the proportion of induced shift relative to that induced by dM25D(+08-12) and dM25D(+06-14), indicating a potential reduction in the opportunity for dM25D(+04-16) or dM25D(+02-18) to anneal to the RNA.

Table 7.1 Estimated amounts of RNA fragment bound and induced to 'shift' due to a conformational change, given as a rating, where 4 represents a complete bandshift.

	Bandshift rating determined after exposure to varied				
deoxy-AO tested	200ng	5ng	2.5ng	1ng	0.5ng
dM21D(+08-12)	4	2	0	0	-
dM21D(+06-14)	4	4	2	0	-
dM21D(+04-16)	4	3	3	1	-
dM21D(+02-18)	4	4	2	0	-
dM22D(+08-12)	4	4	4	2	1
dM22D(+06-14)	4	4	4	2	1
dM22D(+04-16)	4	4	4	4	4
dM22D(+02-18)	4	4	3	1	1
dM25D(+08-12)	4	3	2	1	-
dM25D(+06-14)	4	3	2	1	-
dM25D(+04-16)	4	2	1	0	-
dM25D(+02-18)	4	2	0	0	-

7.1.2 Target selection for exon 20

The length of exon 20 (242bp), was such that it was considered necessary to transcribe two RNA fragments to evaluate the splice sites as potential targets for its 2'OMeAO-induced removal. These two fragments were 329 bases and 353 bases in length, comprising exon 20 and the acceptor or donor flanking intronic sequences respectively.

Four 2'OMeAOs had been designed to target the acceptor splice site and four were directed at the donor splice site of exon 20. The eight deoxy-AOs, dM20A(-18+02), dM20A(-16+04), dM20A(-14+06), dM20A(-12+08), dM20D(+08-12), dM20D(+06-14), dM20D(+04-16) and dM20D(+02-18) were then assessed for their ability to anneal to their specific target and induce a bandshift.

As can be seen in Table 7.1, dM20D(+04-16) and dM20D(+08-12) were able to induce the greatest degree of bandshift when delivered at 5ng. As such, these deoxy-AOs were selected for synthesis as 2'OMeAOs and tested in cell culture. However, subsequent difficulties in inducing exon 20 skipping with these 2'OMeAOs led to the evaluation of an additional four longer deoxy-AOs. dM20A(-15+10) and dM20A(-10+15) were directed at the acceptor site, and dM20D(+10-15) and dM20D(+10-20) targeted the donor site. Although these deoxy-AOs were designed to anneal to a larger region of each splice site, none were able to increase the degree of bandshift induced in the RNA binding studies and so they were not considered for synthesis as 2'OMeAOs. It is not known whether the inability of the longer deoxy-AOs to anneal to the target was related to secondary structure complications from either the deoxy-AO or the synthesised RNA fragment. Results of the binding assay for all 12 deoxy-AOs are summarised in Table 7.2.

Table 7.2 Estimated amounts of RNA fragment bound and induced to 'shift' due to a conformational change, given as a rating, where 4 represents a complete bandshift.

	Bandshift rating after exposure to varied amounts of deoxy-AO(ng)		
deoxy-AO tested	200ng	5ng	1ng
dM20A(-18+02)	0	0	0
dM20A(-16+04)	2	0	0
dM20A(-14+06)	2	0	0
dM20A(-12+08)	2	0	0
dM20A(-15+10)	4	1	0
dM20A(-10+15)	4	0	0
dM20D(+08-12)	4	2	1
dM20D(+06-14)	4	0	0
dM20D(+04-16)	4	2	0
dM20D(+02-18)	4	1	0
dM20D(+10-15)	4	0	0
dM20D(+10-20)	4	0	0

7.1.3 Target selection for exon 24

To assess possible targets for inducing exon 24 skipping, a 390 base pre-mRNA fragment comprising exon 24 and flanking intronic sequences was synthesised. Eight deoxy-AOs were designed, four to target the acceptor splice site, dM24A(-18+02), dM24A(-16+04), dM24A(-14+06) and dM24A(-12+08) and four directed against the donor splice site, dM24D(+08-12), dM24D(+06-14), dM24D(+04-16) and dM24D(+02-18). All eight deoxy-AOs were able to induce a complete bandshift. However, the acceptor site appeared to be slightly less accessible than the donor site to deoxy-AO hybridisation, as only one deoxy-AO, dM24A(-12+08), was able to induce a bandshift which scored a rating of 4 when added at 5ng. It was difficult to discern the degree of shift induced, possibly indicating that when bound, the donor site directed deoxy-AOs did not induce a substantial change in the conformation of the RNA fragment. Nevertheless, dM24D(+08-12) and dM24D(+06-14) did appear to bind most RNA when only 5ng of each was present.

An additional four deoxy-AOs, dM24A(-15+10) and dM24A(-10+15), which were directed at the acceptor site, and dM24D(+10-20) and dM24D(+15-10) which

targeted the donor site, were designed to anneal to a larger region of each splice site. For three of the second generation deoxy-AOs, dM24A(-10+15), dM24D(+10-20) and dM24D(+15-10), 5ng was capable of inducing bandshifts which rated as 4. dM24A(-15+10) was the only second generation deoxy-AO not able to anneal to its target even when added at 200ng. The results are summarised in Table 7.3.

Table 7.3 The amounts of RNA fragment bound and induced to 'shift' have been estimated as a rating, where 4 represents a complete bandshift.

	Bandshift rating after exposure to varied amounts of deoxy-AO(ng)	
deoxy-AO tested	200ng	5ng
dM24A(-18+02)	0	0
dM24A(-16+04)	2	0
dM24A(-14+06)	2	0
dM24A(-12+08)	2	0
dM24A(-15+10)	0	0
dM24A(-10+15)	4	4
dM24D(+08-12)	4	2
dM24D(+06-14)	4	3
dM24D(+04-16)	4	1
dM24D(+02-18)	4	1
dM24D(+10-20)	4	4
dM24D(+10-15)	4	4

7.2 Quality assay of 2'OMeAOs directed at exons 20 - 25

Prior to myotube transfection, all 2'OMeAOs were subject to the standard quality control assessment. As described earlier, ~200ng of each 2'OMeAO was electrophoresed through a denaturing polyacrylamide gel (Figure 7.1). Only 'in-house' 2'OMeAOs were used in this part of the study and all were of an acceptable standard to proceed to cell transfections. In cases where synthesis was not of high quality, eg. M21D(+4-16) and M25D(+6-14), 2'OMeAO concentrations were adjusted and re-evaluated by spectrophotometry prior to cell transfection. Shorter products, while not ideal, still contain some sequence of the full length 2'OMeAO. It should also be noted that the presence of these shorter products does not necessarily compromise the ability of an 2'OMeAO to induce efficient and precise exon skipping (Figures 5.1, 5.6 and 5.15).

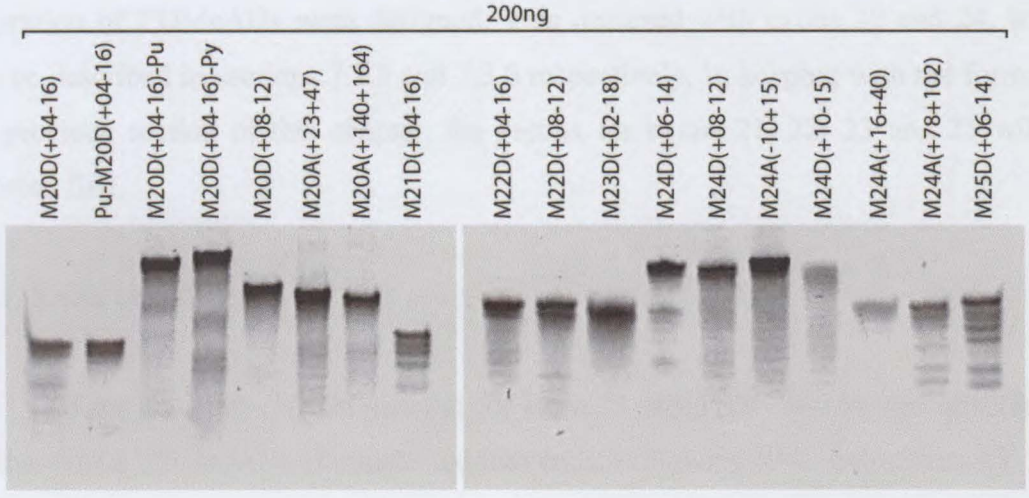

Figure 7.1 Each 2'OMeAO directed at exons 20 to 25 were run on a denaturing polyacrylamide gel. Despite the presence of additional bands, all 2'OMeAOs were judged to be of a sufficiently high standard to proceed to cell transfection studies. Furthermore, 2'OMeAOs of questionable concentration were re-evaluated by spectrophotometry prior to their use in cell culture.

7.3 2'OMeAO-induced Exon Skipping

Deoxy-AOs that were able to induce a bandshift rating of at least 2 when present at a maximum of 5ng per reaction were re-synthesised as 2'OMeAOs for further evaluation in cell culture.

A titration of the transfection concentration of each 2'OMeAO was performed. Total RNA was extracted 24 hours post-transfection and analysed for the presence of exon skipping. Subsequently, any 2'OMeAO-induced products were isolated by bandstab (Wilton et al., 1997b) and subjected to a further 35 cycles of PCR before being purified and directly sequenced. Analysis of the sequences was performed to verify the specific removal of an exon from the mature transcript and to characterise any additional products.

If it was found that the first generation of 2'OMeAOs produced were unable to induce exon skipping at an acceptable transfection dose (300nM or less), a second generation of 2'OMeAOs were designed. This occurred with exons 20 and 24, which will be described in sections 7.3.5 and 7.3.6 respectively. In keeping with the format of the previous section of this chapter, the results for exons 21, 22, 23 and 25 will be reported first.

7.3.1 Exon 21

Of the four deoxy-AOs assayed for exon 21, dM21D(+04-16) was selected for synthesis as a 2'OMeAO and transfected into cells. Following RNA extraction, RT-PCR analysis of the transcripts revealed an unmodified product corresponding to 890bp and a smaller, out-of-frame exon 21-deleted product of 709bp (Figure 7.2). M21D(+04-16) was able to induce the precise and reproducible exon 21-skipped transcript when delivered at a final concentration of 300nM.

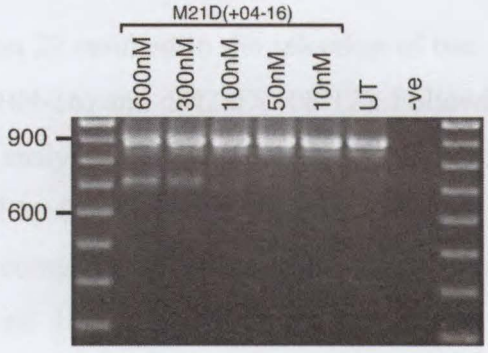

Figure 7.2 Products generated from the nested RT-PCR analysis of *H-2K mdx* mRNA following myotube transfection with a titrated 2'OMeAO, M21D(+04-16), targeting the donor splice site of exon 21. A dose-dependent effect of 2'OMeAO concentration on the abundance of the 709bp transcript fragment was observed, corresponding to the exon 21 skipped product.

Isolation of the shorter transcript fragment by bandstab and direct sequencing confirmed the identity of the 709bp product as exon 20 joined precisely to exon 22, verifying the specific action of M21D(+04-16) to induce exon 21 removal (Figure 7.3).

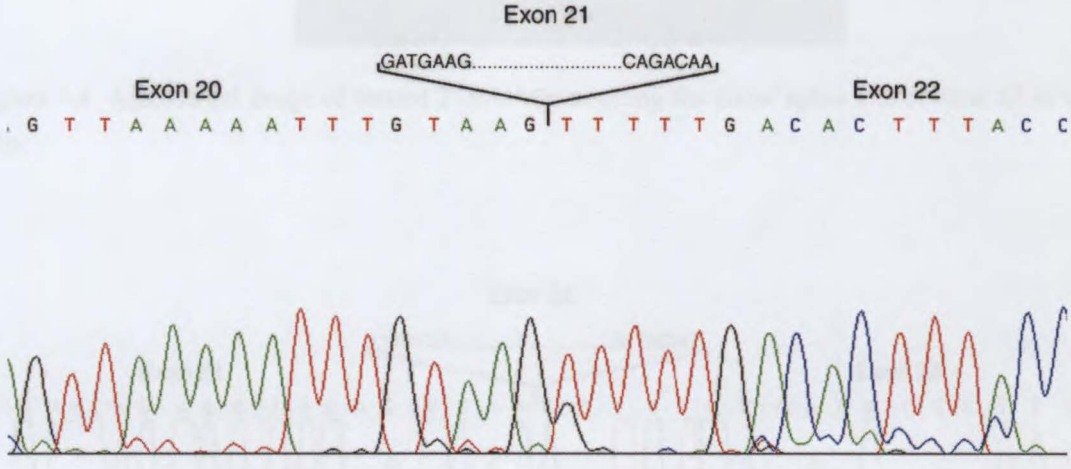

Figure 7.3 DNA sequence chromatogram across the junction of dystrophin exons 20 and 22, indicating the precise removal of exon 21.

7.3.2 Exon 22

The RBA for exon 22 resulted in the selection of two deoxy-AOs for synthesis as 2'OMeAOs, dM22D(+04-16) and dM22D(+08-12). Following cell transfection, total RNA was extracted and analysed for the presence of the out-of-frame exon 22-skipped transcript fragment. M22D(+08-12) and M22D(+04-16) were each able to consistently induce a shorter product corresponding to 627bp, indicating the removal of exon 22, at a final transfection dose of 10nM (Figure 7.4). Subsequent isolation and sequence analysis of the 2'OMeAO-induced product verified that exon 21 was spliced exactly to exon 23, confirming the complete removal of exon 22 from the mature transcript (Figure 7.5).

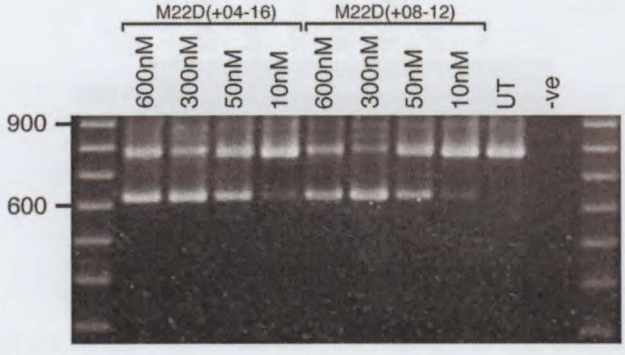

Figure 7.4 Agarose gel image of titrated 2'OMeAOs targeting the donor splice site of exon 22 in *mdx* cells.

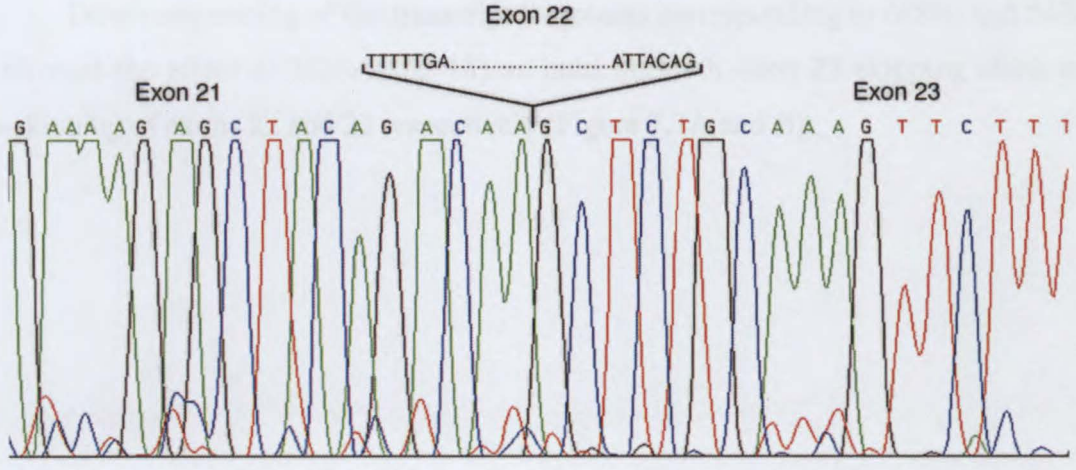

Figure 7.5 DNA sequence chromatogram of the dystrophin gene transcript across exons 21 and 23. The precise excision of exon 22 from *H-2K mdx* dystrophin mRNA, induced by the donor splice site directed 2'OMeAOs, M22D(+04-16) and M22D(+08-12), is shown.

7.3.3 Exon 23

To confirm the findings of Mann et al. (2002), titrated amounts of the 2'OMeAO M23A(+02-18) were transfected into *H-2K mdx* muscle cells. Total RNA was then extracted 24 hours post-transfection, purified and quantified for subsequent analysis by RT-PCR. Consistent with the previously reported results (Mann et al., 2002), transfection doses from 600nM down to 50nM were able to induce two additional transcripts, one in which exon 23 alone was skipped, and a less abundant product missing both exons 22 and 23 (Figure 7.6).

Figure 7.6 A titration of the exon 23 donor site-directed M23D(+02-18), demonstrating the two induced transcript fragments. A dose-dependent effect on the abundance of both the exon 22 skipped product and the product resulting from the co-skipping of exons 22 and 23 was clearly evident.

Direct sequencing of the transcript fragments corresponding to 688bp and 542bp confirmed the effect of M23A(+02-18) as inducing both exon 23 skipping alone and co-skipping of exons 22 and 23 respectively (Figure 7.7A and B).

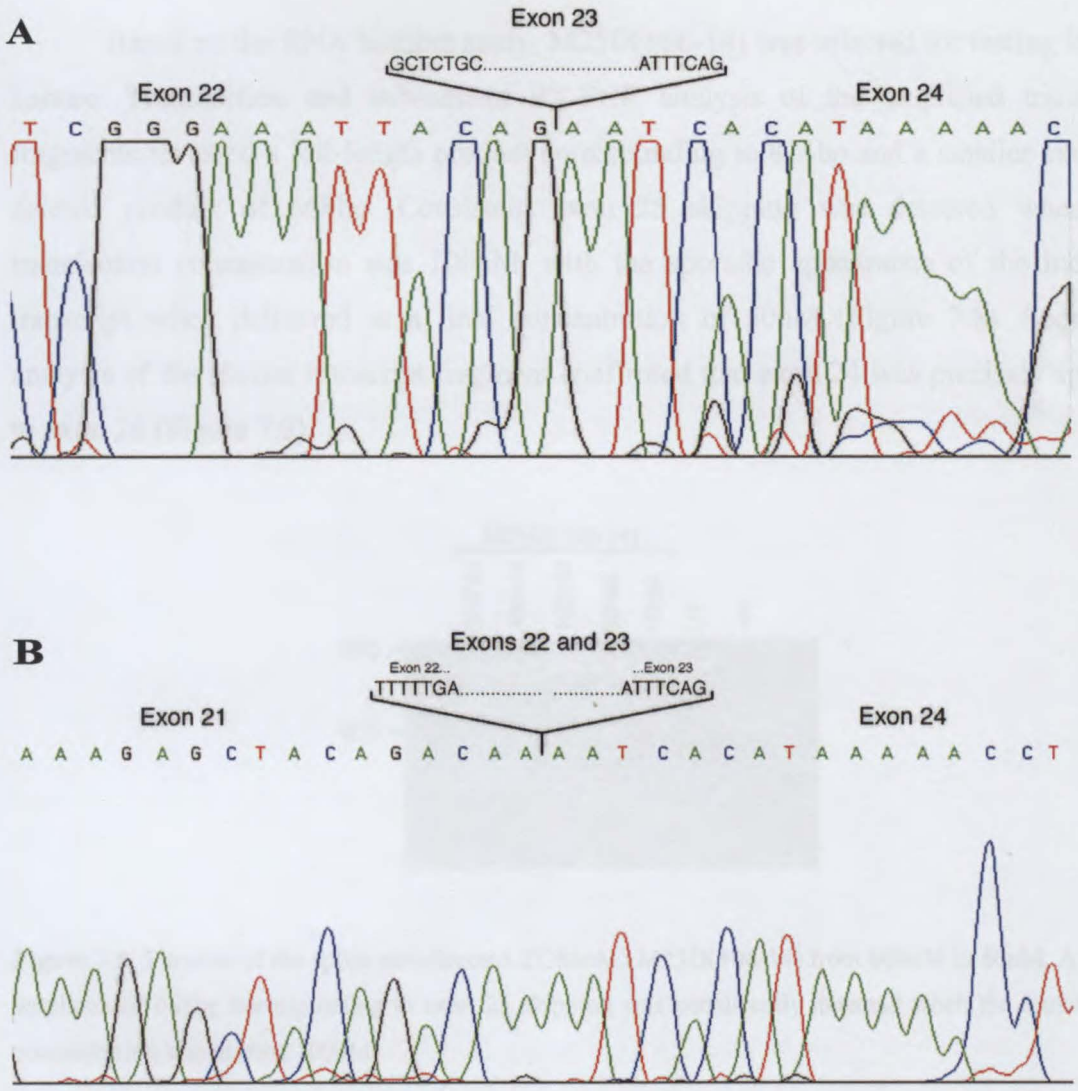

Figure 7.7 DNA sequence chromatograms of the dystrophin gene transcript across exons 22 and 24 and exons 21 and 24. Chromatogram (A) verifies the precise skipping of exon 23 and (B) confirms the co-skipping of exons 22 and 23.

7.3.4 Exon 25

Based on the RNA binding study, M25D(+06-14) was selected for testing in cell culture. Transfection and subsequent RT-PCR analysis of the amplified transcript fragments revealed a full-length product corresponding to 824bp and a smaller exon 25 deleted product of 668bp. Consistent exon 25 skipping was detected when the transfection concentration was 100nM, with the sporadic appearance of the induced transcript when delivered at a final concentration of 50nM (Figure 7.8). Sequence analysis of the shorter transcript fragment confirmed that exon 24 was precisely spliced to exon 26 (Figure 7.9).

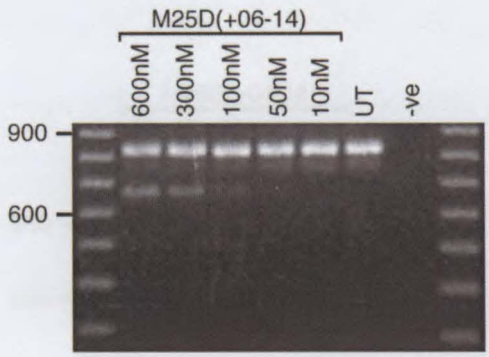

Figure 7.8 Titration of the splice site-directed 2'OMeAO M25D(+06-14) from 600nM to 50nM. A single amplicon of 668bp corresponding to exon 25 skipping was consistently detected when the transfection concentration was at least 100nM.

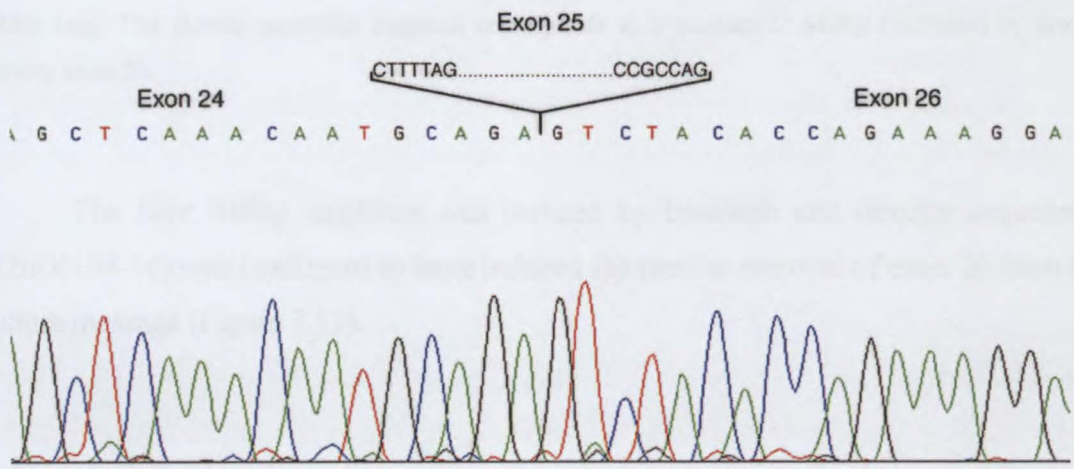

Figure 7.9 DNA sequence chromatogram of the dystrophin gene transcript across exons 24 and 26. The precise excision of exon 25 from *H-2K mdx* mouse muscle mRNA, induced by the donor splice site-directed M25D(+06-14), is shown.

7.3.5 Exon 20

For exon 20, the results of the RBA suggested that the acceptor site was generally less amenable than the donor site to deoxy-AO hybridisation. Therefore dM20D(+04-16) and dM20D(+08-12) were synthesised as 2'OMeAOs and evaluated in cell culture. Despite the indication by the bandshift assay that M20D(+08-12) might bind more efficiently (Table 7.2), it failed to induce exon 20 skipping even at 1000nM. Only M20D(+04-16) was able to consistently induce a detectable, albeit extremely weak, exon 20 skipped transcript provided the transfection concentration was at least 600nM (Figure 7.10).

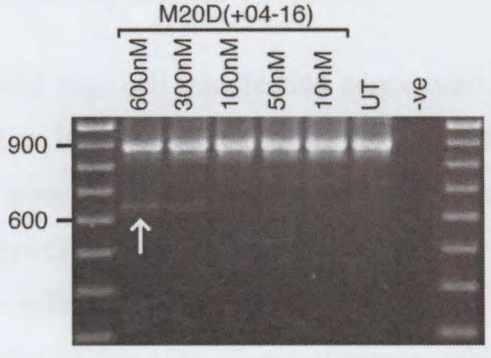

Figure 7.10 Exon 20 skipping induced by M20D(+04-16) in *H-2K mdx* mouse mRNA. RT-PCR analysis of RNA harvested 24 hours after cultured myotubes were transfected with M20D(+04-16) at concentrations ranging from 600nM down to 50nM. The full-length product spanning exons 18 to 23 is 890bp long. The shorter transcript fragment corresponds to a product of 648bp (indicated by arrow) missing exon 20.

The faint 648bp amplicon was isolated by bandstab and directly sequenced. M20D(+04-16) was confirmed to have induced the precise removal of exon 20 from the mature message (Figure 7.11).

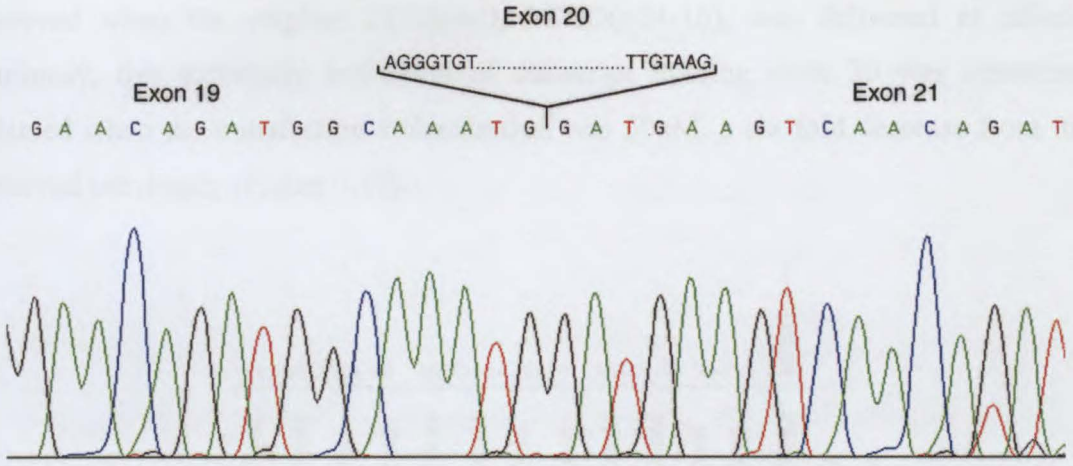

Figure 7.11 DNA sequence chromatogram demonstrating the precise excision of exon 20. M20D(+04-16) was never associated with the removal of other exons or the initiation of splicing from sites other than the consensus splice site sequences flanking exon 20.

Due to the relatively high cell transfection concentration of 2'OMeAO required for exon 20 removal, four longer deoxy-2'OMeAOs were assessed using the RNA binding assay. However, none were able to appreciably increase the degree of bandshift induced and therefore theywere not considered for synthesis as 2'OMeAOs.

In an attempt to enhance the skipping of exon 20, putative exonic splicing silencers were added to the 2'OMeAOs. These elements, which may act to repress or inhibit the inclusion of exons, can be purine or pyrimidine rich and are thought to bind many of the proteins involved in the splicing process (Fairbrother & Chasin, 2000).

Three more 2'OMeAOs were designed by modifying the marginally effective M20D(+04-16) at the 3' or 5' ends to include a purine or pyrimidine rich silencing element (Table 3.2). M20D(+04-16)-Pu and M20D(+04-16)-Py were synthesised with one of either of the silencing motifs (abbreviated from purine and pyrimidine to Pu and Py respectively) included at the 3' end of the molecule. We hypothesised that this modification may have the potential to further enhance 2'OMeAO stability by shielding the 2'OMeAO from exonuclease degradation which is initiated predominately from the 3' end (Agrawal & Ahktar, 1995). For comparison, the third 2'OMeAO, Pu-M20D(+04-16), was synthesised with a purine-rich motif at the 5' end. The addition of these silencing elements also provided an opportunity to assess whether these modifications would play a part in reducing accessibility to the donor site by competing splicing factors.

Regardless of the motif or its position, transfection of the *H-2K mdx* cells with these modified 2'OMeAOs did not increase the level of exon 20 skipping over that

observed when the original 2'OMeAO, M20D(+04-16), was delivered at 600nM. Curiously, this extremely low level of transcript missing exon 20 was sometimes detected when the transfection concentration was 50nM, a six-fold decrease from that observed previously (Figure 7.12).

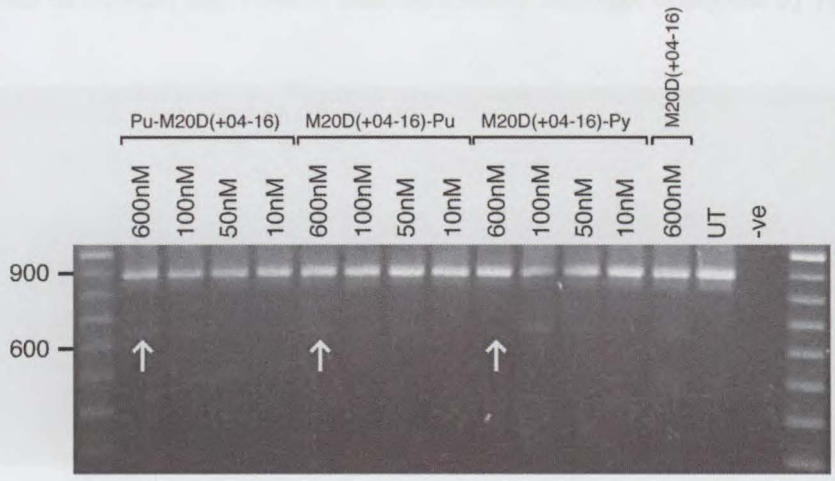

Figure 7.12 A titration in *H-2K mdx* cells of the original 2'OMeAO M20D(+04-16) coupled with one of two putative human splicing silencers (Fairbrother & Chasin, 2000). Similar levels of a product of low abundance corresponding to the exon 20 skipped transcript (indicated by arrows) were consistently detected at transfection concentrations from 600nM down to 50nM.

Due to the fact that neither splice site appeared to be a very effective target for exon 20 skipping (the acceptor splice site rated poorly in the RNA binding assay although its effectiveness as a target for 2'OMeAO-induced exon skipping in cell culture was not assessed), the possibility of targeting exon splicing enhancers (ESEs) was explored. No specific regions within exon 20 have been reported to play a role in its recognition or inclusion, as was the case for exon 19. Therefore, a computer program, RESCUE-ESE, was employed to predict the likely positions of ESEs by the statistical analysis of exon-intron and splice site composition within the given sequences (Fairbrother et al., 2002). Numerous positions were highlighted as sequences likely to possess ESE activity (Figure 7.13).

Based on the predictions made by the RESCUE-ESE program, two 25mer 2'OMeAOs, M20A(+23+47) and M20A(+140+164), were designed to anneal to regions appearing to occupy the greatest concentration of 'ESE-like' motifs. Subsequently, the 2'OMeAOs were transfected separately into *H-2K mdx* muscle cells at final concentrations of 600nM and 100nM and the mature message analysed by RT-PCR.

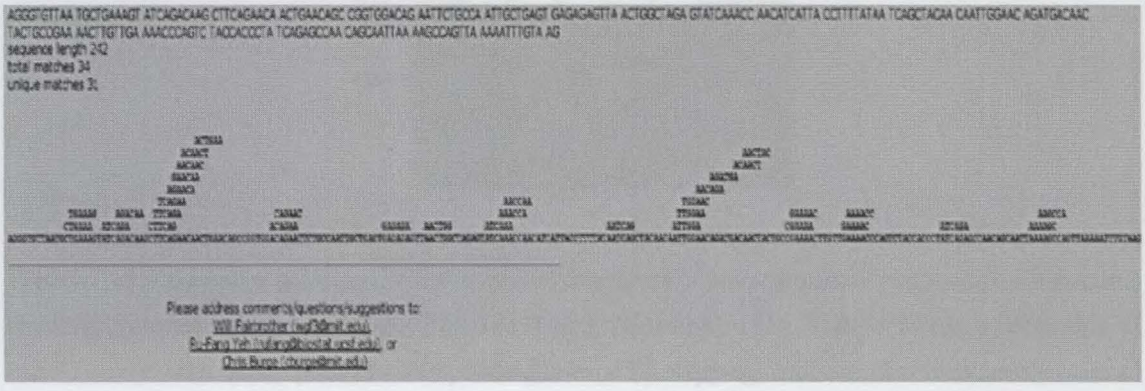

Figure 7.13 The entire exon 20 sequence (242 bases) was submitted for analysis by the ESE prediction program. This is the standard output received upon analysis of the sequence given. Predicted ESE sites were numerous and overlapping.

In addition to the expected full length product, two transcript species were consistently detected in the RNA exposed to M20A(+23+47), a product of low abundance corresponding to exon 20 skipping and a much stronger novel product ~130bp shorter than the full length transcript fragment. M20A(+140+164) was able to induce two products of very low abundance: one corresponding to exon 20 skipping and a novel product of ~570bp (indicated by arrow) in both 600nM and 100nM samples (Figure 7.14).

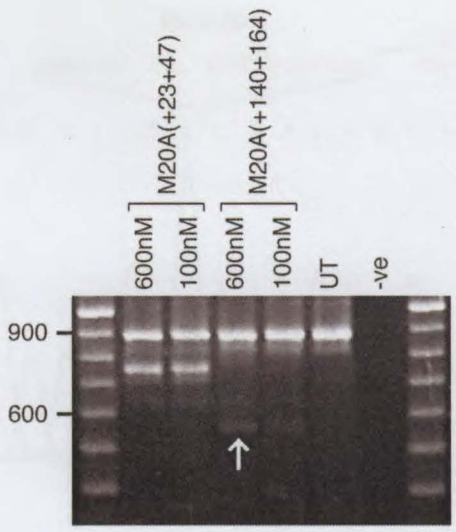

Figure 7.14 An agarose gel image of the amplified fragments of both the natural and modified transcripts resulting from transfection with M20A(+23+47) or M20A(+140+164). Both 2'OMeAOs were able to induce a very weak 648bp product corresponding to exon 20 skipping, and each also consistently induced non-specific skipping. M20A(+23+47) activated a cryptic splice site 135 bases downstream from the consensus acceptor splice site of exon 20, resulting in a novel product (755bp) of high abundance. M20A(+140+164) induced a weak product of 560bp corresponding to the co-skipping of exons 19 and 20 (indicated by arrow).

Each product was isolated by the bandstab method (Wilton et al., 1997b) and directly sequenced. M20A(+23+47) and M20A(+140+164) were confirmed to have induced the precise and repeatable skipping of exon 20 from the final message (Figure 7.11). In addition, the novel product induced by M20A(+23+47) was identified as resulting from the activation of a cryptic acceptor splice site 135 bases downstream from the normal acceptor site of exon 20 (Figure 7.15). As a consequence, the first 134 bases of exon 20 were removed when intron 19 was spliced out. The novel product induced by M20A(+140+164) was confirmed to have resulted from the removal of both exons 19 and 20 (Figure 7.16). This non-specific activity further supports the notion that blocking pre-mRNA sequences containing ESE-like motifs from splicing factors has the potential to interfere with correct exon definition.

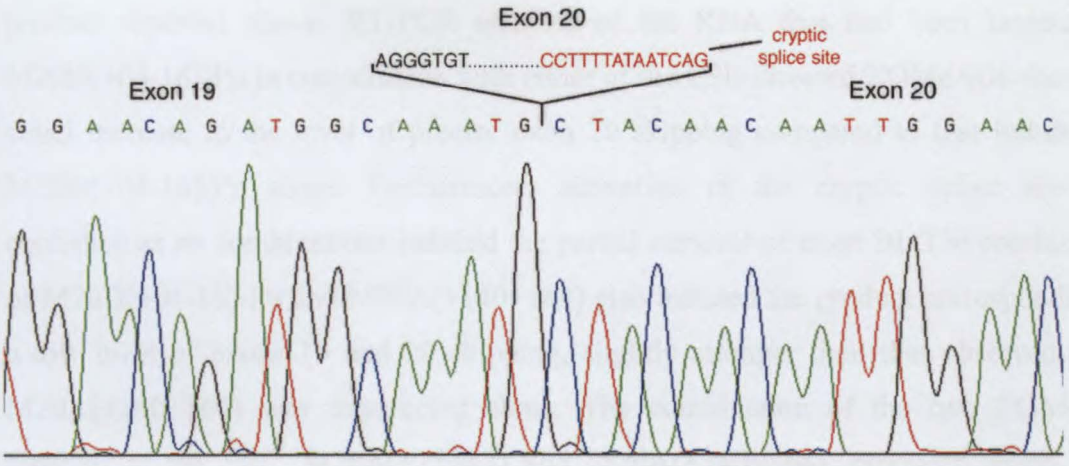

Figure 7.15 DNA sequence chromatogram of the dystrophin gene transcript across exons 19 and 20. Blocking the site recognised by M20A(+23+47) has activated a cryptic acceptor splice site which was 135 bases downstream of the consensus acceptor splice site.

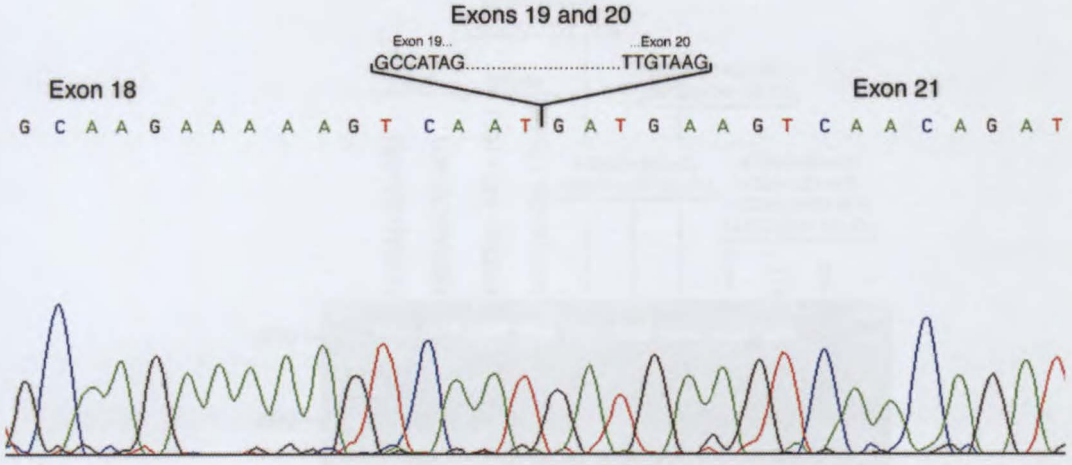

Figure 7.16 DNA sequence chromatogram of the dystrophin gene transcript from exons 18 to 21. The precise excision of exons 19 and 20 from *H-2K mdx* mouse muscle mRNA, induced by the donor splice site directed M20A(+140+164), is demonstrated.

In another attempt to induce exon 20 skipping, cell transfections with combinations of 2'OMeAOs involving M20D(+04-16)-Pu, M20A(+23+47), M20A(+140+164) and the successful exon 19 2'OMeAO, HM19A(+35+65), were performed. HM19A(+35+65) was transfected at 100nM, M20D(+04-16)-Pu and M20A(+140+164) were transfected at 600nM, and M20A(+23+47) was transfected at 100nM, the lowest concentration that was still able to induce the strong novel

product reported above. RT-PCR analysis of the RNA that had been targeted by M20D(+04-16)-Pu in combination with either of the ESE-directed 2'OMeAOs showed a small increase in the level of precise exon 20 skipping compared to that induced by M20D(+04-16)-Pu alone. Furthermore, activation of the cryptic splice site was abolished as no combinations induced the partial removal of exon 20. The combination of M20D(+04-16)-Pu and M20A(+140+164) also induced the product corresponding to a low level of exons 19 and 20 skipping, slightly stronger than that observed when M20A(+140+164) was transfected alone. The combination of the two 2'OMeAOs directed at the ESE, M20A(+23+47) and M20A(+140+164), produced much more abundant exon 20 skipped and exons 19 and 20 co-skipped transcripts (Figure 7.17). However, the combination of all four 2'OMeAOs was not able to increase the level of co-skipping of exons 19 and 20, despite the fact that one of the additional 2'OMeAOs was specifically targeted to exon 19.

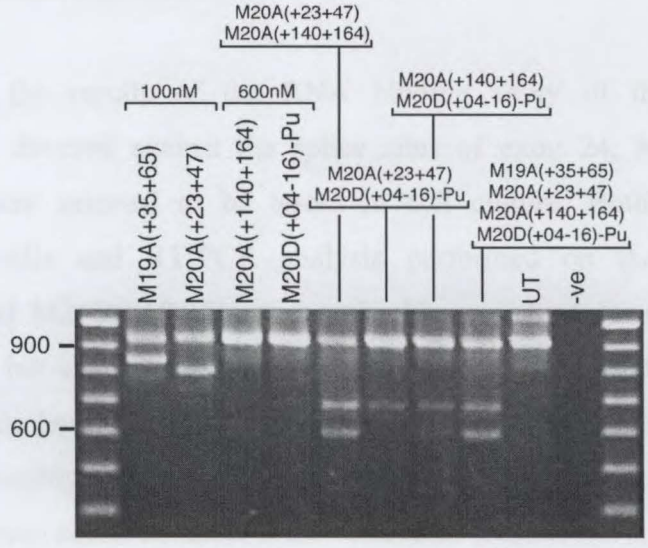

Figure 7.17 Agarose gel image of the RT-PCR products induced by three combinations of 2'OMeAOs directed at various exon 20 motifs. Alone, each was able to modify the splicing pattern to either remove exon 20 entirely at a low level, or imprecisely through cryptic splice site activation. The combination of M20D(+04-16)-Pu and M20A(+140+164) was able to induce the removal of both exons 19 and 20.

7.3.6 Exon 24

From the results of the initial RBA, it was decided to synthesise dM24D(+08-12) and dM24D(+06-14) as 2'OMeAOs. However, neither 2'OMeAO was able to induce a detectable exon 24 skipped transcript, even when the transfection concentration was as high as 1000nM. Therefore, in an attempt to coax out exon 24, combinations of 2'OMeAOs targeting exons 23, 24 and 25 were also transfected into *H-2K mdx* cells. A high degree of cell death was observed post-transfection due to the concomitant increase in Lipofectin concentrations. Moreover, RT-PCR analysis of the RNA extracted did not detect the removal of exon 24 from the mature transcript, although transcripts with either exon 23 or 25 skipped were detected (results not shown).

7.3.6.1 2'OMeAOs directed at splice sites

Based on the results of the RNA binding assay of the additional four deoxy-2'OMeAOs directed against the splice sites of exon 24, M24A(-10+15) and M24D(+10-15) were selected to be tested in cell culture. Both 2'OMeAOs were transfected into cells and RT-PCR analysis performed on the extracted RNA. M24A(-10+15) and M24D(+10-15) were each able to induce consistent and specific exon 24 skipping but at very low levels. However, a dose-dependent effect was not evident, as the same level of induced transcript was observed at concentrations tested down to 50nM, possibly indicating that a maximum level of competition with splicing factors may have been achieved under these conditions (results not shown).

The 685bp amplicons were reamplified by the bandstab procedure (Wilton et al., 1997) and directly sequenced. Both M24A(-10+15) and M24D(+10-15) were confirmed to have induced the precise removal of exon 24 from the final message (Figure 7.18).

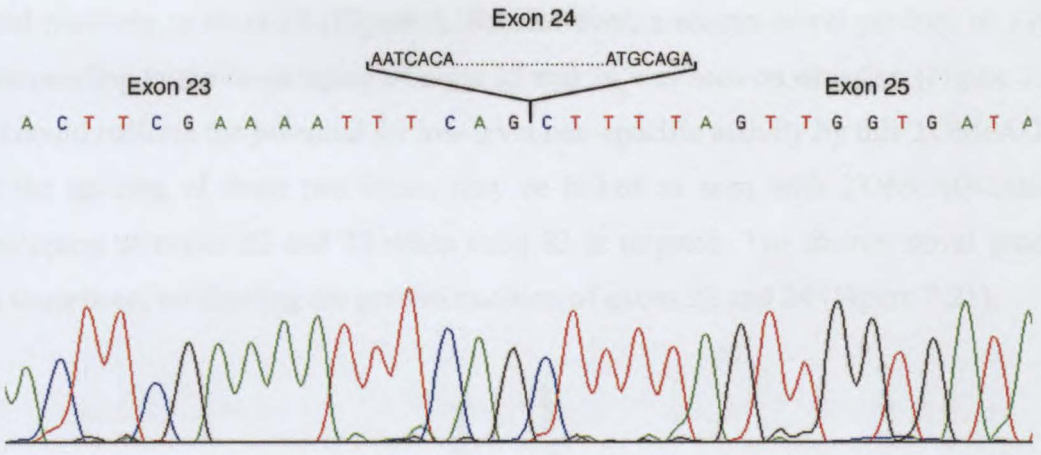

Figure 7.18 DNA sequence chromatogram of exon 24 skipping in *H-2K mdx* mRNA. Both M24A(-10+15) and M24D(+10-15) were able to induce the precise removal of the target exon, where exon 23 was spliced exactly to exon 25.

7.3.6.2 2'OMeAOs directed at ESEs

As with exon 20, the splice sites for exon 24 were not amenable as targets for 2'OMeAO-induced skipping. This discovery was not surprising for the acceptor splice site, considering the splice site score was relatively high (95.3%). However, the donor splice site score of 72.8% could indicate a sub-optimal motif and hence the potential to overwhelm splicing factors and induce exon 24 removal by targeting the donor site. As this was not the case, and as with exon 20, no specific regions within exon 24 have been identified in the literature as playing a role in its definition, the computer program RESCUE-ESE was again employed to predict the likely positions of ESEs within exon 24.

Based on the predictions made by RESCUE-ESE, two 25mer 2'OMeAOs, M24A(+16+40) and M24A(+78+102), were designed to anneal to regions likely to include the greatest concentration of 'ESE-like' motifs. Both 2'OMeAOs were subsequently transfected separately into *H-2K mdx* muscle cells at final concentrations of 600nM and 100nM and the mature message analysed by RT-PCR.

An exon 24 skipped product, of similar abundance to that induced by M24A(-10+15), was detected in the cells transfected with M24A(+16+40). Similar to earlier experiments with the splice site-directed 2'OMeAOs, no difference was observed between the 600nM and 100nM transfection concentrations tested (Figure 7.19). The 2'OMeAO-induced product was isolated for characterisation to ensure that the action of

M24A(+16+40) was specific. Sequencing of the product revealed that exon 23 had been joined precisely to exon 25 (Figure 7.18). However, a shorter novel product of 539bp corresponding to the co-skipping of exon 22 and 24 was seen on occasion (Figure 7.20) This could indicate the potential for low level non-specific activity by this 2'OMeAO, or that the splicing of these two exons may be linked as seen with 2'OMeAO-induced co-skipping of exons 22 and 23 when exon 23 is targeted. The shorter novel product was sequenced, confirming the precise excision of exons 22 and 24 (Figure 7.21).

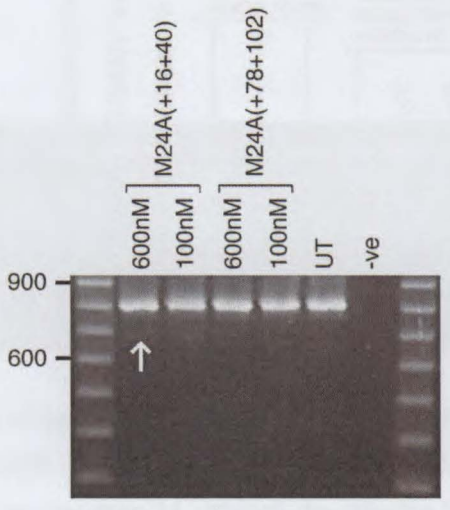

Figure 7.19 RT-PCR analysis showing the natural transcript fragments and the modified transcript fragments resulting from transfection with M24A(+16+40). The same level of induced transcript (indicated by arrow) was detected at both transfection concentrations. M24A(+78+102) consistently failed to induce exon 24 removal.

In another attempt to induce more pronounced exon 24 skipping, cell transfections with combinations of 2'OMeAOs targeting exon 24, M24D(+10-15), M24A(+16+40) and M24A(+78+102), were performed. Each 2'OMeAO was transfected at a final concentration of 300nM to minimise the degree of cell death associated with the high dose of Lipofectin. The 2'OMeAOs were then added to target the four possible combinations of the three splicing motifs. In these combinations, the final concentration was the sum of the concentrations used for each individual 2'OMeAO. RT-PCR analysis of the RNA from cells that had been targeted by each of the three paired combinations of 2'OMeAOs revealed specific exon 24 skipping. The combination of M24A(+16+40) with either M24D(+10-15) or M24A(+78+102) resulted in a skipped product of much higher abundance than that produced following

transfection with any single 2'OMeAO. The combination of M24D(+10-15) and M24A(+78+102) had the same effect but to a lesser degree, inducing a transcript marginally greater in abundance than when the 2'OMeAOs were transfected individually (Figure 7.20).

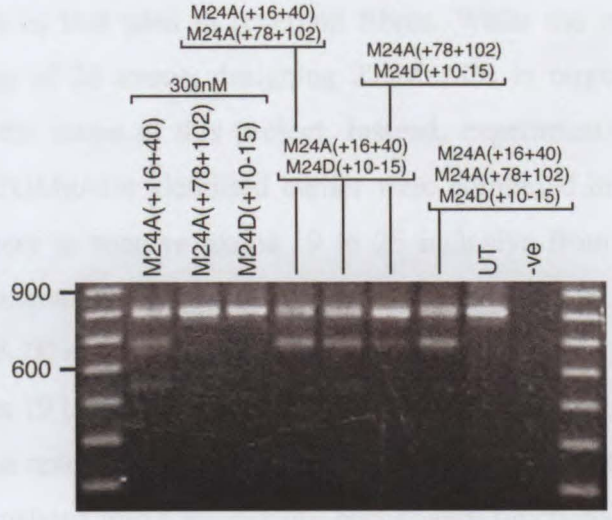

Figure 7.20 Agarose gel image of the RT-PCR products induced by the four combinations of 2'OMeAOs directed at various exon 24 motifs. In individual transfections, only M24A(+78+102) was unable to modify the splicing pattern to remove exon 24 although the skipping induced by M24A(+10-15) was highly inefficient. M24A(+16+40) also induced a novel 539bp product corresponding to the co-skipping of exons 22 and 24. All of the combinations resulted in specific skipping of exon 24.

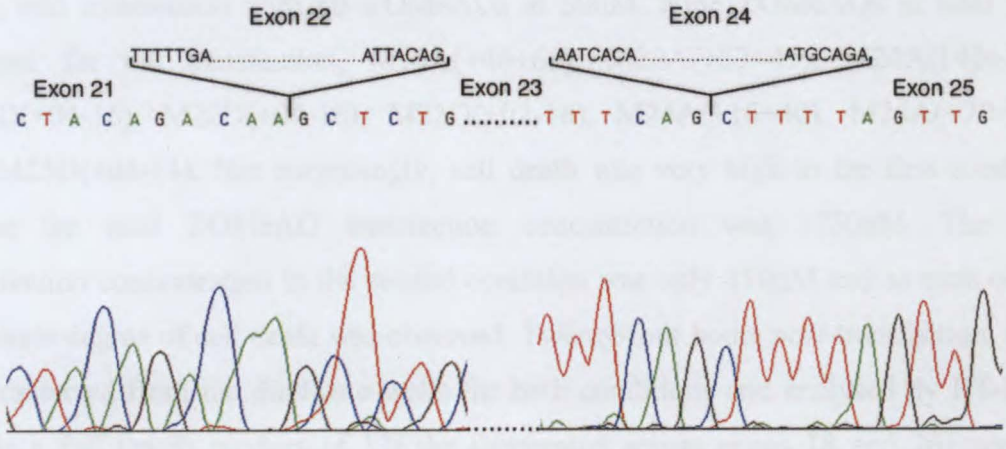

Figure 7.21 DNA sequence chromatogram of precise co-skipping of exons 22 and 24 in *H-2K mdx* mRNA sporadically induced by transfection with M24A(+16+40).

7.3.7 Multiple exon skipping

The focus of this section was to determine appropriate targets for the 2'OMeAO-induced removal of each exon. The ultimate goal was to apply these 2'OMeAOs in combination to *H-2K mdx* muscle cells and to induce the skipping of multiple exons such as that seen in revertant fibres. While the majority of revertant fibres skip in excess of 20 exons, designing 2'OMeAOs to target such a number of exons was beyond the scope of this project. Instead, experiments were performed in which each of the 2'OMeAOs identified earlier were combined in an attempt to force the splicing machinery to remove exons 19 to 25 inclusive from the final transcript. This particular arrangement, while rare, has been detected in naturally occurring revertant fibres in *H-2K mdx* and C57 normal mice (Wilton, et al. 1997). In *mdx* mice, the removal of exons 19 to 25 would not only bypass the nonsense mutation in exon 23, but also maintain the reading frame. This shorter mRNA transcript would therefore be capable of being translated into a shorter but presumably functional dystrophin protein. The same combination of 2'OMeAOs could be applied to any mutation occurring within the targeted exons, resulting in restoration of the reading frame. Therefore, efficient removal of exons 19 to 25 in combination could have broad application to DMD patients exhibiting a range of mutations within this region.

Two experiments were undertaken, transfection with the 2'OMeAOs at the minimum transfection concentration found to induce the removal of the targeted exon, and transfection with all 2'OMeAOs at 50nM. Nine 2'OMeAOs in total were selected for the transfection, M19A(+46+65), M20A(+23+47), M20A(140+164), M21D(+04-16), M22D(+04-16), M23D(+02-18), M24A(+16+40), M24A(+78+102) and M25D(+06-14). Not surprisingly, cell death was very high in the first condition where the total 2'OMeAO transfection concentration was 1750nM. The total transfection concentration in the second condition was only 450nM and as such only a moderate degree of cell death was observed. Twenty-four hours post-transfection, RNA was extracted from the duplicate wells for both conditions and analysed by RT-PCR. While a full length product of 1363bp (generated across exons 18 and 26) was not observed, a novel transcript fragment (223bp) corresponding to the skipping of exons 19 to 25 was detected in both conditions (Figure 7.22).

Additional tests were performed to screen for any non-specific activity of the combined 2'OMeAOs in other regions of the dystrophin transcript. Using the RNA extracted from the *mdx* cells which had been transfected with the two concentrations of combined 2'OMeAOs, regions across exons 1 to 10 and 70 to 79 were amplified. No alterations in the normal splicing patterns were detected other than the specific 2'OMeAO-induced removal of exons 19 to 25 (Figure 7.22).

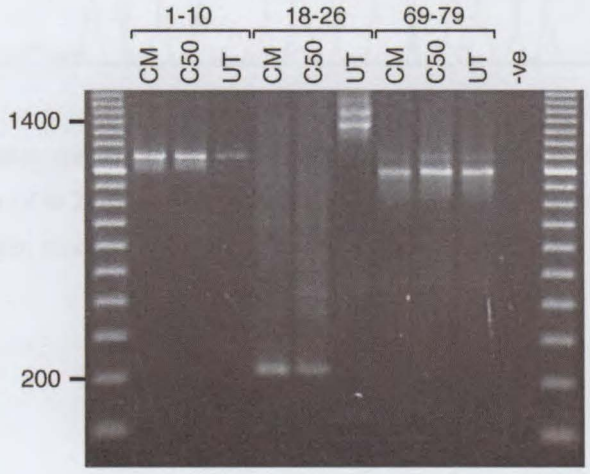

Figure 7.22 An agarose gel image showing the two 223bp products corresponding to exons 19 to 25 skipping detected in *H-2K mdx* mRNA. The combined 2'OMeAOs were transfected at the minimum effective concentration (CM) required to induce the removal of the target exon (where the minimum dose was never below 50nM) or at 50nM each (C50). 2'OMeAOs designed to skip exons 19 to 25 do not alter dystrophin processing in other regions of the gene transcript.

The 223bp amplicon was isolated by the bandstab method, then purified and directly sequenced. Transfection with all nine 2'OMeAOs directed at different motifs within seven exons and flanking introns was successful in inducing the precise removal of exons 19 to 25, such that exon 18 was spliced exactly to exon 26 (Figure 7.23). 2'OMeAO-induced skipping of multiple exons has not been reported previously in the literature.

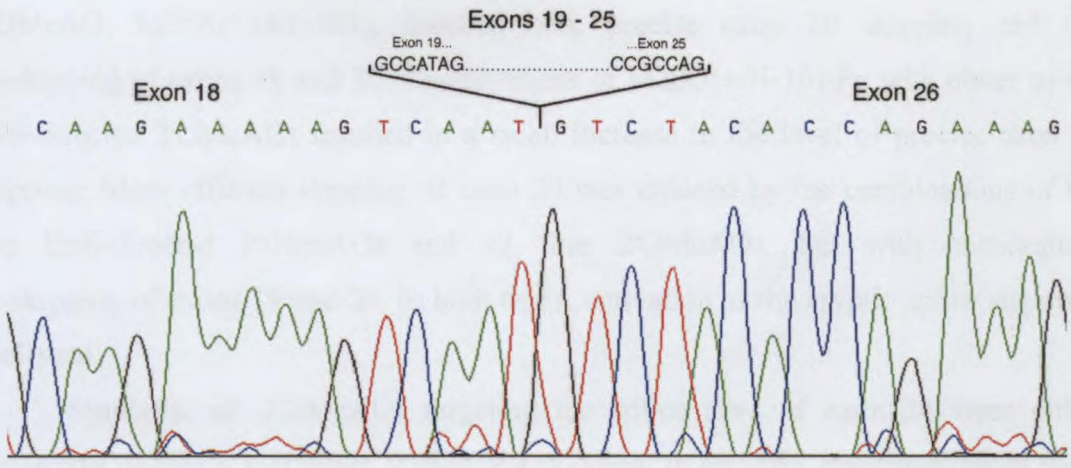

Figure 7.23 DNA sequence chromatogram of the dystrophin gene transcript from exons 18 to 26. The precise excision of exons 19 to 25 from the mature transcript, induced by the combination of 2'OMeAOs directed at each of the seven exons, is demonstrated.

7.4 Summary

This section of the project investigated the possibility of multiple exon removal which occurs naturally in revertant dystrophin-positive fibres. Initial experiments sought to determine the best target for the 2'OMeAO-induced removal of each exon individually. This proved to be a relatively simple process for certain exons and somewhat more challenging for others.

The donor splice sites of exons 21, 22 and 25 proved amenable to 2'OMeAO-induced exon skipping. In each case, 2'OMeAOs directed at the donor splice sites were able to induce consistent and precise removal of the target exon at an acceptable transfection concentration. Highly effective skipping of exon 23 and co-skipping of exons 22 and 23 was induced by targeting the donor splice site, concurring with the previously reported findings of Mann et al. (2001).

Inducing the removal of exon 20 proved more difficult. Of the two 2'OMeAOs targeting the donor splice site of exon 20, only M20D(+04-16) consistently induced skipping of exon 20, and this was at a very low level even at a concentration of 600nM. Modifying this 2'OMeAO with human exonic splicing silencers did not increase the level of skipping. Transfection of the cells with M20A(+23+47), designed to an ESE-like motif within exon 20, resulted in poor skipping of exon 20 as well as a novel

product arising from the activation of a cryptic splice site. A second ESE-directed 2'OMeAO, M20A(+140+164), induced both precise exon 20 skipping and the co-skipping of exons 19 and 20. Combinations of M20D(+04-16)-Pu with either of the ESE-directed 2'OMeAOs resulted in a small increase in the level of precise exon 20 skipping. More efficient skipping of exon 20 was induced by the combinations of the two ESE-directed 2'OMeAOs and all four 2'OMeAOs, but with concomitant co-skipping of exons 19 and 20. In both cases, activation of the cryptic splice sites was abolished.

Similarly, all 2'OMeAOs targeting the splice sites of exon 24 were either ineffective or highly inefficient at inducing skipping. In addition, combinations of these 2'OMeAOs and 2'OMeAOs targeting exons 23 and 25 were unable to induce the removal of exon 24. Low levels of exon 24 skipped transcript were induced by targeting an ESE-like motif with M24A(+16+40), along with the sporadic induction of exons 22 and 24 co-skipping. However, transfection with a combination of M24A(+16+40) and either M24D(+10-15) or M24A(+78+102) increased the abundance of the exon 24 skipped product compared to that produced from transfection with any single 2'OMeAO, without any non-specific activity.

Determining the targets amenable to 2'OMeAO-induced removal of individual exons culminated in the transfection of *H-2K mdx* cells with each of the effective 2'OMeAOs in combination. The ultimate goal of skipping exons 19 to 25 was achieved, using a total of nine 2'OMeAOs. Using this combination resulted in skipping which was far more efficient than that achieved by individual 2'OMeAOs, as no full-length transcript remained. In addition, other regions of the gene transcript were screened, confirming that alterations in the splicing process were localised to the target area.

7.5 Discussion

7.5.1 Exons 21, 22 and 25

Selection of 2'OMeAOs and transfection of exons 21, 22 and 25 will be discussed together as each yielded similar results. First, RNA binding assays were to used to select which deoxy-AOs were to be synthesised as 2'OMeAOs. The limitations of the RBA in predicting the ability of a 2'OMeAO to re-direct splicing have been discussed in the previous chapter. For each exon, four deoxy-AOs were designed to target the donor splice site and assessed for their ability to anneal to their specific target. It was decided to test the donor splice site first, based on studies directed at this region of exon 23 (Mann et al., 2001; Wilton et al., 1999) as well as the results obtained for exon 19 in the current study (Errington et al., 2003). The observation that 2'OMeAOs directed at donor splice sites tend to have greater influence on splicing has also been made by another group (Sierakowska et al., 1996). In the current study, very low doses of each donor site-directed deoxy-AOs tested induced a bandshift sufficient to justify the synthesis of 2'OMeAO homologues. Consequently, other splicing motifs in these exons were not assessed as potential targets for 2'OMeAO induced exon skipping.

For exon 21, the 2'OMeAO M21D(+04-16) was found to induce precise and reproducible skipping at a final concentration of 300nM. While this concentration is considered to be relatively high by our group, it is still comparatively low considering the transfection concentrations reported in other studies (Dunckley et al., 1998; van Deutekom et al., 2001). The splice site score for the donor site of exon 21 is 87% (Senapathy et al., 1990), which may indicate a relatively high level of competition with splicing factors. The final concentration required to induce reliable exon 21 skipping falls within acceptable limits. However, further testing of the acceptor site, which has a score of 76% (indicating a lower competition with splicing factors), or of regions predicted to contain ESE-like motifs, may determine the location of targets more amenable to 2'OMeAO-induced skipping. It is interesting to note that while the RBA was generally correct in predicting the ability of the 2'OMeAO to anneal to the target, it did not reflect the concentration required to induce exon skipping and thus does not predict the efficacy of an 2'OMeAO targeted to a particular region.

Two deoxy-AOs directed at the donor site of exon 22 were selected for synthesis as 2'OMeAOs. Despite a moderate difference in apparent binding efficiencies, both

M22D(+08-12) and M22D(+04-16) appeared equally effective at inducing specific and efficient skipping of exon 22. For this exon, performance of the 2'OMeAOs in cell culture correlated well with the results of the RNA binding assay as both 2'OMeAOs were able to induce specific and efficient skipping of exon 22 at a final transfection dose of 10nM. These results were not unexpected because the splice site score for the donor site, at 79% (Senapathy et al., 1990), indicates a relatively low level of competition with splicing factors. In addition, removal of exon 23 is almost always associated with concomitant removal of exon 22, indicating that the latter exon may be particularly susceptible to 2'OMeAO-induced skipping and that there may be a relationship between the splicing of the two exons (Mann et al., 2002). However, it was interesting to note that targeting exon 22 did not result in the co-skipping of exons 22 and 23 in the current study, possibly reflecting a non-sequential order of exon splicing, as has been observed in other genes (Kessler et al., 1993).

Finally, the donor splice site of exon 25 was evaluated with the 2'OMeAO M25D(+06-14), which induced consistent exon 25 skipping at a transfection dose of 100nM. The donor splice site score, at 84%, was less than that of exon 21, and the lower concentration of 2'OMeAO required to induce skipping of exon 25 may again reflect a comparatively lower level of competition with splicing factors. Again, further testing of the acceptor splice site or regions predicted to contain ESE-like motifs may be desirable to determine the location of targets more amenable to 2'OMeAO-induced skipping of this exon.

It is interesting that similar sequences targeted by the donor site directed deoxy-AOs appeared to induce similar degrees of bandshift between exons (Table 7.1). This reflects the relatively high degree of conservation of the donor splice sites, which would result in similar secondary structures in these regions between exons. However, it is important to note that the RBA only reflects the ability of a deoxy-AO to anneal to an RNA fragment. The secondary structure of the pre-mRNA flanking the fragment may be significantly different, and each splicing motif may contribute to the splicing process in varying degrees (Ito et al., 2001).

7.5.2 Exon 20

Based on the results of the RBA, the acceptor site appeared to be less accessible than the donor site to deoxy-AO hybridisation. Despite the indication by the bandshift assay that M20D(+08-12) might bind more efficiently, only M20D(+04-16) was able to consistently induce a detectable, albeit extremely weak, exon 20 skipped transcript provided the transfection concentration was at least 600nM. As both 2'OMeAOs more than cover the consensus splice site, this may reflect a difference between the structures of the RNA fragment used in the bandshift assay and full-length cellular RNA such that the downstream region is actually more accessible. A further possibility is that the intronic region targeted by M20D(+04-16) may contain motifs more crucial to exon inclusion.

The calculated splice site score of 95% indicates that the donor site of exon 20 might be highly efficient and therefore difficult to obstruct. This, however, does not appear to be constant for all splice sites. For example, a strong positive correlation between splice site score and efficiency of 2'OMeAO induced exon skipping has been observed in other exons. Dystrophin exon 23 skipping was reported to be very efficient when targeting the donor splice site (Mann et al., 2001), which has score of 93.5%. In addition, exon 19 skipping was efficiently induced by targeting the acceptor splice site, which has a score of 91%. It is possible that as splice site scores increase, there is a point at which competition with splicing factors prevents access of the 2'OMeAO to the target site, such that skipping of an apparently highly efficient splice site, for example, the donor splice site of exon 20, becomes very inefficient.

Due to the high transfection concentrations required for exon 20 removal, further 2'OMeAOs were designed in an attempt to improve efficiency. Human silencing motifs thought to repress the inclusion of exons (Fairbrother & Chasin, 2000), were attached to the 3' or 5' ends of the weakly effective M20D(+04-16). The attachment of these motifs to the 3' end was also thought to have potential in improving the stability of the 2'OMeAO by protecting it from exonuclease degradation, which occurs from the 3' end (Agrawal & Ahktar, 1995). However, the three 2'OMeAOs designed with these modifications failed to increase the level of exon 20 skipping over that observed with the parent 2'OMeAO. One possible explanation is that these silencers were derived from human DNA sequence, and that mouse silencing motifs differ in base composition. Additionally, it is possible that the high level of competition with splicing factors

prevented the modified 2'OMeAO from hybridising with the donor splice site, in turn preventing the silencing motif from exerting any effect.

As neither the donor or acceptor splice sites appeared to be very amenable to 2'OMeAO-induced exon 20 skipping, targeting exon splicing enhancers (ESEs) was explored. It is important to note that the acceptor site was not evaluated in cell culture. The splice site score of 85% indicates that it may have been a moderately efficient splice site, but the RBA results suggested that accessibility to the site would have been limited, thus excluding it as a target for this study.

The RESCUE-ESE program (Fairbrother et al., 2002) was utilised to design M20A(+23+47) and M20A(+140+164), which were directed at regions that seemed to contain the greatest concentration of 'ESE-like' motifs. Two transcript species were consistently detected in the RNA exposed to M20A(+23+47), a very weak product corresponding to exon 20 skipping and a much stronger novel product 135 bases shorter than the full length transcript fragment. This suggests that the spliceosome selected a cryptic splice site when a motif (at least) partially responsible for exon inclusion was obscured by M20A(+23+47). The remarkable similarity of the splice site scores of the consensus and cryptic splice sites, at 85% and 84% respectively, highlights the importance of nearby motifs within the exon (or intron) which either enhance the selection of the correct splice site or suppress the selection of the cryptic splice site (Blencowe, 2000; Reed, 1996). It is possible that M20A(+23+47) blocked one of these motifs, removing its effect from the balance of factors determining splice site selection.

A similar effect has been observed in studies which targeted a putative ESE in dystrophin exon 51 (Aartsma-Rus et al. 2002, 2003). As well as specific skipping of the exon, a transcript corresponding to partial skipping of exon 51 was induced as a result of the activation of a cryptic splice site. Several studies have also reported the activation of cryptic splice sites because of disruptions of a donor or acceptor consensus splice site (Fernandez-Cadenas et al., 2003; Fletcher et al., 2001; Tuffery-Giraud, Chambert, Demaille & Claustres, 1999). It thus appears that alterations in either exonic sequences or splice sites can result in non-specific splicing. It has been suggested that targeting exon-internal sequences with 2'OMeAOs might reduce the risk of non-specific splicing aberrations through alteration of secondary structure such that the exon is no longer marked for inclusion (van Deutekom & van Ommen, 2003). However, the results of the current study demonstrate that binding of an 2'OMeAO to exonic sequences will not necessarily result in specific skipping, as targeting certain regions may promote the

selection of a cryptic splice site. Previously, we assumed that this could be circumvented by applying another 2'OMeAO to the cryptic splice site. It now appears that cryptic splice sites can be bypassed by selecting another motif in the pre-mRNA.

In addition, the second of the ESE-directed 2'OMeAOs, M20A(+140+164), also induced the complete removal of both exons 19 and 20. Co-skipping of exons was also reported following targeting of dystrophin exons 2 and 29 with ESE-directed 2'OMeAOs (Aartsma-Rus et al., 2002). It is interesting that in some cases the same co-skipped products were seen in the untreated RNA at weaker levels, suggesting that the 2'OMeAOs may be strengthening a naturally occurring alternative splicing process.

Efficient and precise skipping of exon 20 was finally induced following transfection of cells with combinations of the 2'OMeAOs M20D(+04-16)-Pu, M20A(+23+47) and M20A(+140+164). However, exon 20 removal was specific only in the combination of M20D(+04-16)-Pu and M20A(+23+47), as the other combinations induced concomitant exon 20 and the co-skipping of exon 19 and 20 skipping. This co-skipping was similar to that reported by Mann et al. (2001) for 2'OMeAOs directed at the exon 23 donor splice site. The authors suggested that co-skipping may be due to the intimate relationship between the splicing of introns 22 and 23 rather than a non-specific effect of the 2'OMeAO, particularly as there is no sequence homology between the two exons. As the splicing of downstream introns has been shown to influence the processing of introns upstream (Watakabe et al., 1993), it is possible that a similar intimate relationship exists between exons 19 and 20. M20D(+04-16), when transfected as an individual 2'OMeAO, was never associated with the removal of other exons or the initiation of splicing from sites other than the consensus splice site sequences flanking exon 20. Thus the results of these combined transfections suggest that it was the targeting of the exonic sequences which contributed to the non-specific effects. It is also interesting that the donor splice-site directed 2'OMeAO and the ESE-directed M20A(+140+164) both had the effect of preventing the activation of the cryptic splice site when combined with M20A(+23+47), and that the combination of these 2'OMeAOs resulted in a higher level of specific exon 20 skipping than M20D(+04-16)-Pu alone. This may indicate that both the donor splice site and ESE motifs were significant for correct recognition of the exon 20 boundaries.

7.5.3 Exon 24

Two of the donor site deoxy-2'OMeAOs, dM24D(+08-12) and dM24D(+06-14), identified by RBA as targeting the most accessible regions, were synthesised as 2'OMeAOs and transfected into cells. However, even transfection at 1000nM of either 2'OMeAO was unable to induce detectable exon 24 skipping. The acceptor splice site was not assessed in cell culture at this point due the poor accessibility of the region as indicated by the RBA.

Combinations of 2'OMeAOs directed at exons 23, 24 and 25 were then tested in an attempt to coax out the recalcitrant exon. It was thought that if the splicing of these exons was in some way linked or coordinated, removal of the flanking exons might encourage skipping of the central exon. Such intimate relationships have been demonstrated between exons 22 and 23 (Mann et al., 2001) and between exons 19 and 20 in the current study, in that it was difficult to induce skipping of the downstream exon without co-skipping of the upstream exon. Interestingly, the same effect was not seen for skipping of exon 19 or 22, perhaps reflecting the order in which these exons are removed from the pre-mRNA. It has been demonstrated that while splicing occurs in a general 5' to 3' direction, the order of splicing is not necessarily sequential (Kessler et al., 1993). It is possible that exon 20 is spliced before 19, so that if exon 20 is skipped, certain signals contributing to the inclusion of exon 19 are lost. However, attempts to induce the skipping of exon 24 through this mechanism were not successful, perhaps indicating that a similar link in processing does not exist between exon 24 and its flanking exons.

As these attempts were unsuccessful, longer deoxy-AOs were tested by RBA, resulting in the synthesis of M24A(-10+15) and M24D(+10-15). Despite the seemingly high binding efficiency of these deoxy-AOs, it would appear that the target sites selected were not sensitive to 2'OMeAO activity, as only an extremely weak exon 24 skipped product was detected. The donor splice site score for exon 24 is only 68% (Senapathy et al., 1990), indicating a very low level of efficiency, and therefore obstructing this site may not have been sufficient to prevent inclusion of the exon in the mature transcript. Conversely, the acceptor splice site score is 100%, which indicates an extremely efficient site. It is likely that targeting the acceptor site was unsuccessful due to the very high level of competition with splicing factors inferred by this degree of efficiency.

It would seem logical that a strong acceptor splice site would not be as dependent on internal exon sequences for recognition. However, it has been demonstrated that there is no correlation between the predicted strength of the acceptor splice site and the presence of enhancer sequences (Ito et al., 2001). The significance of putative enhancer sequences in exon 24 was evaluated using two 2'OMeAOs designed to sites predicted to contain ESEs by the RESCUE-ESE program (Fairbrother et al., 2002). Individual transfections with M24A(+16+40) and M24A(+78+102) did not appreciably increase the degree of exon 24 skipping. Combinations of these 2'OMeAOs and the weakly effective M24D(+10-15) were then tested, based on the observation that multiple enhancer elements can synergistically increase the efficiency of splicing (Gravely et al., 1998). Positive results have been observed in similar experiments for exon 19 in the current study, and in a study which simultaneously targeted the splice sites of exon 51 (De Angelis et al., 2002). Consistent with these findings, the combination of M24A(+16+40) with either M24A(+78+102) or M24D(+10-15) or both resulted in a precise and much more abundant exon 24-skipped product. This lends further support to the observation that some exons may require the obstruction of more than one splicing motif to augment their efficient removal from the final transcript, similar to the results from the 2'OMeAO targeting of exon 20. Furthermore, non-specific exon removal was again observed following transfection with an ESE-directed 2'OMeAO. In this case, the skipping of exon 24 induced by M24A(+16+40) was associated with the co-skipping of exon 22. This, in addition to the results of targeting the ESE of exon 20 and the results reported by Aarstma-Rus and colleagues (2002), highlights the potential of exon-internal 2'OMeAOs to induce non-specific effects.

7.5.4 Multiple exon skipping

To assess the possibility of skipping multiple adjacent exons, such as is seen in naturally occurring revertant fibres, the most effective 2'OMeAOs for inducing skipping of exons 19 to 25, nine in total, were co-transfected into *H-2K mdx* cells. Two 2'OMeAOs were targeted against both exons 20 and 24 to improve the skipping efficiency of these two recalcitrant exons. Despite the inevitable cell death associated with high transfection concentrations in the two conditions, efficient and specific skipping of exons 19 to 25 was induced. This would result in an in-frame transcript, resembling a rare, previously characterised, naturally occurring revertant transcript (Lu et al., 2000; Wilton et al., 1997), and thus in a shortened but presumably functional dystrophin. The use of 2'OMeAOs to deliberately induce the skipping of multiple exons and produce an in-frame transcript has not been previously reported. It is not known whether the induced skipping was due only to the fact that a crucial splicing motif for each exon was blocked, or if it was in combination with a low level naturally occurring process (such as alternative splicing) favouring the formation of a revertant fibre.

Findings which appear to support the latter mechanism were reported by Aarstma-Rus and colleagues (2002). In this study, alternative products, corresponding to the skipping of between two and six exons, were observed in untreated primary human muscle cells. Similarly, a subsequent study reported the identification of shorter fragments corresponding to spontaneous skipping of a single exon from the untreated cells of three different DMD patients (Aarstma-Rus et al., 2003). In all but one case, the resulting transcript would be in-frame, perhaps indicating that these transcripts were responsible for populations of revertant fibres. These observations are not surprising considering that revertant fibres are estimated to be present in the muscle of up to 50% of DMD patients (Klein et al., 1992; Uchino et al., 1995). The ESE-directed 2'OMeAOs targeting these cells appeared to enhance this naturally occurring alternative splicing process, such that the skipped product (revertant-like transcript) was much more abundant. This occurred whether or not the exon targeted by the 2'OMeAO was the same exon naturally skipped in the untreated cells. These results are encouraging, particularly since the majority of enhanced alternative transcripts were in-frame.

One concern with any gene therapy approach is that the introduction of a gene product previously absent in a tissue may result in an immune response to that product. The lack of at least a few exons in revertant dystrophins suggests that restoration of

full-length dystrophin (ie. with chimeraplasts), or the introduction of full-length dystrophin by a vector, could be hampered by immunogenic responses (Lu et al., 2000). Many dystrophic individuals will not have been exposed to dystrophin previously and may perceive it as a neoantigen (Ferrer et al., 2000). The extent of this immunogenicity is unclear. Immune responses were not observed following the transfer of full-length or minidystrophin constructs in *mdx* mice by one group (Ferrer et al., 2000), but have been observed following the introduction of full length dystrophin by gene transfer into *mdx* mice in another study (Ohtsuka et al., 1998).

An approach which increases the frequency of revertant-like fibres may avoid the possibility of triggering an immune response. It has been suggested that a panel of functional transgenes could be designed, based on commonly encountered revertant isoforms (Lu et al., 2000). In order to avoid an immune response, it is likely that this process would have to be applied on an individual basis, as the exon skipping required to mimic a naturally occurring revertant transcript would vary between patients. This may not always equate to the minimum number of exons required to restore the reading frame.

Chapter 8 - Conclusions and Future Directions

8.1 Overview

Antisense oligonucleotides were initially investigated as sequence-specific downregulators of gene expression (Weiss, Davidkova & Zhou, 1999). In subsequent studies, chemically modified versions of these molecules have demonstrated the ability to restore the expression of genes inactivated by aberrant splicing (ie. cryptic splice site activation) mutations (Dominski & Kole, 1993; Sierakowska et al., 1996). More relevant to potential DMD therapies, 2'OMeAO-induced modulation of pre-mRNA splicing has been applied to the dystrophin gene to either restore the reading frame in the case of frame-shifting deletions (Aartsma-Rus et al., 2002, 2003; De Angelis et al., 2002; van Deutekom et al., 2001), or to target the disease-causing exons for removal from the final message (Mann et al., 2002; Wilton et al., 1999). In this manner, the induced transcript could be translated into a shorter, but presumably semi-functional, dystrophin.

At the commencement of this project, previous studies had targeted either the splice sites or an ESE but none had compared these regions within the same exon or across species. Therefore, the principal aim of this study was to identify the region(s) of the dystrophin pre-mRNA most amenable to specific and efficient 2'OMeAO-induced exon skipping. An additional aim was to apply the knowledge gained to induce multiple exon skipping to mimic a naturally occurring revertant transcript. We report varying efficiency of 2'OMeAO-induced removal of single and multiple exons of the dystrophin gene by targeting a variety of splicing motifs.

8.2 Target selection

It has been suggested that targeting ESEs may result in more specific exon skipping than targeting splice sites (van Deutekom et al., 2001). In the current study, the ESEs of several exons were targeted, with mixed results. The results of targeting exon 19 appeared to agree with this suggestion, as efficient and specific skipping was induced by 2'OMeAOs directed at ESEs. Conversely, targeting the ESEs of exons 20 and 24 resulted in non-specific antisense activity, such as the activation of a cryptic splice sites and the non-specific removal of an additional exon. Non-specific skipping

and splicing aberrations induced by targeting intra-exonic sequences have since been reported in other studies (Aartsma-Rus et al., 2002, 2003). These effects may be related to the 2'OMeAO target, or could be attributable to the order of splicing of these exons, such that if one exon is skipped, important signals contributing to the inclusion of the preceding exon are removed. A similar intimate relationship has been suggested to exist between exons 22 and 23 (Mann et al., 2001). Furthermore, even though targeting the ESE of exon 19 resulted in highly efficient skipping, this was not applicable to all exons investigated in this study. Targeting the ESE of exon 46 resulted in very inefficient skipping, and two ESE-directed 2'OMeAOs were required to induce the skipping of both exons 20 and 24. This also reflects the increased degree of difficulty in inducing the skipping of some exons compared to others.

In contrast to some of the results from exon skipping induced by ESE-directed 2'OMeAOs, highly specific and efficient skipping has been observed when targeting splice sites. The level of skipping induced by targeting the donor splice site of exon 19 was only marginally less efficient than that induced by targeting the ESE. The donor splice sites of exons 21, 22 and 25 also proved amenable to 2'OMeAO-induced exon skipping, with varying degrees of efficiency from moderate to very high. In contrast, targeting of the donor splice sites of exons 20 and 24 resulted in only very inefficient skipping, and no detectable skipping of exon 46 was observed when a 2'OMeAO was directed to this motif. Specificity of exon removal, however, was constant between exons, as targeting of the donor splice site was never associated with aberrant splicing of the exons evaluated in this study. The acceptor splice site was also targeted in exon 19, resulting in skipping which was only marginally less efficient than that induced by targeting the donor splice site. However, targeting the acceptor splice sites of exons 24 and 46 resulted in very inefficient skipping. The acceptor splice site was not assessed in the other exons as RNA binding assays predicted these sites to be relatively inaccessible. Since there was not always a correlation between strong binding and efficient exon skipping, future studies could re-examine these acceptor splice sites as potential targets. Although not observed in this study, targeting of the acceptor splice site has been reported to induce the co-skipping of exons (Mann et al., 2001). Thus the specificity of exon removal does not appear to be a function of target acquisition but rather reflects the exon properties and position in the gene transcript relative to adjacent exons.

The increased efficiency of exons 19, 20 and 24 skipping induced by combinations of 2'OMeAOs suggests that targeting a combination of splicing motifs can improve the efficiency of skipping. Similar results were reported in a study which simultaneously targeted the splice sites of exon 51 (De Angelis et al., 2002). It is also likely that multiple enhancer elements can additively increase the efficiency of splicing (Gravely, Hertel & Maniatis, 1998). Furthermore, the necessity of targeting more than one site to achieve efficient skipping of exons 20 and 24 lends further support to the observation that some exons may require the obstruction of more than one splicing motif to augment their efficient removal from the final transcript. This agrees with the suggestion that the significance of various splicing motifs and enhancers to exon inclusion varies between exons (Ito et al., 2001).

8.3 Future directions

The final aspects of this project sought to apply the knowledge gained regarding target selection to assess the possibility of multiple exon removal. Due to time constrainsts the evaluation of possible targets was not exhaustive, and further testing of the acceptor splice site or regions predicted to contain ESE-like motifs may determine the location of targets more amenable to 2'OMeAO-induced skipping. Nevertheless, the ultimate goal of skipping exons 19 to 25 was achieved, thus demonstrating the feasibility of this approach in modulating splicing patterns to mimic a naturally occurring revertant transcript. These results are very encouraging, particularly as the initial attempt was successful and the multiple exon removal appeared to be very efficient in that there were no other products of intermediate splicing. In addition, this approach has the potential to avoid triggering an immune response such as that seen following the introduction of full-length dystrophin into previously dystrophin-deficient tissues (Lu et al., 2000; Ohtsuka et al., 1998). In a therapeutic setting, each mutation would have to be evaluated on an individual basis, as the exon removal required to mimic a naturally occurring revertant transcript would vary between patients. Exon mapping has demonstrated that the most common revertant fibres arise from the skipping of 10 or more exons (Lu et al., 2000); thus the minimum number of skipped exons required to mimic an already occurring revertant fibre in a given cell population may not always be the same as the minimum number of exons required to restore the reading frame. Further *in vitro* studies will be required to evaluate the skipping of other

combinations of exons to achieve a variety of revertant-type transcripts, as the exons skipped in the current study would only be applicable to patients with mutations in exons 19 - 25. This would result in the development of a range of 2'OMeAOs which could be administered in various combinations ('cocktails') to treat many different mutations. *In vivo* studies will also need to be undertaken to verify that the shortened dystrophin is functional and non-immunogenic.

One limitation of this approach is that while transfection with the combination of 2'OMeAOs resulted in very efficient and specific skipping, it was also associated with a moderately high level of cell death. Further studies could assess the possibility of achieving the same multiple exon skipping using only selected 2'OMeAOs, particularly since the splicing of some exons appeared to be linked. This would reduce the total concentration required for transfection. One promising study has recently reported the development of two 2'OMeAOs which can skip multiple exons. In this novel approach, the two 2'OMeAOs, joined by a ten base uracil linker, are directed simultaneously at splicing motifs within the first and last exons of the multiple exon segment to be removed (Aarstma-Rus et al., 2004). Such an approach would minimise the number of 2'OMeAOs required and thus reduce the toxicity associated with the delivery of multiple 2'OMeAOs. Further studies will be required to determine the maximum number of exons which can be skipped using this technique.

The current study employed 2'OMeAOs, which are modified for increased stability and resistance to nuclease degradation (Altmann et al., 1998; Lavrovsky et al., 1997; Dias & Stein, 2002; Seeberger & Caruthers, 1998). One concern, however, is that the phosphorothioate backbone modification may incite toxic or nonspecific effects *in vivo* (Agrawal, 1999). Further modifications of antisense oligonucleotides may yield improvements in sequence-specificity, nuclease resistance and cellular uptake (van Deutekom & van Ommen, 2003). The development of several relatively new and promising chemical modifications, including locked nucleic acids, peptide nucleic acids (Sazani et al., 2002) and morpholino antisense oligonucleotides (Gebski, Mann, Fletcher & Wilton, 2003; Sazani et al., 2002) is ongoing.

Even when antisense oligonucleotide chemistries, pre-mRNA target selection and transfection conditions have been optimised, delivery of the therapeutic molecule(s) to all dystrophin deficient tissues will remain a major challenge to this form of genetic therapy. Skeletal muscle is the most obvious target, but as most DMD patients die as a result of cardiac or respiratory complications, and some suffer from a degree of mental

impairment (Emery, 2002), it is crucial that the other affected tissues are also treated. Intraperitoneal injection of morpholino oligonucleotides and PNAs has demonstrated uptake and activity in muscle and heart tissue (Sazani et al., 2002). However, because the blood-brain barrier prevents access of oligonucleotides to the cortex (Sazani et al., 2002), delivery to the brain will be particularly challenging. Persistence of the therapeutic molecule is also an issue, as it is not known how long a revertant-type dystrophin will persist or whether it will accumulate over time, and therefore how often repetitive administration will be required. Although repeated intramuscular injections of 2'OMeAOs into *mdx* mice can result in the persistent production of the dystrophin protein and an improvement in muscle function (Lu et al., 2003), a less invasive and impractical method capable of delivery to all affected tissues will be required. As long as a suitable means for the administration of antisense oligonucleotides can be developed, reading frame correction by these molecules represents a promising therapeutic approach for many DMD patients.

8.4 Summary

The complexity of the dystrophin gene and its protein have been a major challenge to those seeking to find a successful therapy for DMD. Reports of the successful reading-frame restoration in the primary cells of DMD patients are starting to emerge (Aartsma-Rus et al., 2002, 2003; De Angelis et al., 2002), increasing optimism for an antisense oligonucleotide therapy based on re-directing gene transcript processing. However, lack of efficiency and delivery represent major obstacles to be overcome before clinical success is attained. In addition, this approach could only benefit those patients whose particular dystrophin gene mutation can be by-passed with specific exon skipping combinations which do not involve essential functional domains. The focus of the present study was to determine the best targets for the 2'OMeAO-induced removal of certain individual exons. The results presented suggest that the sensitivity of either acceptor, donor or ESE splicing motifs to modulation by 2'OMeAOs is unique to the exon selected for removal and less dependent on the targeted sites. Therefore, there does not appear to be one specific splicing motif that can be universally targeted. Each mutation may have to be treated individually, assessing the best motifs on an exon to exon basis.

9.0 References

Aartsma-Rus, A., Bremmer-Bout, M., Janson, A. A. M., den Dunnen, J. T., van Ommen, G. B., & van Deutekom, J. C. T. (2002). Targeted exon skipping as a potential gene correction therapy for Duchenne muscular dystrophy. Neuromuscular Disorders, 12, S71 - S77.

Aartsma-Rus, A., Janson, A. A. M., Kaman, W. E., Bremmer-Bout, M., den Dunnen, J. T., Baas, F., van Ommen, G. B., & van Deutekom, J. C. T. (2003). Therapeutic antisense-induced exon skipping in cultured muscle cells from six different DMD patients. Human Molecular Genetics, 12 (8), 907 - 914.

Aartsma-Rus, A., Janson, A. A. M., Kaman, W. E., Bremmer-Bout, M., van Ommen, G. B., den Dunnen, J. T., Baas, F., & van Deutekom, J. C. T. (2004). Antisense-induced multiexon skipping for Duchenne muscular dystrophy makes more sense. American Journal of Human Genetics, 74, 83 - 92.

Acsadi, G., Dickson, G., Love, D. R., Jani, A., Walsh, F. S., Gurusinghe, A., Wolff, J.A., & Davies, K. E. (1991). Human dystrophin expression in *mdx* mice after intramuscular injection of DNA constructs. Nature, 352, 815 - 818.

Adams, M. D., Rudner, D. Z., & Rio, D. C. (1996). Biochemistry and regulation of pre-mRNA splicing. Current Opinion in Cell Biology, 8, 331 - 339.

Agrawal, S. (1992). Antisense oligonucleotides as antiviral agents. Trends in Biological Technology, 10, 152 - 158.

Agrawal, S. & Akhtar, S. (1995). Advances in antisense efficacy and delivery. Trends in Biological Technology, 13 (6), 197 - 199.

Agrawal, S. (1996). Antisense oligonucleotides: towards clinical trials. Trends in Biotechnology, 14 (10), 376 - 387.

Agrawal, S. (1999). Importance of nucleotide sequence and chemical modifications of antisense oligonucleotides. Biochimica et Biophysica Acta, 1489 (1), 53 - 68.

Ahn, A. H., & Kunkel, L. M. (1993). The structural and functional diversity of dystrophin. Nature Genetics, 3, 283 - 291.

Altmann, K.-H., Cuenound, B. and Von Matt, P. (1998). Novel Chemistry. Applied Antisense Oligonucleotide Technology. C. A. Stein and A. Kreig. New York, Wiley-Liss.

Anderson, M. S., & Kunkel, L. M. (1992). The molecular and biochemical basis of Duchenne muscular dystrophy. Trends in Genetics, 17, 289 - 292.

Baker, B., Condon, T., Koller, E., McKay, R., Siwikowski, A., Vickers, T., Monia, B. (2001). Discovery and analysis of antisense oligonucleotide activity in cell culture. Methods, 23, 191 - 198.

Bennett, C. F. (1998). Use of Cationic Lipid Complexes for Antisense Oligonucleotide Delivery. Applied Antisense Oligonucleotide Technology. C. A. Stein and A. Kreig. New York, Wiley-Liss.

Berget, S. M. (1995). Exon recognition in vertebrate splicing. Journal of Biological Chemistry, 10, 2411 - 2414.

Bertoni, C., & Rando, T. A. (2002). Dystrophin gene repair in *mdx* muscle precursor cells in vitro and in vivo mediated by RNA-DNA chimeric oligonucleotides. Human Gene Therapy, 13, 707 - 718.

Bies, R. D., Phelps, S. F., Cortez, M. D., Roberts, R., Caskey, C. T., & Chamberlain, J. S. (1992). Human and murine dystrophin mRNA transcripts are differentially expressed during skeletal muscle, heart and brain development. Nucleic Acids Research, 20 (7), 1725 - 1731.

Black, D. L. (1995). Finding splice sites within a wilderness of RNA. RNA, 1 (8), 763 - 771.

Blau, H. M., & Springer, M. L. (1995). Molecular medicine: muscle-mediated gene therapy. New England Journal of Medicine, 333 (23), 1554 - 1556.

Blencowe, B. J. (2000). Exonic splicing enhancers: mechanism of action, diversity and role in human genetic diseases. Trends in Biochemical Science, 25, 106 - 110.

Boussif, O., Lezoualc'h, F., Zanta, M. A., Mergny, M. D., Scherman, D., Demeneix, B., & Behr, J. (1995). A versatile vector for gene and oligonucleotide transfer into cells in culture and in vivo: polyethylenimine. Proceedings of the National Academy of Science, USA, 92, 7297 - 7301.

Branch, A. D. (1996). A hitch-hiker's guide to antisense and non-antisense biochemical pathways. Hepatology, 24, 1517 - 1529.

Bulman, D. E., Murphy, E. G., Zubrzycka-Gaarn, E. E., Worton, R. G., & Ray, P. N. (1991). Differentiation of Duchenne and Becker muscular dystrophy phenotypes with amino- and carboxy-terminal antisera specific for dystrophin. American Journal of Human Genetics, 48, 295 - 304.

Cartegni, L., Chew, S., & Krainer, A. (2002). Listening to silence and understanding nonsense: exonic mutations that affect splicing. Nature Reviews Genetics, 3 (4), 285 - 298.

Cerletti, M., Negri, T., Cozzi, F., Colpo, R., Andreeta, F., Croci, D., Davies, K. E., Cornelio, F., Pozza, O., Karpati, G., Gilbert, R., & Mora, M. (2003). Dystrophic phenotype of canine X-linked muscular dystrophy is mitigated by adenovirus-mediated utrophin gene transfer. Gene Therapy, 10, 750 - 757.

Chabot, B. (1996). Directing alternative splicing: cast and scenarios. Trends in Genetics, 12 (11), 472 - 478.

Chaubourt, E., Voisin, V., Fossier, P., Baux, G., Israel, M., & De La Porte, S. (2002). Muscular nitric oxide synthase (muNOS) and utrophin. Journal of Physiology - Paris, 96, 43 - 52.

Chelly, J., Kaplan, J. C., Maire, P., Gautron, S., & Kahn, A. (1988). Transcription of the dystrophin gene in human and non-muscle tissue. Nature, 333 (6176), 858 - 860

Cooper, B. J. (1989). Animal models of Duchenne and Becker muscular dystrophy. British Medical Bulletin, 45, (3), 703 - 718.

Cooper, B. J. (1993). Animal models of muscular dystrophy: characteristics and applications. Lab Animal, 22, 33 - 37.

Coovert, D. D., & Burghes, A. H. M. (1994). Gene therapy for muscle diseases. Current Opinion in Neurology, 7, 463 - 470.

Coulter, L. R., Landree, M. A., & Cooper, T. A. (1997). Identification of a new class of exonic splicing enhancers by in vivo selection. Molecular and Cellular Biology, 17 (4), 2143 - 2150.

Crooke, S. T., & Bennett, C. F. (1996). Progress in antisense oligonucleotide therapeutics. Annual Review of Pharmacological Toxicology, 36, 107 - 129.

Crooke, S. T. (1999). Molecular mechanisms of action of antisense drugs. Biochimica et Biophysica Acta, 1489, 31 - 44.

Culligan, K. G., Mackey, A. J., Finn, D. M., Maguire, P. B., & Ohlendieck, K. (1998). Role of dystrophin isoforms and associated proteins in muscular dystrophy (Review). International Journal of Molecular Medicine, 2, 639 - 648.

Dagle, J. M., & Weeks, D. L. (2001). Oligonucleotide-based strategies to reduce gene expression. Differentiation, 69, 75 - 82.

Davies, K. E. (1997). Challenges in Duchenne muscular dystrophy. Neuromuscular Disorders, 7, 482 - 486.

De Angelis, F. G., Sthandier, O., Berarducci, B., Toso, S., Galluzzi, G., Ricci, E., Cossu, G., & Bozzoni, I. (2002). Chimeric snRNA molecules carrying antisense sequences against the splice junctions of exon 51 of the dystrophin pre-mRNA induce exon skipping and restoration of a dystrophin synthesis in Δ48-50 DMD cells. Proceedings of the National Academy of Science, USA, 99 (14), 9456 - 9461.

DelloRusso, C., Scott, J. M., Hartigan-O'Connor, D., Salvatori, G., Barjot, C., Robinson, A. S., Crawford, R. W., Brooks, S. V., & Chamberlain, J. S. (2002). Functional correction of adult *mdx* mouse muscle using gutted adenoviral vectors expressing full-length dystrophin. Proceedings of the National Academy of Science, USA, 99 (20), 12979 - 12984.

Dias, N. & Stein, C. A. (2002). Antisense oligonucleotides: basic concepts and mechanisms. Molecular Cancer Therapeutics, 1, 347 - 353.

Dickson, G., Hill, V., & Graham, I. R. (2002). Screening for antisense modulation of dystrophin pre-mRNA splicing. Neuromuscular Disorders, 12, S67 - S70.

Dominski, Z., & Kole, R. (1993). Restoration of correct splicing in thalassemic pre-mRNA by antisense oligonucleotides. Proceedings of the National Academy of Science, USA, 90, 8673 - 8677.

Dominski, Z., & Kole, R. (1994). Identification and characterisation by antisense oligonucleotides of exon and intron sequences required for splicing. Molecular and Cellular Biology, 14 (11), 7445 - 7454.

Dominski, Z., & Kole, R. (1996). Effects of exon sequences on splicing of model pre-mRNA substrates *in vitro*. Acta Biochimica Polonica, 43 (1), 161 - 174.

Duchler, M., Pengg, M., Brunner, S., Muller, M., Brem, G., & Wagner, E. (2001). Transfection of epithelial cells is enhanced by combined treatment with mannitol and polyethyleneglycol. Journal of Genetic Medicine, 3, 115 - 124.

Dunckley, M. G., Manoharan, M., Villiet, P., Eperon, I. C., & Dickson, G. (1998).Modification of splicing in the dystrophin gene in cultured *mdx* muscle cells by antisense oligoribonucleotides. Human Molecular Genetics, 7 (7), 1083 - 1090.

Emery, A. E. H. (2002). The muscular dystrophies. The Lancet, 359, 687 - 695.

England, S. B., Nicholson, L. V., Johnson, M. A., Forest, S. M., Love, D. R., Zubrzycka-Gaarn, E. E., Bulman, D. E., Harris, J. B., & Davies, K. E. (1990). Very mild muscular dystrophy associated with the deletion of 46% of dystrophin. Nature, 343, 180 - 182.

Errington, S. J., Mann, C. J., Fletcher, S., & Wilton, S. D. (2003). Target selection for antisense oligonucleotide induced exon skipping in the dystrophin gene. The Journal of Gene Medicine, 5, 518 - 527.

Fabb, S. A., Wells, D. J., Serpente, P., & Dickson, G. (2002). Adeno-associated virus vector gene transfer and sarcolemmal expression of a 144 kDa micro-dystrophin effectively restores the dystrophin-associated protein complex and inhibits myofibre degeneration in nude/*mdx* mice. Human Molecular Genetics, 11 (7), 733 - 741.

Fairbrother, W. G. & Chasin, L. A. (2000). Human genomic sequences that inhibit splicing. Molecular and Cellular Biology, 20 (18), 6816 - 6825.

Fairbrother, W. G., Yeh, R., Sharp, P. A., & Burge, C. B. (2002). Predictive identification of exonic splicing enhancers in human genes. Science, 297, 1007 - 1013.

Fanin, M., Danieli, G. A., Cadaldini, M., Miorin, M., Vitiello, L., & Angelini, C. (1995). Dystrophin-positive fibres in Duchenne dystrophy: origin and correlation to clinical course. Muscle and Nerve, 18, 1115 - 1120.

Fanin, M., Freda, D. A., Vitiello, L., Danieli, G. A., Pegoraro, E., & Angelini, C. (1996). Duchenne phenotype with in-frame deletion removing major portion of dystrophin rod: threshold effect for deletion size? Muscle and Nerve, 19, 1154 - 1160.

Feener, C. A., Koenig, M., & Kunkel, L. M. (1989). Alternative splicing of human dystrophin mRNA generates isoforms at the carboxy terminus. Nature, 338 (6215), 509 - 511.

Fernandez-Cadenas, I., Andreu, A. L., Gamez, J., Gonzalo, R., Martin, M. A., Rubio, J. C., & Arenas, J. (2003). Splicing mosaic of the myophosphorylase gene due to a silent mutation in McArdle disease. Neurology, 61, 1432 - 1434.

Ferrari, G., Cusella-De Angelis, G., Colletta, M., Paolucci, E., Stornaiuolo, A., Cossu, G., & Mavilio, F. (1998). Muscle regeneration by bone-marrow-derived myogenic progenitors. Science, 279, 1528 - 1530.

Ferrer, A., Wells, K. E., & Wells, D. J. (2000). Immune responses to dystrophin: implications for gene therapy of Duchenne muscular dystrophy. Gene Therapy, 7 (17), 1439 - 1446.

Fisher, R., Tinsley, J. M., Phelps, S. R., Squire, S. E., Townshend, E. R., Martin, J. E., & Davies, K. E. (2001). Non-toxic ubiquitous over-expression of utrophin in the *mdx* mouse. Neuromuscular Disorders, 11, 713 - 721.

Fletcher, S., Wilton, S. D., & Howell, J. M. (2000). Gene therapy and molecular approaches to the treatment of hereditary muscular disorders. Current Opinion in Neurology, 13, 553 - 560.

Fletcher, S., Ly, T., Duff, R. M., Howell, J., & Wilton, S. D. (2001). Cryptic splicing involving the splice site mutation in the canine model of Duchenne muscular dystrophy. Neuromuscular Disorders, 11, 239 - 243.

Frenkel, P. A., Chen, S., Thai, T., Shohet, R. V., & Grayburn, P. A. (2002). DNA-loaded albumin microbubbles enhance ultrasound-mediated transfection *in vitro*. Ultrasound in Medicine & Biology, 28 (6), 817 - 822.

Furdon, P. J., Dominski, Z., & Kole, R. (1989). RnaseH cleavage of RNA hybridised to oligonucleotides containing methylphosphomate, phosphorothioate and phosphodiester bonds. Nucleic Acids Research, 17 (22), 9193 - 9204.

Galderisi, U., Cascino, A., & Giordana, A. (1999). Antisense oligonucleotides as therapeutic agents. Journal of Cellular Physiology, 181, 251 - 257.

Gamper, H. B., Cole-Strauss, A., Metz, R., Parekh, H., Kumar, R., & Kmiec, E. B. (2000). A plausible mechanism for gene correction by chimeric oligonucleotides. Biochemistry, 39, 5808 - 5816.

Gao, X., & Huang, L. (1995). Cationic liposome-mediated gene transfer. Gene Therapy, 2, 710 - 722.

Gillis, J. M. (2002). Multivariate evaluation of the functional recovery obtained by the overexpression of utrophin in skeletal muscles of the *mdx* mouse. Neuromuscular Disorders, 12, S90 - S94.

Goncz, K. K., Colosimo, A., Delapiccola, B., Gagne, L., Hong, K., Novelli, G., Papahadjopioulos, D., Sawa, T., Schreier, H., Wiener-Kronisch, J., Xu, Z., & Gruenert, D. C. (2001). Expression of ΔF508 CFTR in normal mouse lung after site-specific modification of CFTR sequences by SFHR. Gene Therapy, 8, 961 - 965.

Gorecki, D. C., Monaco, A. P., Derry, J. M., Walker, A. P., Barnard, E. A., & Barnard, P. J. (1992). Expression of four alternative dystrophin transcripts in brain regions regulated by different promoters. Human Molecular Genetics, 1 (7), 505 - 510.

Graveley, B. R., Hertel, K. J., & Maniatis, T. (1998). A systematic analysis of the factors that determine the strength of pre-mRNA splicing factors. The EMBO Journal, 17 (22), 6747 - 6756.

Guga, P., Koziolkiewicz, A., Okruszek, A., & Stec, W. J. (1998). Oligo(nucleoside phosphorothioate)s. Applied Antisense Oligonucleotide Technology. C. A. Stein and A. Kreig. New York, Wiley-Liss.

Gussoni, E., Soneoka, Y., Strickland, C. D., Buzney, E. A., Khan, M. K., Flint, A. F., Kunkel, L. M., & Mulligan, R. C. (1999). Dystrophin expression in the *mdx* mouse restored by stem cell transplantation. Nature, 401, (6751), 390 - 394.

Harper, S. Q., Hauser, M. A., DelloRusso, C., Duan, D., Crawford, R. W., Phelps, S. F, Harper, H. A., Robinson, A. S., Englehardt, J. F., Brooks, S. V., & Chamberlain, J. S. (2002). Modular flexibility of dystrophin: implications for gene therapy of Duchenne muscular dystrophy. Nature Medicine, 8 (3), 253 - 261.

Hartigan-O'Connor, D., & Chamberlain, J. S. (2000). Developments in gene therapy for muscular dystrophy. Microscopy Research and Technique, 48, 223 - 238.

Hauser, M. A., Amalfitano, A., Kumar-Singh, R., Hauschka, S., & Chamberlain, J. S. (1997). Improved adenoviral vectors for gene therapy of Duchenne muscular dystrophy. Neuromuscular Disorders, 7, 277 - 283.

Heald, A., Anderson, L. V., Bushby, K. M., & Shaw. P. J. (1994). Becker muscular dystrophy with onset after 60 years. Neurology, 44 (12), 2388 - 2390.

Hodgetts, S. I., Spencer, M. J., & Grounds, M. D. (2003). A role for natural killer cells in the rapid death of cultured donor myoblasts after transplantation. Transplantation, 75 (6), 863 - 871.

Hoffman, E. P., Brown, R. H., & Kunkel, L., M. (1987). Dystrophin: the protein product of the Duchenne muscular dystrophy locus. Cell, 51, 919-928.

Hoffman, E. P., Fischbeck, K. H., Brown, R. H., Johnson, M., Medori, R., Loike, J. D., Harris, J. B., Waterston, R., Brooke, M., & Specht, L. (1988). Characterisation of dystrophin in muscle-biopsy specimens from patients with Duchenne's or Becker's muscular dystrophy. New England Journal of Medicine, 318 (21), 1363 - 1368.

Hoffman, E. P., Morgan, J. E., Watkins, S. C., & Partridge, T. A. (1990). Somatic reversion / suppression of the mouse *mdx* phenotype *in vivo*. Journal of the Neurological Sciences, 99, 9 - 25.

Horowitz, D. S. & Krainer, A. R. (1994). Mechanisms for selecting 5' splice sites in mammalian pre-mRNA splicing. Trends in Genetics, 10 (3), 100 - 106.

Howell, J. M., Fletcher, S., O'Hara, A., Johnsen, R. D., Lloyd, F., & Kakulas, B. A. (1998). Direct dystrophin and reporter gene transfer into dog muscle *in vivo*. Muscle and Nerve, 21, 159 - 165.

Ito, T., Takeshima, Y., Sakamoto, H., Nakamura, H., & Matsuo, M. (2001). Purine-rich exon sequences are not necessarily splicing enhancer sequence in the dystrophin gene. Kobe Journal of Medical Science, 47, 193 - 202.

Jat, P. S., Noble, M. D., Ataliotis, P., Tanaka, Y., Yannoutsos, N., Larsen, L., & Kiossis, D. (1991). Direct derivation of conditionally immortal cell lines from an H-2K-tsA58 transgenic mouse. *Proceedings of the National Academy of Science, USA*, 88, 5096 - 5110.

Kapsa, R., Quigley, A., Lynch, G., Steeper, K., Kornberg, A. J., Gregorevic, P., Austin, L., & Byrne, E. (2001). *In vivo* and *in vitro* correction of the *mdx* dystrophin gene nonsense mutation by short-fragment homologous replacement. Human Gene Therapy, 12, 629 - 642.

Karpati, G., & Acsadi, G. (1993). The potential for gene therapy in Duchenne muscular dystrophy and other genetic muscle diseases. *Muscle & Nerve*, 16, 1141 - 1153.

Kessler, O., Jiang, Y., & Chasin, L. A. (1993). Order of intron removal during splicing of endogenous adenine phosphoribosyltransferase and dihydrofolate reductase pre-mRNA. Molecular and Cellular Biology, 13 (10), 6211 - 6222.

Kichler, A., Leborgne, C., Coeytaux, E., & Danos, O. (2001). Polyethylenimine-mediated gene delivery: a mechanistic study. The Journal of Gene Medicine, 3, 135 - 144.

Klein, C. J., Coovert, D. D., Bulman, D. E., Ray, P. N., Mendell, J. R., & Burghes, A. H. (1992). Somatic reversion / suppression in Duchenne Muscular Dystrophy (DMD): evidence supporting a frame-restoring mechanism in rare dystrophin-positive fibres. American Journal of Human Genetics, 50, 950 - 959.

Kochanek, S., Clemens, P. R., Mitani, K., Chen, H., Chan, S., & Caskey, C. T. (1996). A new adenoviral vector: replacement of all viral coding sequences with 28 kb of DNA independently expressing both full-length dystrophin and β-galactosidase. Proceedings of the National Academy of Science, USA, 93, 5731 - 5736.

Koenig, M., Hoffman, E. P., Bertelson, C. J., Monaco, A. P., Feener, C., & Kunkel, L. M. (1987). Complete cloning of the Duchenne muscular dystrophy (DMD) cDNA and preliminary genomic organisation of the DMD gene in normal and affected individuals. Cell, 50, 509 - 517.

Koenig, M., Monaco, A. P., & Kunkel, L. M. (1988). The complete sequence of dystrophin predicts a rod-shaped cytoskeletal protein. Cell, 53, 219 - 228.

Koenig, M., Beggs, A. H., Moyer, M., Scherpf, S., Heindrich, K., Bettecken, T., Meng, G., Muller, C. R., Lindlof, M., & Kaariainen, H. (1989). The molecular basis for Duchenne versus Becker muscular dystrophy: correlation of severity with type of deletion. American Journal of Human Genetics, 45, 498 - 506.

Kole, R. & Sazani, P. (2001). Antisense effects in the nucleus: modification of splicing. Current Opinion in Molecular Therapies 3, 229-234.

Lam, B. J., & Hertel, K. J. (2002). A general role for splicing enhancers in exon definition. RNA, 8, 1233 - 1241.

Lavrovsky, Y., Chen, S., & Roy, A. K. (1997). Therapeutic potential and mechanism of action of oligonucleotides and ribozymes. Biochemical and Molecular Medicine, 62, 11 - 22.

Lebedeva, I., & Stein, C. A. (2001). Antisense oligonucleotides: promise and reality. Annual Review of Pharmacology and Toxicology, 41, 403 - 419.

Lin, S. & Burgunder, J. M. (2000). Utrophin may be a precursor of dystrophin during skeletal muscle development. Brain Research. Developmental Brain Research, 119, 289 - 295.

Liu, H-X., Zhang, M., & Krainer, A. R. (1998). Identification of functional exonic splicing enhancer motifs recognised by individual SR proteins. Genes & Development, 12, 1998 - 2012.

Liu, H-X., Chew, S. L., Cartegni, L., Zhang, M.Q, & Krainer, A. R. (2000). Exonic splicing enhancer motif recognised by human SC35 under splicing conditions. Molecular and Cellular Biology, 20 (3), 1063 - 1071.

Liu, H-X., Cartegni, L., Zhang, M. Q., & Krainer, A. R. (2001a). A mechanism for exon skipping caused by nonsense or missense mutations in BRCA1 and other genes. Nature Genetics, 27, 55 - 58.

Liu, L., Rice, M. C., & Kmiec, E. B. (2001b). *In vivo* gene repair of point and frameshift mutations directed by chimeric RNA/DNA oligonucleotides and modified single-stranded oligonucleotides. Nucleic Acids Research, 29 (20), 4238 - 4250.

Love, D. R., Byth, B. C., Tinsley, J. M., Blake, D. J., & Davies, K. E. (1993). Dystrophin and dystrophin-related proteins: a review of protein and RNA studies. Neuromuscular Disorders, 3 (1), 5 - 21.

Lu, Q. L., Morris, G. E., Wilton, S. D., Ly, T., Artem'yeva, O. V., Strong, P., & Partridge, T. A. (2000). Massive idiosyncratic exon skipping corrects the nonsense mutation in dystrophic mouse muscle and produces functional revertant fibres by clonal expansion. Journal of Cell Biology, 148 (5), 985 - 995.

Lu, Q. L., Mann, C. J., Lou, F., Bou-Gharios, G., Morris, G. E., Xue, S. A., Fletcher, S., Partridge, T. A., & Wilton, S. D. (2003). Functional amounts of dystrophin produced by skipping the mutated exon in the mdx dystrophic mouse. Nature Medicine 9 (8), 1009 - 14.

Mann, C. J., Honeyman, K., Cheng, A. J., Ly, T., Lloyd, F., Fletcher, S., Morgan, J. E., Partridge, T. A., & Wilton, S. D. (2001). Antisense-induced exon skipping and synthesis of dystrophin in the *mdx* mouse. Proceedings of the National Academy of Science, USA, 98 (1), 42 - 47.

Mann, C. J., Honeyman, K., McClorey, G., Fletcher, S., &Wilton, S. D. (2002). Improved oligonucleotide induced exon skipping in the *mdx* mouse model of muscular dystrophy. Journal of Gene Medicine, 4 (6), 644 - 654.

Maquat, L. E. (1995). When cells stop making sense: effects of nonsense codons on RNA metabolism in vertebrate cells. RNA, 1 (5) 453 - 465

Marshall, D. J., & Leiden, J. M. (1998). Recent advances in skeletal-muscle-based gene therapy. Current Opinion in Genetics and Development, 8, 360 - 365.

Matsuo, M., Masamura, T., Nakajima, T., Kitoh, Y., Takumi, T., Nishio, H., Koga, J., & Nakamura, H. (1990). A very small frame-shifting deletion within exon 19 of the Duchenne muscular dystrophy gene. Biochemical and Biophysical Research Communications, 170 (2), 963 - 967.

Matsuo, M., Masamura, T., Nishio, H., Nakajima, T., Kitoh, Y., Takumi, T., Koga, J. & Nakamura, H. (1991). Exon skipping during splicing of dystrophin mRNA precursors due to an intragenic deletion in the dystrophin gene of Duchenne muscular dystrophy Kobe. Journal of Clinical Investigation, 87, 2127 - 2131.

Matsuo, M. (1996). Duchenne / Becker muscular dystrophy: from molecular diagnosis to gene therapy. Brain and Development, 18, 167 - 172.

Matveeva, O., Felden, B., Tsodikov, A., Johnston, J., Monia, B., Atkins, J. F., Gesteland, R. F., & Freier, S. M. (1998). Prediction of antisense oligonucleotide efficacy by in vitro methods. Nature Biotechnology, 16, 1374 - 1375.

Mendell, J. R., Kissel, J. T., Amato, A. A., King, W., Signore, L., Prior, T. W., Sahenk, Z.,Benson, S., McAndrew, P. E., Rice, R., Nagaraja, H., Stephens, R., Lantry, L., Morris, G. E., & Burghes, A. H. M. (1995). Myoblast transfer in the treatment of Duchenne muscular dystrophy. New England Journal of Medicine, 333, 832 - 838.

Mercatante, D. R., Bortner, C. D., Cidlowski, J. A., & Kole, R. (2001). Modification of alternative splicing of Bcl-x pre-mRNA in prostate and breast cancer cells. The Journal of Biological Chemistry, 276 (19), 16411 - 16417.

Monaco, A. P., Bertelson, C. J., Liechti-Gallati, S., Moser, H., & Kunkel, L. M. (1988). An explanation for phenotypic differences between patients bearing partial deletions of the DMD locus. Genomics, 2, 90 - 95.

Moore, M. J., Query, C. C., & Sharp, P. A. (1993). Splicing of precursors to mRNA by the spliceosome. In G. R. F. & A. J. F. (Eds.), The RNA World (pp. 303 - 357). Cold Spring Harbor: Cold Spring Harbor Laboratory Press.

Morgan, J. (1994). Cell and gene therapy in Duchenne muscular dystrophy. Human Gene Therapy, 5, 165-173.

Morgan, J. E., Beauchamp, J. R., Pagel, C. N., Peckham, M., Ataliotis, P., Jat, P. S., Noble, M. D., Farmer, K., & Partridge, T. A. (1994). Myogenic cell lines derived transgenic mice carrying a thermolabile T antigen: a model system for the derivation of tissue-specific and mutation-specific cell lines. Developmental Biology, 162 (2), 486 - 498.

Mountain, A. (2000). Gene therapy: the first decade. Trends in Biological Technology, 18, 119 - 128.

Nicholson, L. V. B. (1993). The 'rescue' of dystrophin synthesis in boys with Duchenne muscular dystrophy. Neuromuscular Disorders, 3, 525 - 531.

Nonaka, I. (1998). Animal models of muscular dystrophies. Laboratory Animal Science, 48 (1), 8 - 17.

Ohtsuka, Y., Udaka, K., Yamashiro, Y., Yagita, H., & Okumura, K. (1998). Dystrophin acts as a transplantation rejection antigen in dystrophin-deficient mice: implication for gene therapy. The Journal of Immunology, 160, 4635 - 4640.

Orr, R. M. (2001). Technology evaluation: fomivirsen, Isis Pharmaceuticals Inc/CIBA vision. Current Opinion in Molecular Therapies, 3 (3), 288 - 294.

Pearce, M., Blake, D. J., Tinsley, J. M., Byth, B. C., Campbell, L., Monaco, A. P., & Davies, K. E. (1993). The utrophin and dystrophin genes share similarities in genomic structure. Human Molecular Genetics, 2 (11), 1765 - 1772.

Petrof, B. J., Shrager, J. B., Stedman, H. H., Kelly A. M., & Sweeney, H. L. (1993). Dystrophin protects the sarcolemma from stresses developed during muscle contraction. Proceedings of the National Academy of Science (USA), 90 (8), 3710 - 3714.

Politz, J. C., Taneja, K. L., & Singer, R. H. (1995). Characterisation of hybridisation between synthetic oligodeoxynucleotides and RNA in living cells. Nucleic Acids Research, 23 (24), 4946 - 4953.

Pramono, Z. A., Takeshima, Y., Alimsardjono, H., Ishii, A., Takeda, S., & Matsuo, M. (1996). Induction of exon skipping of the dystrophin transcript in lymphoblastoid cells by transfecting an antisense oligodeoxynucleotide complementary to an exon recognition sequence. Biochemical and Biophysical Research Communications, 226, 445 - 449.

Prior, T. W., Papp, A. C., Snyder, P. J., Burghes, A. H. M., Bartolo, C., Sedra, M. S., Western, L. M., & Mendell, J. R. (1993). A missense mutation in a Duchenne muscular dystrophy patient. Nature Genetics, 4, 357 - 360.

Radojevic, V., Lin, S., & Burgunder, J. M. (2000). Differential expression of dystrophin, utrophin, and dystrophin-associated proteins in human muscle culture. Cell Tissue Research, 300, 447 - 457.

Ragot, T., Vincent, N., Chafey, P., Vigne, E., Gilgenkrantz, H., Couton, D., Cartaud, J., Briand, P., Kaplan, J., Perricaudet, M., & Kahn, A. (1993). Efficient adenovirus-mediated transfer of a human minidystrophin gene to skeletal muscle of *mdx* mice. Nature, 361, 647 - 650.

Rando, T. A. & Blau, H. M. (1994). Primary mouse myoblast purification, characterisation, and transplantation for cell-mediated gene therapy. Journal of Cell Biology, 125 (6), 1275 - 1287.

Rando, T. A., Disatnik, M., & Zhou, L. Z. (2000). Rescue of dystrophin expression in *mdx* mouse muscle by RNA/DNA oligonucleotides. Proceedings of the National Academy of Science, USA, 97 (10), 5363 - 5368.

Reed, R. (1996). Initial splice-site recognition and pairing during pre-mRNA splicing. Current Opinions in Genetics and Development, 6, 215 - 220.

Roberts, R. G., Coffey, A. J., Bobrow, M., & Bentley, D. R. (1992a). Determination of the exon structure of the distal portion of the dystrophin gene by vectorette PCR. Genomics, 13, 942 - 950.

Roberts, R. G., Bobrow, M., & Bentley, D. R. (1992b). Point mutations in the dystrophin gene. Proceedings of the National Academy of Science, USA, 97, 2331 - 2335.

Romano, G., Micheli, P., Pacilio, C., & Giordano, A. (2000). Latest developments in gene transfer technology: achievements, perspectives, and controversies over therapeutic applications. Stem Cells, 18, 19 - 39.

Romero, N. B., Benveniste, O., Payan, C., Braun, S., Squiban, P., Herson, S., & Fardeau, M. (2002). Current protocol of a research phase I clinical trial of full-length dystrophin plasmid DNA in Duchenne/Becker muscular dystrophies; part II: clinical protocol. Neuromuscular Disorders, 12, S45 - S48.

Sadoulet-Puccio, H. M., & Kunkel, L. M. (1996). Dystrophin and its isoforms. Brain Pathology, 6, 25 - 35.

Sakamoto, M., Yuasa, K., Yoshimura, M., Yokota, T., Ikemoto, T., Suzuki, M., Dickson, G., Miyagoe-Suzuki, Y., & Takeda, S. (2002). Micro-dystrophin cDNA ameliorates dystrophic phenotypes when introduced into *mdx* mice as a transgene. Biochemical and Biophysical Research Communications, 293, 1265 - 1272.

Sampaolesi, M., Torrente, Y., Innocenzi, A., & Tonlorenzi, R. (2003). Cell therapy of (alpha)-sarcoglycan null dystrophic mice through intra-arterial delivery of mesoangioblasts. Science, 301 (5632), 487 - 492.

Sazani, P., Gemignani, F., Kang, S., Maier, M. A., Manoharan, M., Persmark, M., Bortner, D., & Kole, R. (2002). Systemically delivered antisense oligomers upregulate gene expression in mouse tissues. Nature Biotechnology, 20, 1228 - 1233.

Sazani, P., & Kole, R. (2003). Therapeutic potential of antisense oligonucleotides as modulators of alternative splicing. The Journal of Clinical Investigation, 112 (4), 481 - 486.

Schatzberg, S. J., Anderson, L. V. B., Wilton, S. D., Kornegay, J. N., Mann, C. J., Solomon, G. G., & Sharp, N. J. H. (1998). Alternative dystrophin gene transcripts in golden retriever muscular dystrophy. Muscle & Nerve, 21, 991 - 998.

Seeberger, P. H., & Caruthers, M. H. (1998). Modified oligonucleotides as antisense thaerapeutics. Applied Antisense Oligonucleotide Technology. C. A. Stein and A. Kreig. New York, Wiley-Liss.

Seigneurin-Venin, S., Bernard, V., & Tremblay, J. P. (2000). Telomerase allows the immortalization of T antigen-positive DMD myoblasts: a new source of cells for gene transfer application. Gene Therapy, 7, 619 - 623.

Senapathy, P., Shapiro, M. B., & Harris, N. (1990). Splice junctions, branch point sites and exons: sequence statistics, identification, and applications to genome project. Methods in Enzymology, 183, 252 - 278.

Shapiro, M. B., & Senapathy, P. (1987). RNA splice junctions of different classes of eukaryotes: sequence statistics and functional implications in gene expression. Nucleic Acids Research, 15, 7155 - 7174.

Sharp, N. J., Kornegay, J. N., Van Camp, S. D., Herbstreith, M. H., Secore, S. L., Kettle, S., Hung, W. -Y, Constantinou, C. D., Dykstra, M. J., Roses, A. D., & Bartlett, R. J. (1992). An error in dystrophin mRNA processing in Golden Retriever muscular dystrophy, an animal homologue of Duchenne muscular dystrophy. Genomics, 13, 115 - 121.

Sherratt, T. G., Vulliamy, T., Dubowitz, V., Sewry, C. A., & Strong, P. N. (1993). Exon skipping and translation in patients with frameshift deletions in the dystrophin gene. American Journal of Human Genetics, 53, 1007 - 1015.

Sicinski, P., Geng, Y., Ryder-Cook, A. S., Barnard, E. A., Darlison, M. G., & Barnard, P. J. (1989). The molecular basis of muscular dystrophy in the *mdx* mouse: a point mutation. Science, 244, 1578 - 1579.

Sierakowska, H., Sambade, M. J., Agrawal, S., & Kole, R. (1996). Repair of thalassemic human β-globin mRNA in mammalian cells by antisense oligonucleotides. Proceedings of National Academy of Sciences, USA, 93, 12840 - 12844.

Sironi, M., Cagliani, R., Pozzoli, U., Bardoni, A., Comi, G. P., Giord, R., & Bresolin, N. (2002). The dystrophin gene is alternatively spliced throughout its coding sequence. FEBS Letters, 517, 163 – 166.

Smythe, G. M., Hodgetts, S. I., & Grounds, M. D. (2000). Immunobiology and the future of myoblast transfer therapy. Molecular Therapy, 1 (4), 304 - 313.

Stein, C. A., & Krieg, A. M. (1994). Problems in interpretation of data derived from in vitro and in vivo use of antisense oligodeoxynucleotides. Development, 4(2), 67 - 69.

Stein, C. A. (2001). The experimental use of antisense oligonucleotides: a guide for the perplexed. The Journal of Clinical Investigation, 108(5), 641 - 644.

Stephenson, M. L., & Zamecnik, P. C. (1978). Inhibition of Rous sarcoma viral RNA translation by a specific oligodeoxyribonucleotide. Proceedings of the National Academy of Science, USA, 75 (1), 285 - 288.

Takeshima, Y., Nishio, H., Sakamoto, H., Nakamura, H., & Matsuo, M. (1995). Modulation of *in vitro* splicing of the upstream intron by modifying an intron-exon sequence which is deleted from the dystrophin gene in dystrophin Kobe. Journal of Clinical Investigation, 95 (2), 515 - 520.

Takeshima, Y., Wada, H., Yagi, M., Ishikawa, Y., Ishikawa, Y., Minami, R., Nakamura, H., & Matsuo, M. (2001). Oligonucleotides against a splicing enhancer sequence led to dystrophin production in muscle cells from a Duchenne muscular dystrophy patient. Brain Development, 23(8), 788 - 790.

Tanaka, K., Watakabe, A., & Shimura, Y. (1994). Polypurine sequences within a downstream exon function as a splicing enhancer. Molecular Cell Biology, 14, 1347 - 1354.

Tennyson, C. N., Klamut, H. J., & Worton, R. G. (1995). The human dystrophin gene requires 16 hours to be transcribed and is cotranscriptionally spliced. Nature Genetics, 9 (2), 184 - 190.

Thanh, L. T., Man, N., Helliwell, T. R., & Morris, G. E. (1995). Characterisation of revertant muscle fibres in Duchenne muscular dystrophy, using exon-specific monoclonal antibodies against dystrophin. American Journal of Human Genetics, 56, 725 - 731.

Tsukamoto, H., Wells, D. J., Brown, S. C., Serpente, P., Strong, P. N., Drew, J., Inui, K., Okada, S., & Dickson, G. (1999). Enhanced expression of recombinant dystrophin following intramuscular injection of Epstein-Barr virus (EBV)-based mini-chromosome vectors in *mdx* mice. Gene Therapy, 6, 1331 - 1335.

Tinsley, J. M., Potter, A. C., Phelps, S. R., Fisher, R., Trickett, J. I., & Davies, K. E. (1996). Amelioration of the dystrophic phenotype of *mdx* mice using a truncated utrophin transgene. Nature, 384, 349 - 353.

Tuffery-Giraud, S., Chambert, S., Demaille, J., Claustres, M. (1999). Point mutations in the dystrophin gene: evidence for frequent use of cryptic splice sites as a result of splicing defects. Human Mutations, 14 (5), 359 - 368.

Uchino, M., Tokunaga, M., Mita, S., Uyama, E., Ando, Y., Teramoto, H., Miike, T., & Ando, M. (1995). PCR and immunocytochemical analyses of dystrophin-positive fibres in Duchenne muscular dystrophy. Journal of the Neurological Sciences, 129, 44 - 50.

Valentine, B. A., Winand, N. J., Pradhan, D., Moise, N. S., de Lahunta, A., Kornegay, J. N., & Cooper, B. J. (1992). Canine X-linked muscular dystrophy as an animal model of Duchenne muscular dystrophy: a review. American Journal of Medical Genetics, 42, 352 - 356.

van Deutekom, J. C. T., Floyd, S., Booth, D. K., Oligino, T., Krisky, D., Marconi, P., Glorioso, J. C., & Huard, J. (1998). Implications of maturation for viral gene delivery to skeletal muscle. Neuromuscular Disorders, 8, 135 - 148.

van Deutekom, J. C. T., Bremmer-Bout, M., Janson, A. A. M., Ginjaar, I. B., Baas, F., den Dunnen, J. T., & van Ommen, G. B. (2001). Antisense-induced exon skipping restores dystrophin expression in DMD patient derived muscle cells. *Human Molecular Genetics*, 10 (15), 1547 - 1554.

van Deutekom, J. C. T. & van Ommen, G. B. (2003). Advances in Duchenne muscular dystrophy gene therapy. Nature Reviews Genetics, 4, 774 - 783.

Vickers, T. A., Wyatt, J. R., & Freier, S. M. (2000). Effects of RNA secondary structure on cellular antisense activity. Nucleic Acids Research, 28 (6), 1340 - 1347.

Vilquin, J. T., Brussee, V., Asselin, I., Kinoshita, I., Gigras, M., & Tremblay, J. P. (1998). Evidence of *mdx* mouse skeletal muscle fragility *in vivo* by eccentric running exercise. Muscle and Nerve, 21, 567 - 576.

Vilquin, J. T., Kennel, P. F., Paturneau-Jonas, M., Chapdelaine, P., Boissel, N., Delaere, P., Tremblay, J. P., Scherman, D., Fiszmann, M. Y., & Schwartz, K. (2001). Electrotransfer of naked DNA in the skeletal muscles of animal models of muscular dystrophies. Gene Therapy, 8, 1097 - 1107.

Wakefield, P. M., Tinsley, J. M., Wood, M. J., Gilbert, R., Karpati, G., & Davies, K. E. (2000). Prevention of the dystrophic phenotype in dystrophin/utrophin-deficient muscle following adenovirus-mediated transfer of a utrophin minigene. Gene Therapy, 7, 201 - 204.

Watakabe, A., Tanaka, K., & Shimura, Y. (1993). The role of exon sequences in splice site selection. Genes and Development, 7, 407 - 418.

Weiss, B., Davidkova, G., & Zhou, L. W. (1999). Antisense RNA gene therapy for studying and modulating biological processes. Cellular & Molecular Life Sciences, 55, 334 - 358.

Wilson, L. A., Cooper, B. J., Dux, L., Dubowitz, V., & Sewry, C. A. (1994). Expression of utrophin (dystrophin-related protein) during regeneration and maturation of skeletal muscle in canine X-linked muscular dystrophy. Neuropathology and Applied Neurobiology, 20, 359 - 367.

Wilton, S. D., Dye, D., & Laing, N. (1997a). Dystrophin gene transcripts skipping the *mdx* mutation. Muscle & Nerve, 20, 728 - 734.

Wilton, S. D., Lim, L., Dye, D., & Laing, N. (1997b). Bandstab: a PCR-based alternative to cloning PCR products. Biotechniques, 22, 642 - 645.

Wilton, S. D., Dye, D. E., Blechynden, L. M., Laing, N. G. (1997c). Revertant fibres: a possible genetic therapy for Duchenne muscular dystrophy? Neuromuscular Disorders, 7, 329 - 335.

Wilton, S. D., Lloyd, F., Carville, K., Fletcher, S., Honeyman, K., Agrawal, S., & Kole, R. (1999). Specific removal of the nonsense mutation from the *mdx* dystrophin mRNA using antisense oligonucleotides. Neuromuscular Disorders, 9, 330 - 338.

Winnard, A. V., Mendell, J. R., Prior, T. W., Florence, J., & Burghes, A. H. M. Frameshift deletions of exons 3-7 and revertant fibres in Duchenne muscular dystrophy: mechanisms of dystrophin production. American Journal of Human Genetics, 56, 158 - 166.

Wolff, J. A., Malone, R., Williams, P., Chong, W., Acsadi, G., Jani, A., & Felgner, P. L. (1990). Direct gene transfer into mouse muscle in vivo. Science, 247, 1465 - 1468.

Woolf, T., Melton, D. A., & Jennings, C. G. B. (1992). Specificity of antisense oligonucleotides in vivo. Proceedings of the National Academy of Science, USA, 89, 7305 - 7309.

Worton, R. G. (1992). Duchenne muscular dystrophy: gene and gene product; mechanism of mutation in the gene. Journal of Inherited Metabolic Diseases, 15 (4), 539 - 550.

Xu, R., Teng, J., & Cooper, T.A. (1993). The cardiac troponin T alternative exon contains a novel purine-rich positive splicing element. Molecular Cell Biology, 13, 3660 - 3674.

Yuasa, K., Sakamoto, M., Miyagoe-Suzuki, Y., Tanouchi, A., Yamamoto, H., Li, J., Chamberlain, J. S., Xiao, X., & Takeda, S. (2002). Adeno-associated virus vector-mediated gene transfer into dystrophin deficient skeletal muscles evokes enhanced immune response against the transgene product. Gene Therapy, 9 (23), 1576 - 1588.

Zelenin, A. V., Kolesnikov, V. A., Tarasenko, O. A., Shafei, R. A., Zelenina, I. A., Mikhailov, V. V., Semenova, M. L., Kovalenko, D. V., Artemyeva, O. V., Ivaschenko, T. E., Evgrafov, O. V., Dickson, G., & Baranovand, V. S. (1997). Bacterial β-galactosidase and human dystrophin genes are expressed in mouse skeletal muscle fibres after ballistic transfection. FEBS Letters 414, 319 - 322.

Zelphati, O., & Szoka, F. C. (1996). Mechanism of oligonucleotide release from cationic liposomes. Proceedings of the National Academy of Science, USA, 93, 11493 - 11498.

Zubrzycka-Gaarn, E. E., Hutter, O. F., Karpati, G., Klamut, H. J., Bulman, D. E. (1991). Dystrophin is tightly associated with the sarcolemma of mammalian skeletal muscle fibers. Experimental Cell Research, 192 (1), 278 - 288.

Zubrzycka-Gaarn, E. E., Bulman, D. E., Karpati, G., Burghes, A. H. M., Belfall, B., Klamut, H. J., Talbot, J., Hodges, R. S., Ray, P. N., & Worton, R. G. (1988). The Duchenne muscular dystrophy gene product is localised in sarcolemma of human skeletal muscle. Nature, 333, 466 - 469